UNIVERSITY OF CALGARY

Boron Isotope Geochemistry During Burial Diagenesis

by

Lynda B. Williams

A THESIS

SUBMITTED TO THE FACULTY OF GRADUATE STUDIES

IN PARTIAL FULFILLMENT OF THE REQUIREMENTS FOR THE

DEGREE OF DOCTOR OF PHILOSOPHY

DEPARTMENT OF GEOLOGY AND GEOPHYSICS

CALGARY, ALBERTA

APRIL, 2000

ABSTRACT

This research was conducted to test the hypothesis that boron isotopes in deep sedimentary basins can be used to monitor fluid/rock/organic interactions during thermal maturation. The thermal maturation of hydrocarbons occurs at temperatures corresponding to the major diagenetic silicate reaction of smectite to illite. If B is mobilized from a source rock along with the generated hydrocarbons, its interaction with authigenic illite in reservoirs could provide a useful tracer of migrating hydrocarbon-related fluids.

Experiments were conducted to measure the B-isotope fractionation between mineral and water during the illitization of smectite. The temperature dependence of the isotope fractionation was tested at 300° and 350°C. Isotopic equilibrium was approached after 4-5 months when the illite/smectite (I/S) displayed long-range structural ordering (~70% illitization). Results were used to construct a new B-isotope fractionation curve.

Methods were developed and tested for analyzing B and O-isotopes in clay minerals by secondary ion mass spectrometry (SIMS). A method for analyzing B in organic matter by thermal ionization mass spectrometry was also tested, but analyses by SIMS are simpler. A comparison of results of the two analytical methods shows consistency.

The fractionation curve was tested in a variety of natural geologic settings, including hydrocarbon reservoirs in the U.S. Gulf of Mexico basin, and the Alberta basin. Samples from a contact metamorphic aureole in the Cretaceous Pierre shale (Colorado) provided a test of the temperature dependence of the curve, outside the realm of

diagenetic temperatures. The results presented demonstrate that the B-fractionation curve can be applied over a large range of temperatures (diagenetic to metamorphic).

The importance of this research is that it provides new isotopic data that describes B-isotope systematics in sedimentary basins undergoing diagenesis. The magnitude of B-isotope fractionation is large compared to other stable isotopic systems, and the fractionation applies to a variety of diagenetic silicates. The substitution of B in authigenic illite, with an isotopic composition reflecting the fluid chemistry at the temperature of precipitation, may provide a useful diagenetic monitor for the migration of hydrocarbon-related fluids in reservoirs.

Acknowledgements

I thank Ian Hutcheon (UC) for making the opportunity for me to work with him and my committee for their helpful suggestions. I have greatest appreciation for Rick Hervig, my mentor at Arizona State University. His constant optimism and inquisitive nature led me through this work. I also thank John Holloway (ASU) for teaching me how hydrothermal experiments work. I enjoyed working with Mike Wieser (UC) who taught me how to do thermal ionization mass spectrometry.

From other universities I thank Fred Longstaffe, (UWO) who gave me valuable advice, encouragement and analyses throughout my research. I also thank Bill Leeman (Rice Univ.) for analyses of standards, Ray Ferrell (LSU) for assistance in Walsenburg, CO. Jon Dudley formerly of Imperial for Cold Lake samples, and Neeley Bostick (USGS) for sharing his great coal collection.

The following people are appreciated for technical assistance. Maurice Shevalier was a critical link for me accomplishing my goals in the time allotted. I appreciate his conversations and moral support as well. Steve Taylor provided inspiration when spectrometers misbehaved, and took pity when needed. Nenita Lozano, Jesusa Pontoy and Maria Mihailescu delighted my days in the lab at UC, and took good care of me.

At ASU I enjoyed the assistance and humor of Al Higgs, who was critical to electronic repairs on the SIMS. David Wright assisted in setting up the hydrothermal lab and vacuum extractions. Jon Mull, Nina Barr, Paul Perkes, Joan Bahamonde and Sue Selkirk assisted with computer and graphics difficulties. They are highly valued.

Funding was from the U.S. Department of Energy grant DE-FG03-94ER14414 and partial support by the Imperial Oil Charitable Foundation to Ian Hutcheon.

Finally, this research required immense patience and perseverance of my family through very difficult times that completely disrupted their lives. I will always love them.

Dedication

To my mother

TABLE OF CONTENTS

List of Tables

List of Figures

I believe that imagination is stronger than knowledge,
That myth is more potent than history,
That dreams are more powerful than facts,
That hope always triumphs over experience,
That laughter is the only cure for grief,
And I believe that love is stronger than death.

Robert Fulghum, All I Really Need to Know I Learned in Kindergarten

CHAPTER ONE: INTRODUCTION

The chemical dynamics of sedimentary basins undergoing burial diagenesis are so complex that even the most fundamental questions focussing on how water moves and transports elements through the rock, have consumed generations of researchers. One of the most productive branches of geochemistry for enhancing our knowledge of processes affecting fluid/rock interactions has been the study of stable isotopes. A variety of stable isotopic systems of major elements (C, H, O, N, S) have been applied to deriving important information about how rocks exchange components with aqueous fluids and hydrocarbons during burial diagenesis; approaching equilibrium under constantly changing physical conditions such as increasing temperature and pressure. Boron isotope systematics have not been as widely applied to geologic problems in the sedimentary environment because B is a trace element, and therefore it has been more difficult to measure and understand its isotopic variations in nature. Advances in analytical methods for measuring B-isotopes in minerals by secondary ion mass spectrometry (e.g. Hervig, 1996; Chaussidon,et al., 1997) have made this research possible. This thesis attempts to build on the broad foundation of stable isotopic studies by using boron isotope variations to elucidate processes in diagenetic systems.

Boron isotopes are appealing to use in studying clastic sedimentary rocks because B has only one oxidation state (+3) so it does not participate in redox reactions. Boron, with an atomic number of 5, has many chemical characteristics similar to carbon and silicon. Because it is a strong electron pair acceptor (a Lewis acid) it has a very high affinity for oxygen (Hawthorne et al., 1996). Thus it is expected to behave in silicate

hydrocarbon reservoirs in a manner similar to the C and Si that dominate the system. Its behavior, therefore, may trace the diagenetic modifications to the fluid, rock, and organic matter.

Mechanisms of mineral modifications in sedimentary rocks have been difficult to constrain because of the large number of phases (minerals) contributing the same components (e.g. oxygen) involved in several complex reactions. For example if the O-isotopic composition of a quartz cement in sandstone is variable, it suggests that there were changes in the water $\delta^{18}O$ or temperature during cementation. Even if temperature can be constrained, it is not possible to say what chemical reactions contributed to changing the water $\delta^{18}O$ because oxygen might be derived from carbonates, silicates or transported fluids that have migrated into the reservoir. Boron can be a more sensitive tracer of fluid/rock interactions in deep sedimentary basins because it is not a significant component of many diagenetic silicates (primarily only clay minerals contain >100 ppm B), so the variables that affect the isotope ratios can be more easily constrained.

Boron has two stable isotopes, ^{10}B and ^{11}B, with average relative abundance of 20% and 80%, respectively. It occurs in natural waters predominantly as $B(OH)_3$ or $B(OH)_4^-$. The heavy isotope, ^{11}B, forms more stable bonds in trigonal coordination, whereas ^{10}B is predominantly in tetrahedral coordination (Palmer and Swihart, 1996). It is this coordination preference that causes ^{10}B-enrichment of minerals that provide tetrahedral sites. Clay minerals, specifically smectite and illite, are the dominant host for B in clastic sedimentary rocks (Goldschmidt and Peters, 1932). Boron substitutes for silicon in tetrahedral layers of clay structures (Palmer and Swihart, 1996) during

illitization of smectite (Perry, 1972). Under surface depositional conditions, however, B is adsorbed on the clay minerals surfaces. This adsorbed-B is not related to the crystallization of the mineral, and therefore has a distinctly different isotopic composition reflecting the surficial water chemistry.

The sedimentary cycle of B-isotopes was studied nearly a decade ago by several researchers (Spivack et al., 1987; Ishikawa and Nakamura, 1993; You et al., 1993) who established that adsorbed-B on clay minerals was critically important for understanding marine sediments and B fluxes in the ocean. Boron is a mobile element in the aqueous phase because it is incompatible with most minerals. Desorption of the surface adsorbed-B in marine sediments was found to make it useful as a tracer of sediment derived fluids (^{10}B-enriched) in subduction zones (You et al., 1993). These earlier studies all examined bulk marine sediments (<4μm fraction) including a mixture of detrital minerals (clay minerals, quartz and carbonate). They recognized that illite was the major host for boron in the sediments and suggested that B is incorporated in illite during diagenesis. However, lacking experimental data on the fractionation factors as a function of temperature, these investigators were unable to predict equilibrium conditions for fluids and authigenic minerals during burial. This important earlier work clearly called for experimental measurements of boron isotope fractionation during illitization of smectite. Furthermore, B-isotopes in organic matter have not been previously examined. Many coal deposits contain significant quantities of B (Banerjee and Goodarzi, 1990) indicating that organic matter can be a significant source of B when it is thermally degraded. Since

kerogen is an important reactive constituent of most sedimentary basins it is examined in this research.

The main hypothesis of this research is that boron may be generated during thermal maturation of hydrocarbon source rocks with a characteristic isotopic ratio that will be recorded by exchange reactions with authigenic clay minerals (illite/smectite, I/S). Knowledge of the isotopic fractionation factors of B at temperatures of burial diagenesis is required, and forms the basis of this research. The goals were,

1) To experimentally measure the equilibrium isotope fractionation of B between mineral and water during the reaction of smectite to illite.
2) To examine the B-content and isotope ratios of diagenetic silicates, organic matter and waters in natural environments in order to determine their potential as sources of B.
3) To utilize the knowledge of the boron isotope fractionation as a function of temperature to interpret the fluid/rock interactions in hydrocarbon reservoirs.

The thesis is a collection of four papers addressing the above goals. The first paper (Chapter 2) was submitted to Chemical Geology and has been accepted pending revision. It describes a study of the potential sources of B in a sedimentary basin. Sources of B in hydrocarbon bearing basins are important to identify if B is to be used as a geochemical tracer. Samples of rock, oil and water from hydrocarbon reservoirs and source rocks in the U.S. Gulf of Mexico sedimentary basin were examined. Methods were developed and tested for extracting B from organic matter for isotope ratio analysis, in order to evaluate its potential impact on the chemistry of formation fluids. Results

showed that kerogen contained as much B as clay minerals (>100 ppm), but that oils contained negligible quantities (ppb). The $\delta^{11}B$ of the kerogen was negative, indicating that organic matter is a potential source of isotopically light B during late stages of organic maturation. The $\delta^{11}B$ and B-content of authigenic clay minerals in the reservoir sandstones did not change over the depth interval examined (3.5 – 4.3 km) indicating that they are not a source of B at the diagenetic temperatures represented (90°-125°C).

The second paper (Chapter 3) has been submitted to Geochimica et Cosmochimica Acta. It is the main body of the research and describes three experiments that were conducted over two years to measure the changes in B-isotopes during the illitization of smectite. Design and construction of the hydrothermal experimental apparatus was essential for extraction of samples on a routine basis. Several sealed samples were taken during each experiment in order to monitor the kinetics of B and O isotopic exchange. Due to the slow reaction kinetics at diagenetic temperatures the experiments were run at elevated temperatures (300°C and 350°C). It took 4-5 months for the experiments to approach equilibrium. Changes in oxygen isotopes were monitored as a method of defining the approach to equilibrium. Oxygen isotopic equilibrium ratios for illite at the temperatures of the experiment are known (Savin and Lee, 1988). Boron substitution in illite is chemically linked to oxygen isotope exchange because as B substitutes for Si the Si-O bonds in the mineral must be broken. Changes in the O-isotope composition of the water are sensitive to the B-isotopic exchange. The equilibrium isotopic fractionation value for B was used to construct a fractionation curve. The results place two points on a fractionation line, which are in line with other experiments at

higher and lower temperatures. These data provide a basis for a fractionation equation unlike previously published fractionation estimates based on theory (Kakihana et al., 1977). The new fractionation data is used to interpret the B-isotope ratios measured on mudstones and sandstone reservoirs from the U.S. Gulf Coast basin.

The third paper (Chapter 4) is also submitted to Geochimica et Cosmochimica Acta as another example of the application of the experimental fractionation data to a natural geological environment. It is a study of the B-isotopic changes observed in a contact metamorphosed black-shale from Colorado. The contact aureole contains a bentonite layer that shows a complete recrystallization of smectite to illite with increasing temperature, proximal to the dike. The B-isotope ratios of the I/S showed a large decline (~20‰) with increasing temperature which could be interpreted using the new B-isotope fractionation data and applying a Rayleigh distillation model to the results. The importance of this paper is that it shows that the isotopic fractionation curve applies to metamorphic temperatures as well as diagenetic temperatures. It was also discovered that a sample near the dike that had experienced 500°C temperatures and contained 500 ppm B. This shows that illite does not break down or lose B even at metamorphic temperatures so it is an unlikely source of B at diagenetic temperatures. This validates the idea that illite will retain the $\delta^{11}B$ it acquires during crystallization, and should be a useful archive of the fluid chemistry at that time.

The final paper (Chapter 5) is an application of the B-isotope fractionation curve to a hydrocarbon reservoir in the Alberta basin. This paper will be submitted to Applied Geochemistry. The samples examined were from a steam injection recovery project at

Cold Lake. The sediments have a major component of volcanic lithic fragments (pumice) that appear to be the most reactive phases with respect to boron. Examination of core samples from before and after steam injection show significant differences in the $\delta^{11}B$ and B-content of the pumice. This information, combined with an earlier study of the $\delta^{11}B$ variations in produced waters from the reservoir (Wieser, 1998), provide an ideal test for the experimental isotope fractionation data. The water $\delta^{11}B$ could be predicted by the temperature dependence of the rock-fluid isotope fractionation. The importance of this paper is that it shows that the isotopic fractionation of B is not dependent on mineralogy. The fractionations measured in the clay mineral experiments also described the fractionation due to isotopic exchange with pumice. This means that B-isotopes can be used as a geothermometer in a variety of geologic settings (Hervig et al., in review).

By monitoring the geochemistry of B during burial diagenesis, the complex reactions between inorganic and organic substances in hydrocarbon reservoirs might be better understood. Authigenic illite in deep sedimentary basins provides a snapshot of the $\delta^{11}B$ of fluids during crystallization that can be used to constrain variables in the geochemical environment and ultimately aid our understanding of the chemical dynamics of hydrocarbon reservoirs.

CHAPTER TWO:

THE INFLUENCE OF ORGANIC MATTER ON THE BORON ISOTOPE GEOCHEMISTRY OF THE GULF COAST SEDIMENTARY BASIN, USA

2.1. ABSTRACT

Large variations in the boron isotopic composition of sedimentary environments make boron an attractive monitor of fluid/rock interactions during diagenesis. Studies of B in marine sediments have shown that preferential adsorption of ^{10}B on clay minerals leaves pore waters enriched in ^{11}B. During diagenesis, clay minerals recrystallize and incorporate ^{10}B into the mineral structure (Spivack et al., 1987). This process should cause a depletion of B-content and an increase in the $\delta^{11}B$ of pore water; however, in the Gulf Coast sedimentary basin (USA) there is a general increase in B-content and decrease in $\delta^{11}B$ with depth. This suggests that another source of ^{10}B exists in deep basinal environments. Oil reservoir brines are commonly enriched in boron (Collins, 1975), therefore this study examines organic matter as a possible source of boron during thermal maturation.

Samples of water, oil, and cored sediments were collected from three stacked hydrocarbon reservoirs in the Gulf of Mexico sedimentary basin at a depth of 3500-4350 m. Extraction of boron from organic matter (oil and kerogen) was done by Parr Bomb volatilization, with mannitol used as a B-complexing agent. The isotope ratios were measured using negative thermal ionization and compared to in situ analyses using secondary ion mass spectrometry.

The $\delta^{11}B$ values of pore filling clays in sandstone reservoirs is $-2\pm2‰$. The B-content of the clay averages 144 ppm. Oil field waters show a range in B-content from 8-85 ppm and $\delta^{11}B$ values from +28 to +37‰, increasing from the lowest to the uppermost reservoir. There is apparent ^{11}B-enrichment of fluids with progressive migration through clay-rich sediments. Very little B (ppb) was found in the oil, but kerogen extracted from the

oil source rock (Sassen, 1990) contains significant B (140 ppm) with a $\delta^{11}B$ of $-2\pm2‰$, similar to the authigenic illite in the sandstones. While kerogen comprises only ~2% of the sedimentary basin, its influence can be significant if B with distinctly low $\delta^{11}B$ is released over a specific temperature interval during thermal maturation. The release of B from organic compounds could cause the observed regional ^{10}B enrichment in waters deep in the Gulf Coast basin.

2.2. INTRODUCTION

In order to evaluate the B-isotope systematics of sedimentary basins, it is necessary to know the relative amount of B derived from organic matter during thermal maturation and its isotopic composition. The objective of this study is to determine the contribution of boron from oil and kerogen in a hydrocarbon-producing region of the Gulf Coast sedimentary basin and to evaluate its effect on the isotopic composition of associated water and minerals.

Boron is an important constituent of clastic sedimentary basins because it is concentrated in clay minerals, causing shales to contain 1-2 orders of magnitude more boron than other crustal or mantle silicates (Goldschmidt and Peters, 1932). Detrital clay minerals initially adsorb boron onto the mineral surface, but with increasing burial, boron is substituted in tetrahedral sites of the clay structure, replacing Si (Couch and Grim, 1968). This B is non-desorbable or 'fixed-B'. Perry (1972) studied boron fixation in clay minerals from natural sediments by isolating <1μm size fraction clays from samples of the Gulf of Mexico sedimentary basin (USA). He showed that fixed-B concentrations increase with increasing quantity of authigenic illite (Fig. 2.1a), and proposed that the source for B

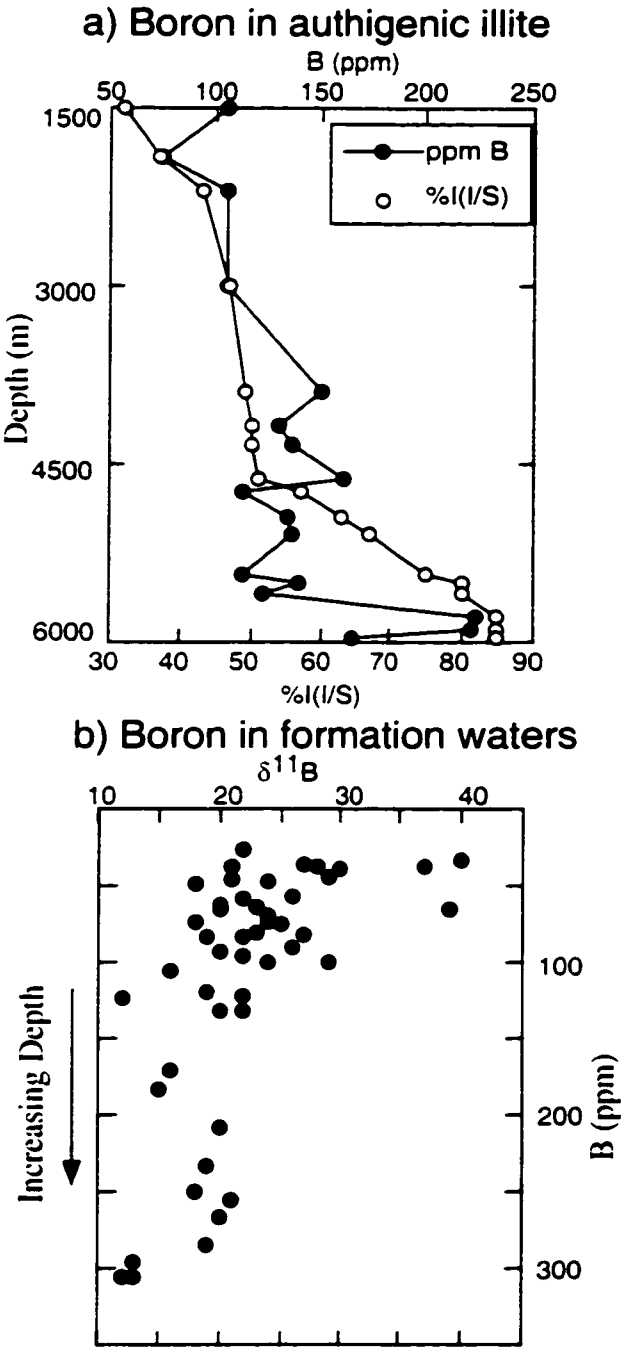

Figure 2.1 a) Variation in the B-content of authigenic illite with depth of burial in the Gulf Coast sedimentary basin, USA (Perry 1972) and b) concurrent changes in B-content and $\delta^{11}B$ of formation waters from clastic reservoirs in the Gulf Coast sedimentary basin (Land and Macpherson, 1992).

in authigenic illite was the adsorbed-B from detrital minerals, perhaps redistributed during breakdown of detrital illite (also a supply of K^+). Boron isotope systematics during progressive burial and illitization were not examined.

Recent B-isotope studies have focused on B in shallow marine sediments (<2 km) where adsorption on clay-rich sediments has a significant effect on the isotopic composition of the associated pore fluids (Vengosh et al., 1991; Brumsack and Zulegar, 1992; You et al., 1995a,b). Generally, high $\delta^{11}B$ waters are thought to result from preferential adsorption of ^{10}B onto clay mineral surfaces, causing a reduction of the B-content of the water as well (Brumsack and Zulegar, 1992). Therefore, in shallow marine sediments the B-content of pore waters commonly decreases with depth while the $\delta^{11}B$ increases.

In the deep Gulf of Mexico basin, however, this variation of B-content and $\delta^{11}B$ of formation water is not observed. Boron increases with depth from 20 - 300 ppm and $\delta^{11}B$ decreases from a maximum of 40‰ to a minimum near 12‰ (Fig. 2.1; Land and Macpherson, 1992; Moldovanyi and Walter, 1992). There is considerable scatter in the $\delta^{11}B$ of water, which combines analyses from a number of localities. Such variations presumably indicate local differences in the chemistry of the sediments. However, the regional trend indicates the existence of an additional, isotopically light source of B not observed in shallow marine sediments.

Organic matter in the Gulf of Mexico sedimentary basin is a potential source of boron that has not been previously investigated. Available literature on the B content of kerogen is sparse, but B is often mentioned as a substantial component of organic compounds. Boron in oil has been found in concentrations up to 70 ppm B (Gulyayeva et

al., 1966) and coals have been found with as much as 500 ppm B (Goodarzi and Swain, 1994). Gulyayeva et al., (1966) studied boron in various fractions of oil and found boron primarily associated with napthenic acids in the resinous oil components. Elevated concentrations of boron are common in oil field waters (Collins, 1975) suggestive of organically-derived B. No data are available on the isotopic composition of boron in hydrocarbons and kerogen, therefore the objective of this research is to explore the potential influence of organically-derived B on the B-isotopic composition of basin waters.

2.3. FIELD AREA

Samples of water, oil and cored sediments were collected from drill holes that intersected three stacked hydrocarbon reservoirs in Fordoche Field, located in the Eocene Wilcox Fm of south-central Louisiana (Fig. 2.2). These samples allowed examination of the role of B in clays, organic matter and pore water during thermal maturation. The samples collected are from a locality where the structural, stratigraphic and mineralogic details as well as the thermal maturity of organic matter are known (Williams et al., 1995). The source region for the oils has been identified using biomarkers and oil-source rock correlations (Sassen, 1990), and thermal maturity indices (Rock Eval pyrolysis) shows the source rock to contain mixed type II and III organic matter with a moderate generative potential and averaging 2% TOC. The ratio of H/C is approximately twice that of O/C indicative of a mature source (Williams et al., 1995).

The Wilcox Fm is comprised of a thick sequence of organic-rich shales with interbedded sandstones that were deposited along a prograding delta. Fordoche Field

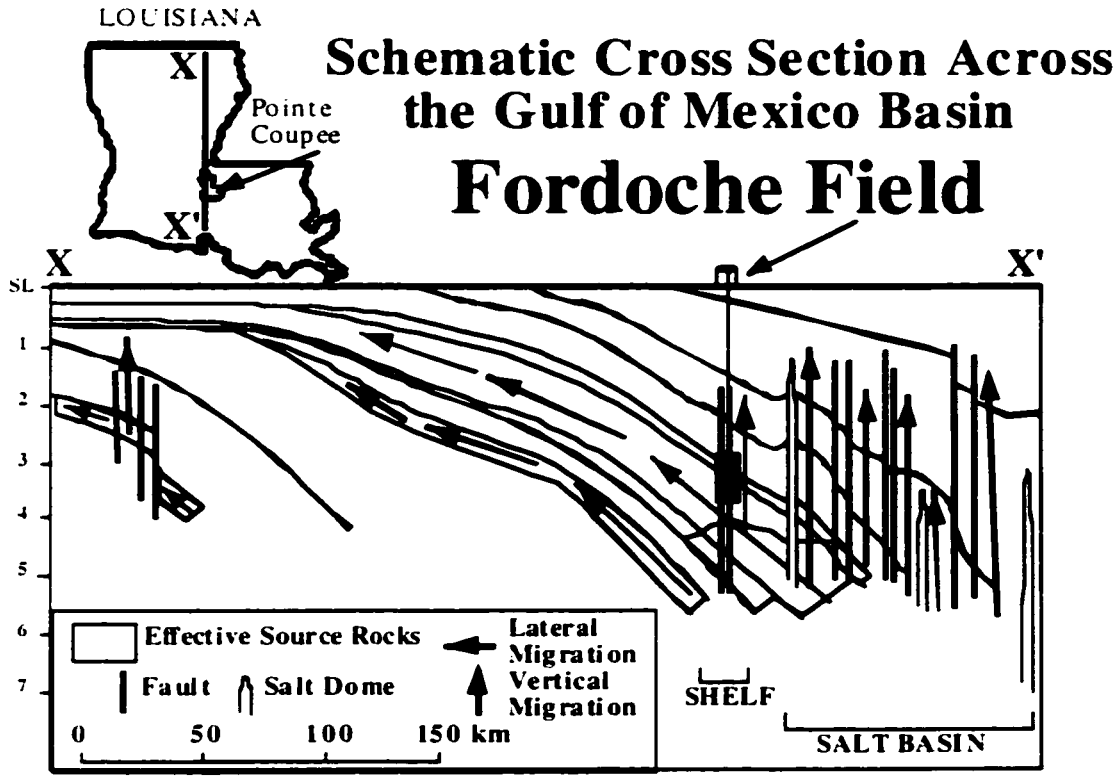

Figure 2.2 Stratigraphic cross section across central Louisiana (N-S). The Fordoche field is located in the Eocene Wilcox Fm, directly above the inferred hydrocarbon source rock (Sassen 1990).

reservoirs are located just above the source region for the oils (Sassen, 1990). Previous investigations of this field (Williams et al., 1995) indicated that hydrocarbons were introduced into the three reservoirs along a normal growth fault that bounds the field to the northwest. The direction of hydrocarbon migration is up dip, away from the fault. The API gravity of the hydrocarbons increases from the deepest (46.9° API) to the middle reservoir (44.9° API) and uppermost reservoir (40° API).

A cross section of Fordoche Field from the major growth fault toward the southeast (Fig. 2.3) shows the structural relationship of the three reservoirs sampled (W-12, W-8 and Sparta B reservoirs). Kerogen was extracted from mudstones located below the reservoirs at 14,200 ft (4.3 km). This region is slightly above the depth of source rocks, but the thermal maturity is very close to the threshold for hydrocarbon generation (Williams et al., 1995). The distance of fluid migration from the source region increases from the deepest toward the shallowest reservoir, and from the fault toward the southeast end of each reservoir in the field. The oil and water samples were taken from wells where cores were retrieved from the same production intervals. It was not possible to sample oil and water from each cored well across the field because some were out of production, but samples were taken across the deepest reservoir (W-12) along the section line and near the fault in the two shallower reservoirs (W-8 and Sparta B).

2.4. METHODS

Two different mass spectrometric techniques were used in this study: Thermal ionization mass spectrometry utilizing negative BO_2^- ion emission (NTIMS; Heumann and Zeininger, 1985; Vengosh et al., 1989; Klötzli, 1992; Hemming and Hanson, 1994), and

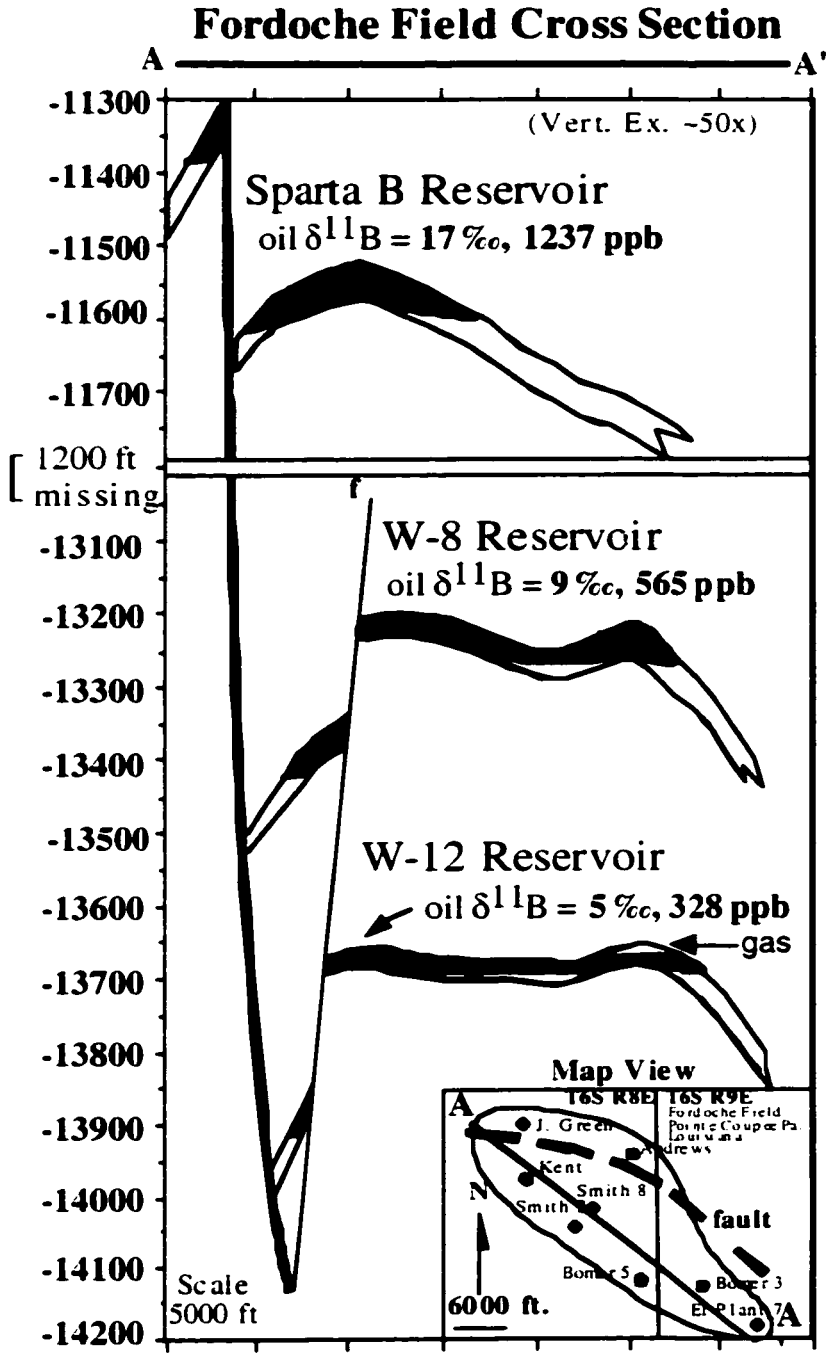

Figure 2.3 Cross section of Fordoche field showing the structural and stratigraphic relationships of the three sandstone reservoirs sampled. Black denotes oil-saturated zones of the sandstone.

secondary ion mass spectrometry (SIMS) (Chaussidon et al., 1997) which analyzes positive ions of B. The isotopic abundance ratio, $^{11}B/^{10}B$, is expressed in delta notation as $\delta^{11}B = [(^{11}B/^{10}B)_{sample} / (^{11}B/^{10}B)_{standard} - 1] \times 1000$ (‰). The standard is NBS SRM-951 (boric acid) with $^{11}B/^{10}B$ ratio of 4.0437 (NIST certified).

2.4.1. Analytical Techniques

2.1.1a. Thermal Ionization Mass Spectrometry

Negative thermal ionization mass spectrometry (NTIMS) is a conventional technique for analysis of solutions with very small amounts of B (Heumann and Zeininger, 1985; Vengosh et al., 1989; Klötzli, 1992). The ionization efficiency for negative ions is greater than for positive ions, therefore analyses can be made on samples containing as little as 10ng of B (Hemming and Hanson, 1994). Typically 1-3μL of sample solution is loaded on an outgassed rhenium filament, along with 3μL of a $Ba(OH)_2$ solution (10 μg Ba) as an emission activator. The filament is introduced into the spectrometer with a vacuum of ~2 x 10^{-7} Torr, floated to -5 kV, and heated by a current of ~1800 mA. A stable emission current was normally generated at temperatures of 850°-900°C.

Analyses yielded errors on the order of ±2‰. These errors are greater than those obtained by PTIMS techniques using cesium metaborate (Swihart, 1996), however, given the large variations in $\delta^{11}B$ observed in the diagenetic environment (>60‰), the errors should not preclude interpretation of the data. Measurements of the boron isotope standard NBS SRM 951 (Catanzaro et al., 1970) yielded a $^{11}B/^{10}B$ ratio of 4.0337±0.0041, which is slightly higher than that reported by other labs using NTIMS (Vengosh et al., 1991; Hemming and Hanson, 1994). However, repeated analysis of seawater collected from the

Pacific ocean yielded a $\delta^{11}B$ value of +39.8±3‰, which is in excellent agreement with that measured in other laboratories (Hemming and Hanson, 1994).

2.4.1b. Secondary Ion Mass Spectrometry

SIMS analyses do not yield the high precision results of TIMS (Tonarini et al., 1997), but they allow better spatial resolution and control of the analyzed area based on textural observation. This can be essential for the analysis of authigenic pore-filling clay minerals that are impossible to separate from detrital clays during extraction from a core. It is sometimes possible to focus an analysis on a thick cement of a particular clay mineral, thus avoiding the complexity of analyzing multiple types of clay minerals. The general method for analysis of B-isotope ratios in silicates by SIMS is described by Chaussidon et al. (1997).

The SIMS was calibrated for analysis of clay minerals by comparing results of analyses on standards to analyses done by TIMS. A standard illite (IMt-1) was rinsed three times in B-free water, and centrifuged to select the <2μm fraction. Aliquots of this standard were analyzed (by W.P. Leeman, Rice University) by the method of Tonarini et al. (1997) using alkali carbonate fusion and ion-exchange separation for boron purification, and PTIMS using $Cs_2BO_2^+$. Three replicate analyses average –8.66±0.23 ‰. Another aliquot was analyzed by NTIMS (built in-house at Univ. of Calgary) with an average of 2 analyses of –9.86±0.65 ‰. Using an average $\delta^{11}B$ value of -9‰ for the IMt-1 illite standard, the instrumental mass fractionation (IMF) for the SIMS is determined during each analytical session by measuring the B-isotope ratio on an aliquot of standard. During the clay analysis sessions, the IMF has varied between -44 and -51 ‰, depending on the instrumental set

up. The IMF remains constant (within error) during each analytical session, allowing the correction for $\delta^{11}B$ relative to NBS 951. As noted by Chaussidon et al. (1997), there is not a significant matrix effect on B-isotope analyses, therefore it can be assumed that there is no significant difference in the IMF for different clay minerals.

2.4.2. Sample Preparation

2.4.2a. Formation Water

Eight water samples were filtered and acidified to pH~2 when collected, in order to prevent bacterial alteration of the samples. The samples were never in contact with borosilicate glass, and were stored in polypropylene bottles. The B-contents of waters were determined by inductively coupled plasma- atomic emission spectroscopy (ICP-AES). The levels of boron in the waters were high enough that no ion exchange was necessary in order to concentrate the B in solution for $\delta^{11}B$ analysis. The isotope ratios were measured by NTIMS.

2.4.2b. Organic Matter

Oils were collected from the same wells as waters and stored in polypropylene containers. Attempts to extract bitumen from powdered core samples failed because the core samples had been stored for several years so bitumen was lost. However, kerogen was extracted from mudstones by dissolution of the silicates in HF (Durand, 1980). The undigested kerogen was filtered out and dried. No published method for extracting and analyzing B-isotopes in organic matter was found, therefore the sample preparation was tested and is described in detail.

Gulyayeva et al. (1966) used a Parr Bomb technique to extract B from oils for analysis of B-content. The Parr bomb is a steel cylinder in which a stainless steel vessel containing ~1g of sample is suspended (Fig. 2.4). A nickel alloy ignition wire is placed just above the sample and about 4 ml of an absorbent (NaOH or water) is placed in the bottom of the cylinder. "B-free" water (deionized water filtered through Amberlite resin to remove B) was used in these preparations. ICP analysis indicates a B-content of the 'B-free' water below the detection limit of 4 ppb. The bomb was then sealed, loaded with 25-30 atm. oxygen, and submerged in water. A current supplied to the ignition wire ignited it, and the organic matter was volatilized.

There was minimal boron recovery in the aqueous solution within the bomb, perhaps due to loss of certain volatile forms of B, such as BCl_3, which is gaseous at 12.5°C, and therefore might not have been trapped in solution. The relatively high salinity of oil field brines suggests an abundance of Cl^-, therefore there is a likelihood of BCl_3 being lost along with CO_2 and other gases released when the bomb is opened. To remedy this, a boron complexing agent, mannitol, was used in the Parr Bomb. Mannitol is a polyhydric alcohol ($CH_2OH\ (CHOH)_4\ CH_2OH$), that is used to eliminate significant B loss from acidic solutions during silicate digestion (Ishikawa and Nakamura, 1990; Nakamura et al., 1992). A solution of 1.82% mannitol (Leeman et al., 1991) was added to the Parr Bomb. BCl3 in the released gas was trapped by purging the gas through an external container of the mannitol solution (Fig. 2.4). The B-contents of solutions collected from inside the Parr Bomb were compared to the external solution and it was discovered that 90-95% of the total-B extracted was in the external solution. Tests were made for the

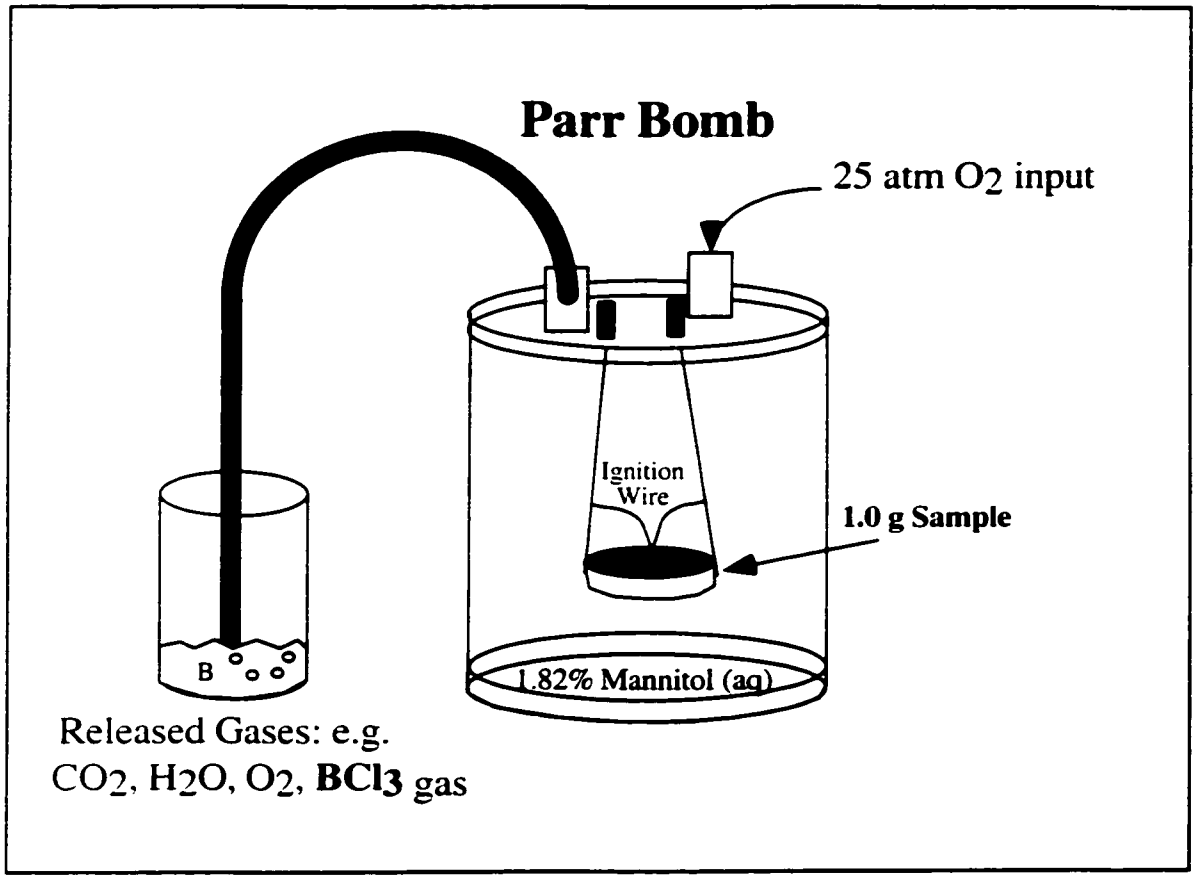

Figure 2.4 Schematic diagram of the Parr bomb apparatus for extraction of B from organic matter.

appropriate purge flow rate to yield the highest boron recovery. Initial purge rates took 20 minutes to empty the ~1 liter volume of gas in the cylinder (~50 ml/minute). The highest yields were obtained at a flow rate of ~15 ml/min, however this does not guarantee complete recovery. A double trap (two external solutions) is recommended as the most effective method for trapping the volatile boron.

Kerogen was initially extracted from six powdered mudstone samples by dissolution of silicates in 5N HF-1N HCl. The undigested kerogen and amorphous silica residue were filtered out of the acid solution. This filtrate was Parr bombed to remove B from kerogen. Because of the variable content of undissolved silica in the organic concentrate (referred to as "ash" by organic petrologists), a small amount of ethanol was added to the sample to enhance ignition (just enough alcohol to dampen the sample). When pure organic compounds (e.g. oil) are Parr bombed there is no residue as volatilization is nearly complete, however silicate material trapped in the kerogen leaves considerable residue in the form of ash or glass beads. These residues were weighed in order to estimate the amount of kerogen volatilized during the Parr bomb procedure. In each sample the ratio of organic matter to ash was ~0.3. Insufficient B was recovered from 1 g samples of shale, however a 50g sample of organic-rich shale from beneath the Fordoche reservoirs yielded ~18g of kerogen (plus silica). The Parr bomb ignition was performed in batches since the capacity of each bomb is approximately 1g of sample. The total ash recovered was 13g, indicating that only about one third of this residue was organic matter (~5 g; consistent with the ratio of organic matter to ash found previously). This kerogen provided enough B for ICP and TIMS analyses.

2.4.2c. Clay Minerals

SIMS analyses of $\delta^{11}B$ were done on thin sections of sandstone and mudstone from the Fordoche cores. B-contamination of minerals in thin section can occur during processing by polishing materials and epoxy. Experiments indicate that ultrasonic cleaning of the thin section with B-free water, and pre-sputtering of the analyzed area decreases B contamination to the level of 0.01 ppm (Chaussidon et al., 1997). However, clay minerals are sponges for boron. The adsorbed-B can exchange in a few hours depending on the clay type (Bassett, 1976). Boron introduced with drilling fluids might significantly affect the isotopic composition of the adsorbed-B in core samples. By definition, clays are particles <2μm in size so the primary ion beam with a diameter of 20-50μm may sputter many clay surfaces at various orientations during a single SIMS analysis. The resulting analysis would be some combination of adsorbed plus fixed-B. Therefore it is important to remove adsorbed-B from the thin-sectioned minerals before analysis.

Removal of adsorbed-B from clay minerals was tested on clay mineral separates and compared to pore-filling and mudstone clay minerals in thin section from the same cored interval. Many authors (e.g., Keren and Mezuman, 1981; Palmer et al., 1987; Spivack et al., 1987) have removed adsorbed-B by rinsing the sample several times in deionized water. This is standard procedure for separating out <2μm size fractions because Cl must be removed from the sample in order to prevent clay mineral flocculation. It was found, however, that this does not consistently remove the adsorbed-B, especially if the clay sample is enriched in smectite. A comparison was made of B-isotope ratios of a standard smectite (SWy-1) rinsed 5 times in B-free water and centrifuged to separate the

<2μm size fraction, with an aliquot of the standard that was K-saturated (shaken in 1N KCl for 24 hrs then rinsed to remove Cl), and another aliquot that was washed in 1.82% mannitol solution for 2 hours. A few drops of clay slurry was dried (60°C) on a B-free glass slide or silicon wafer and Au-coated for SIMS analysis. The results showed that the water-washed smectite has a $\delta^{11}B$ of +12.1±1.3‰, while the $\delta^{11}B$ of the K-saturated sample is -3.0±1.0‰, and the mannitol-washed sample has a $\delta^{11}B$ of -1.1±0.6‰. Removal of adsorbed-B on kaolinite, smectite and illite by washing in mannitol has been tested (Hingston, 1963) and shown to be the most effective treatment. Mannitol also prevents B-isotope fractionation during evaporation (Xiao et al., 1997).

In order to test the effectiveness of mannitol on removing B from thin-sectioned minerals, the $\delta^{11}B$ of a thin section was measured before and after soaking it in 1.82% mannitol solution. The sample was a mudstone taken just below the uppermost reservoir (3535 m). The clays were a mixture of detrital and authigenic material, but the texture, grain size and mineralogy appeared homogeneous. The clay fraction of the mudstone was composed of 44% kaolinite, 30% smectite, 15% chlorite and 11% illite/smectite. The initial analysis of clays in the untreated sample (ultrasonicated in deionized water) gave a $\delta^{11}B$ value of +6.6±2.9‰. The thin section was soaked in mannitol ~72 hrs, ultrasonicated and rinsed to see if the solution could remove adsorbed-B from the surface of the section. SIMS analytical craters are <5μm deep therefore the mannitol must penetrate the surface to at least that depth in order to be effective. After soaking, the area of the thin section previously analyzed gave a significantly lower $\delta^{11}B$ value of -18.9±3.5‰ (13 analyses). In order to check this result, the surface of the section was polished again to remove the

Au-coat and analytical craters and re-analyzed without a second soaking in mannitol, giving an average of -18.7±1.3‰ (3 analyses). This indicates that adsorbed-B was successfully removed from the thin section and that the analyses represent the composition of the fixed-B component.

2.5. RESULTS

2.5.1. Water and Oil

The results of total-B analyses by ICP and isotope ratio measurements by NTIMS are shown in Table 2.1. The B-content of the oil field waters range from 8 to 85 ppm. These data and the $\delta^{11}B$ results are plotted in Figure 2.5. Fluids were introduced to the sandstones through the fault, therefore the distance of migration increases away from the fault, and from the deepest (W-12) to shallowest reservoir (Sparta B). The B-content of most of the reservoir waters is in the range of 10 to 20 ppm, however there is a slight increase in the B-content at the edges of the field. The highest B-content was found in the shallowest reservoir in a well located closest to the regional fault (Fig. 2.5). The $\delta^{11}B$ of the reservoir waters is in the range of values reported for oil field brines (e.g. Vengosh et al, 1994), but notably the deepest reservoir has $\delta^{11}B$ values ~10‰ lower than the upper reservoirs. The exception to this is the water from a gas well at the edge of the field where $\delta^{11}B$ values are similar to the upper reservoirs.

The analyses of the oil are given in Table 2.1 and indicated on Figure 2.3. Results reflect the ~10‰ difference in $\delta^{11}B$ between the deepest reservoir (5‰) and shallowest reservoir (17‰), but the B-contents of the oils are very low (ppb levels), suggesting that B is partitioned into the aqueous phase.

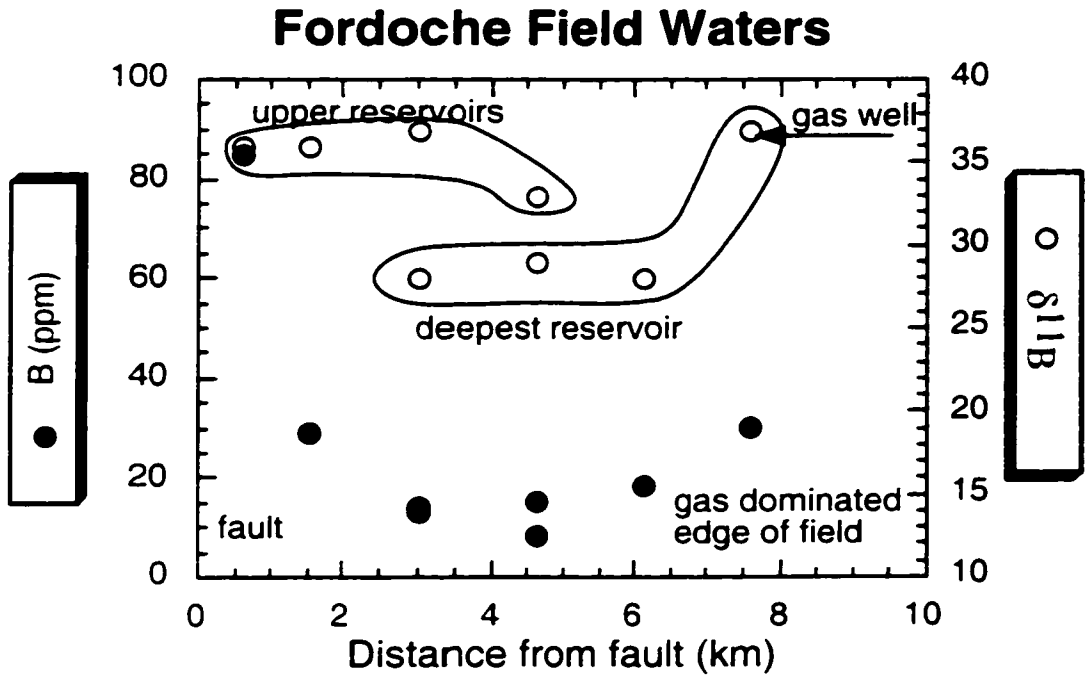

Figure 2.5 Variations in B-content and $\delta^{11}B$ of formation waters across Fordoche Field.

Table 2.1. Boron contents of oil field waters and oils from the Fordoche Field. Waters measured by atomic absorption spectroscopy with a detection limit of 2 ppm. Oils measured by induced coupled plasma spectroscopy with a 4 ppb detection limit.

Waters

Sample	Reservoir	AA (ppm)	S.D.	$^{11}B/^{10}B$	S.D.	$\delta^{11}B$ (‰)
John Green 1	Sparta B	85.1	±0.7	4.1787	±0.0093	36±2.2
Andrews 2	Sparta B	29.3	±1.5	4.1804	±0.0190	36±4.5
Kent 1	W-8	14.6	±0.9	4.1844	±0.0057	37±1.4
Smith 2	W-8	15.6	±0.1	4.1514	±0.0087	33±2.1
Kent 1D	W-12	13.1	±0.3	4.1479	±0.0160	28±3.9
Smith 2D	W-12	8.3	±1.8	4.1688	±0.0081	29±1.9
Bomer 3	W-12	18.6	±1.5	4.1480	±0.0068	28±1.6
El Plant 5	W-12	30.2	±2.4	4.1817	±0.0084	37±2.0

Oils

Sample	Reservoir	ICP (ppb)	S.D.	$^{11}B/^{10}B$	S.D.	$\delta^{11}B$ (‰)
Andrews 2	Sparta B	1527	±3.7	4.1035	±0.0052	17±1.3
Andrews 2D	Sparta B	947	±2.4			
Kent 1	W-8	433	±3.5			
Smith 2	W-8	696	±1.3	4.0702	±0.0089	9±2.2
Kent 1D	W-12	228	±2.6			
Smith 2D	W-12	452	±1.8	4.0532	±0.0130	5±3.2
Bomer 3	W-12	341	±1.5			
El Plant 5	W-12	289	±0.4			

Kerogen		ICP (ppm)	S.D.	$^{11}B/^{10}B$	S.D.	$\delta^{11}B$ (‰)
Kimball	Source Rock	140	±1.4	4.0268	±0.0085	−2±2.1

S.D. is standard deviation. ICP and AA analyses are averages of 4 analyses per sample.

2.5.2. Clay Minerals

Analyses of the $\delta^{11}B$ of clay minerals in Fordoche Field were done by SIMS on thin sections of a representative mudstones and sandstones. To test for changes in $\delta^{11}B$ with burial depth, samples were examined from the shallowest (3540 m) and deepest (4212 m) sandstone reservoirs, and from mudstones at 3536 m and near the oil source region at 4334 m. There is no significant change in the average isotopic composition of the clays over this depth interval (Table 2.2). The pore-filling clays from sandstone had an average $\delta^{11}B$ value of -2.5±0.2‰ in the shallowest reservoir and -2.1±1.7‰ in the deepest reservoir. The mudstones surrounding the sandstone reservoirs contains clays with a much lower fixed B-isotope composition averaging –19±3‰.

2.5.3. Kerogen

The kerogen extracted from mudstone beneath the Fordoche reservoirs (4334 m) contained as much B (140±1.4 ppm) as is commonly found in clay minerals. The high-B concentration allowed analysis by NTIMS without need for ion exchange. The results (Table 2.3) indicated a $\delta^{11}B$ value of –2±2.2‰. In order to test this result, kerogen was analyzed directly by SIMS in a thin section taken from the same core depth (14220 ft.; 4334 m) as the extracted kerogen. Adsorbed-B had been removed by soaking the whole sample in mannitol solution. Seven analyses, each <50μm in diameter, were made on a large kerogen fragment found in this section. Assuming an IMF similar to that used for the clay minerals during that analytical session (-48‰), the $\delta^{11}B$ values measured by SIMS average –4.7±4.1‰, and confirm that the $\delta^{11}B$ of kerogen is negative. This result also suggests that the technique for extraction of B from kerogen by Parr Bomb does not

Table 2.2 B-isotope analyses of clay minerals in A) sandstone and B) mudstone thin sections soaked in mannitol. Standard IMt-1 is analyzed to determine IMF for each analytical session. This value is subtracted from the delta value. S.D. is standard deviation of the ratio. S.E. is standard error of the average. Predicted error is the best possible error based on counting statistics.

A) SANDSTONE ANALYSES

Sample	11/10	S.D.	error ‰	pred. error ‰	IMF	S.E.
IMt-1 Standard	3.8084	0.0042	0.6	0.4	-49.2	
240 ppm B	3.8135	0.0046	0.7	0.5	-47.9	
	3.8139	0.0047	0.7	0.5	-47.8	
				AVERAGE	**-48**	**0.8**
Sample	11/10	S.D.	error ‰	pred. error ‰	δ11B	S.E.
LNB 11614 SS	3.8396	0.0126	1.8	1.0	-2.2	
mannitol washed	3.8374	0.0112	1.6	1.0	-2.7	
228 ppm B	3.8395	0.0119	1.7	1.0	-2.2	
	3.8366	0.0205	2.9	1.5	-2.9	
	3.8394	0.0180	2.6	1.9	-2.2	
	3.8345	0.0171	2.4	1.1	-3.4	
	3.8431	0.0218	3.1	1.9	-1.3	
	3.8350	0.0263	3.8	2.1	-3.3	
				AVERAGE	**-2.5**	**0.2**
Sample	11/10	S.D.	error ‰	pred. error ‰	δ11B	S.E.
Holloway 13820 SS	3.8464	0.0101	1.4	0.7	-0.5	
mannitol washed	3.8432	0.0241	3.4	2.3	-1.3	
157 ppm B	3.8221	0.0051	0.7	0.7	-6.5	
	3.8155	0.0128	1.8	1.4	-8.1	
new pore	3.8522	0.0163	2.3	1.6	0.9	
new pore	3.8589	0.0132	2.2	1.9	2.6	
				AVERAGE	**-2.1**	**1.7**

Continued on next page

Continued Table 2.2

B) MUDSTONE ANALYSES

Sample	11/10	± S.D.	error ‰	pred. error ‰	IMF	S.E.
IMt-1 Standard	3.7947	0.0034	0.5	0.4	-52.6	
240 ppm B	3.7989	0.0052	0.7	0.4	-51.5	
	3.8065	0.0050	0.7	0.4	-49.7	
				AVERAGE	**-51.3**	**0.9**
Sample	11/10	S.D.	error ‰	pred. error ‰	δ11B	S.E.
LNB 11607	3.7584	0.0173	2.5	1.8	-19.3	
MUDSTONE	3.7646	0.0157	2.2	1.8	-17.7	
258 ppm B	3.7517	0.0185	2.6	1.8	-20.9	
	3.7649	0.0175	2.5	1.8	-17.6	
	3.7696	0.0214	3.1	1.6	-16.5	
	3.7565	0.0185	2.6	1.8	-19.7	
	3.7609	0.0193	2.8	1.9	-18.6	
	3.7985	0.0175	2.5	2.0	-9.3	
	3.7516	0.0173	2.5	2.0	-20.9	
	3.7659	0.0205	2.9	1.9	-17.4	
	3.7459	0.0217	3.1	1.9	-22.3	
	3.7417	0.0186	2.7	2.1	-23.4	
	3.7500	0.0230	3.3	1.9	-21.3	
				AVERAGE	**-18.9**	**1.0**
Re-test of mannitol washed mudstone clay						
Sample	11/10	S.D.	error ‰	pred. error ‰	IMF	S.E.
IMt-1 Standard	3.8265	0.0043	0.6	0.4	-44.7	
240 ppm B	3.8387	0.0039	0.6	0.5	-41.7	
	3.8301	0.0054	0.8	0.5	-43.8	
	3.8197	0.0049	0.7	0.4	-46.4	
				AVERAGE	**-44.2**	**1.0**
Sample	11/10	S.D.	error ‰	pred. error ‰	δ11B	S.E.
LNB 11607 MS	3.7951	0.0110	1.6	1.5	-17.3	
re-polished	3.7876	0.0119	1.2	1.2	-19.1	
no additional	3.7848	0.0111	1.6	1.6	-19.8	
mannitol wash				**AVERAGE**	**-18.7**	**0.8**
Sample	11/10	S.D.	error ‰	pred. error ‰	IMF	S.E.
Kimball 14220 MS	3.8041	0.0081	2.1	1.7	-16.8	
mannitol washed	3.7776	0.0129	3.4	2.8	-23.7	
196 ppm B	3.8087	0.0087	2.3	1.9	-15.6	
	3.7838	0.0090	2.4	2.2	-22.1	
	3.8094	0.0105	2.7	2.2	-15.5	
				AVERAGE	**-18.7**	**1.7**

Table 2.3. TIMS analyses of kerogen extracted from source rock, compared to SIMS analyses of kerogen in thin section from the same depth (4334 m).

TIMS analyses of extracted kerogen

mass 11/10	Std. Dev	± 1 SD ‰	std. error	$\delta^{11}B$		
4.0100	0.0183	4.5	1.1	-6.9		
4.0280	0.0191	4.7	1.1	-2.4		
4.0356	0.0149	3.7	0.9	-0.5		
4.0233	0.0126	3.1	0.7	-3.6		
4.0236	0.0112	2.8	0.7	-3.5		
4.0279	0.0142	3.5	0.8	-2.4		
4.0408	0.0128	3.2	0.7	0.8		
4.0225	0.0126	3.1	0.7	-3.8		
4.0399	0.0125	3.1	0.7	0.5		
4.0273	0.0145	3.6	0.8	-2.6		
4.0387	0.0112	2.8	0.7	0.2		
4.0277	0.0123	3.0	0.7	-2.5	**S.D.**	**S.E.**
AVERAGE				**-2.2**	**±2.2**	**0.6**

SIMS analyses in situ using 5 nA primary current and defocussed beam.

mass 11/10	Std. Dev	± 1 SD ‰	std. error	$\delta^{11}B$		
3.8410	0.02020	2.9	2.3	-2.1		
3.8009	0.02050	2.1	2.4	-12.0		
3.8158	0.02791	4.0	2.1	-8.4		
3.8339	0.02812	4.0	2.3	-3.9		
3.8430	0.02785	4.0	2.1	-1.6		
3.8455	0.02638	3.8	2.1	-1.0		
3.8353	0.02565	3.7	2.1	-3.5	**S.D.**	**S.E.**
AVERAGE				**-4.7**	**±4.1**	**1.5**

significantly fractionate the boron.

2.6. DISCUSSION

The geochemistry of the pore waters in the Gulf Coast basin should reflect chemical changes in the sediments because of the high rock:water ratio. Evaluation of B-trends thus requires an understanding of how B interacts with the clastic sediments. It is known that boron is incorporated in clay minerals during diagenesis (Perry, 1972). This interaction is complicated by the fact that B is both adsorbed onto clay surfaces and fixed into tetrahedral sites of authigenic clays. The amount of boron adsorption on detrital clay minerals depends on the specific clay type (Keren and Mezuman, 1981), but ^{10}B shows a preference for tetrahedral coordination at clay surfaces (Palmer and Swihart, 1996) causing a fractionation between aqueous B(OH)3 and adsorption sites of clay minerals in excess of 31‰ (Palmer et al., 1987) at surface temperatures. Spivack et al. (1987) showed that adsorbed-B accounts for <20% of the total-B in shallow marine sediment and has a mean $\delta^{11}B$ of +14‰. The quantity of fixed-B in marine sediments is greater than adsorbed-B and has $\delta^{11}B$ values between 0 and -5 ‰ (Spivack et al., 1987). The illite formed during illitization of smectite is apparently a sink for ^{10}B during diagenesis, not a source.

In the sedimentary environment, smectite is the greatest adsorber of B (Keren and Mezuman, 1981), perhaps due to its high expandability and surface area. On the other hand illite has a greater proportion of fixed-B than smectite. Other clays also contain B, but the predominant clay reaction in the Gulf Coast basin is the illitization of smectite. In general the Wilcox mudstones contain 25-30% clay minerals, while the sandstones contain <10% clay minerals, predominantly illite/smectite (Williams et al., 1995). The Fordoche Field

reservoirs are located at a depth where illite-forming reactions are nearly complete (70-80% authigenic illite, T~120°C). By ~150°C, illitization and oil production has ceased and kerogen begins to break down to dry gas and char or graphite (Fig. 2.6). It is important to realize that after illitization stops continued release of B from kerogen could significantly affect the $\delta^{11}B$ of pore waters.

In order to evaluate the potential influence of organic matter on the B-isotope systematics of basin fluids, the B trends and factors that could cause the observed isotopic changes within Fordoche Field will be discussed first. These factors include fractionation due to pH, temperature changes causing mineral/water or organic/water fractionation, a gas phase separation, isotope exchange due to mineralogical changes, and fluid migration. After evaluation of these variables on a local scale, the regional B trends will be assessed in light of the new B-isotope data for kerogen.

2.6.1. Fordoche Field Boron

2.6.1a. pH and Temperature

Aqueous-B speciation is pH and temperature dependent (Keren and Mezuman, 1981). The predominant species are boric acid ($B(OH)_3$), which shows a preference for ^{11}B, and borate anion ($B(OH)_4^-$), which prefers ^{10}B. At low pH (<7), boron occurs primarily as boric acid, $B(OH)_3$. Under diagenetic temperatures in the Gulf Coast (up to 200°C) siliciclastic reactions buffer the pore water pH to values between 5-6 where $B(OH)_3$ species dominate (Bassett, 1980). Therefore the possibility of isotopic fractionation due to variable aqueous speciation can be dismissed. The effect of polynuclear B-species that might form at high concentrations of B (Bassett, 1976), has not been assessed.

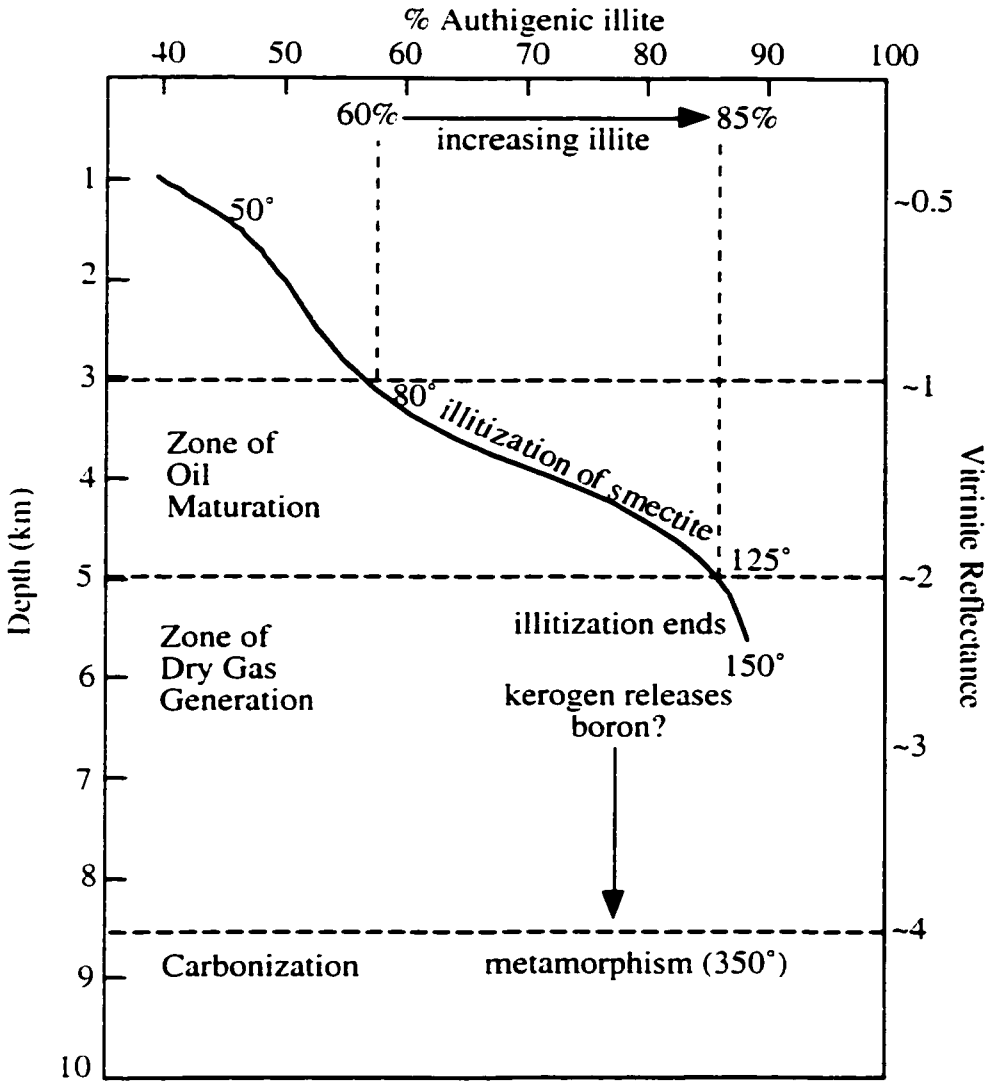

Figure 2.6 Schematic diagram showing the progress of illitization during stages of organic matter maturation in a sedimentary basin. It is inferred that kerogen begins to release B at temperatures >150° after illitization ends.

The temperature difference between W-12 and Sparta B reservoirs is ~25°C. Although this temperature difference seems small, the potential for B-fractionation between the clay minerals and water, or organic matter and water must be evaluated.

2.6.1b. Clay Mineral/Water Fractionation

There is no significant change in the fixed-B content or $\delta^{11}B$ of pore-filling clay minerals in the sandstone reservoirs over the cored interval examined. There is however a significant difference in the water $\delta^{11}B$ from an average of 28‰ in the W-12 reservoir (excluding the gas well) to 36‰ in the shallower Sparta B reservoir. Although sandstone reservoirs are unquestionably rock-dominated, the volume of fluid flow through the rock is much greater than in mudstones and thus trace elements may potentially be transferred from the fluid into pore-filling authigenic minerals. If this is the case, one might expect a difference in the $\delta^{11}B$ of authigenic clays in Fordoche reservoirs that reflects the differences in water chemistry. If the illite had released ^{10}B to lower the water $\delta^{11}B$ in the W-12 reservoir, the fixed-B in clay should be ^{11}B- enriched relative to the shallower Sparta B reservoir. As this is not the case, it appears that the clay minerals are an unlikely source of ^{10}B-enriched waters at depth.

The $\delta^{11}B$ of fixed-B in the mudstone at 11,600 ft (3535 m) and in the source rock (14,220 ft; 4334 m) is much lower (-18‰) than that measured in clays from the adjacent sandstones (-2‰; Table 2.2). The clay minerals in the mudstone are dominated by authigenic I/S (Perry, 1972), and they contain 200 – 300 ppm fixed-B. This is twice as much B as equivalent sediments at the surface (Spivack et al., 1987). New measurements (Table 2.2) show that the clay minerals in the sandstone have similarly high B-contents,

and their textures indicate that they also formed in-situ (authigenic). The high-B content and negative $\delta^{11}B$ of the authigenic clay minerals at this depth (4 km) supports further that authigenic clays retain ^{10}B rather than releasing it to the pore fluid. Based on recent experimental work to determine the B-isotope fractionation between illite and water (Williams et al., 1999) it is expected that pore waters in equilibrium with -18‰ I/S will be isotopically light at these reservoir temperatures (<10‰). If there were large-scale exchange of fluids between mudstones and sandstones, one would expect the authigenic pore-filling clays in the sandstone to have a more negative $\delta^{11}B$, similar to the mudstones. Since this is not the case, it suggests that the reservoir waters were either diagenetically altered or migrated into the sandstone. It is also possible that the sandstone clay minerals formed at an earlier time (lower temperature) in equilibrium with fluids that previously passed through the unit. Regardless of the timing, it is clear that authigenic clay minerals in the sandstone reflect equilibrium with a different fluid than the fluid that originally filled the pore space. The mudstones on the other hand are probably in equilibrium with pore fluids that have not migrated far, and may represent original pore fluids that have been diagenetically altered.

2.6.1c. Oil /Water Fractionation

The variation in $\delta^{11}B$ of oil samples reflects the trend of lighter values with depth shown by the waters, but the B-content of the oils are so low that their effect on $\delta^{11}B$ of coexisting water is unlikely to be significant. It would be more reasonable to attribute these trends to incorporation of some B from the water into the oil.

2.6.1d. Gas Phase Separation

The water $\delta^{11}B$ changes observed across the field (Fig 2.5) may be complicated by the fact that the gas reservoirs within the field are found where the highest $\delta^{11}B$ values are found. It is possible that ^{11}B is fractionated preferentially into a gas phase (Palmer and Sturchio, 1990). Leeman et al. (1992) found a fractionation of only ~3‰ between water and vapor at 150°C; however, that work focused primarily on $B(OH)_3$ species alone. No information is available on possible fractionation of B between water and gaseous organic compounds. If ^{11}B is preferentially associated with a gas phase, and the gas accumulates in the uppermost regions of the hydrocarbon reservoirs, then there may be some ^{11}B enrichment of fluids in contact with those gases. The variations in $\delta^{11}B$ and B-content of the waters may be correlated with the gas/oil ratios in each reservoir.

2.6.1e. Isotope Exchange

The mechanism of B-isotope exchange between clay minerals and water is important to the interpretation of field data. During oxygen isotope exchange, a Si-O bond is broken to allow redistribution of O-isotopes. In order to increase the fixed-B content of illite, four oxygen bonds must be broken to release Si and substitute B. This would require substantial recrystallization and therefore B-isotope equilibration may be more difficult to achieve than O-isotope equilibration. If there is a solid-state redistribution of B from adsorbed-sites to fixed-sites of a *detrital* clay mineral, it is likely that a portion of the fixed-B is inherited from the original crystal. However, in the Gulf Coast, the B-content of the authigenic portion of mixed-layered illite/smectite increases by more than 100 ppm with depth (Perry, 1972). These sediments originated partly as volcanic ash (Bloch et al., 1998)

which gradually recrystallized to smectite and illite during burial (Perry and Hower, 1972). Another mechanism for formation of authigenic illite is through dissolution/precipitation. If detrital smectite dissolves and precipitates as more stable illite during burial, the authigenic mineral may not retain the $\delta^{11}B$ inherited from the original detritus. Instead, the B incorporated into the structure will reflect the chemistry of the diagenetic fluid present during recrystallization. This fluid has been modified by siliciclastic reactions occurring at that depth, and could be substantially influenced by organic reactions taking place concurrently, especially in hydrocarbon-rich environments.

2.6.1f. Fluid Migration

The range of values for B-content and $\delta^{11}B$ of formation waters in the Fordoche reservoirs is consistent with the range of values reported for Cenozoic reservoirs throughout the Gulf Coast (Fig. 2.1). There is a minor increase in B-content and $\delta^{11}B$ in the uppermost reservoir over the lower Wilcox reservoirs that may reflect variability in the original porewaters, or may reflect differences related to diagenesis. The Wilcox reservoirs are overpressured and less saline than the uppermost reservoir (Sparta), suggesting addition of water from the dehydration of smectite (Bruce, 1984). This dilution effect could result in the lower B content of these waters. According to experimental studies of B-adsorption (You et al., 1996) the K_d between adsorbed-B and water approaches 0 at 100-120°C. The temperatures of the reservoirs are 90-126°C (Williams et al., 1995) therefore adsorption processes plays a minor role in the variations in B-content of the water. Nonetheless, as recrystallization of smectite is occurring at temperatures >100 °C, ^{10}B is preferentially substituted in the silica tetrahedron, therefore waters migrating through the

rock should become gradually ^{10}B depleted with migration distance.

2.6.2. Regional Boron

The regional trends for boron in waters from the Gulf Coast sedimentary basin (Macpherson and Land, 1989; Land and Macpherson, 1992; Moldovanyi et al., 1994) show an increase in B-content and decrease in $\delta^{11}B$ with depth basin wide (Fig. 2.1). At depths equivalent to Fordoche Field, B-contents are as high as 300 ppm, and $\delta^{11}B$ values as low as 12‰, but a majority of the water analyses have $\delta^{11}B$ values between 18-30‰. The B-content of Fordoche Field is slightly low in comparison to regional waters, but this could be explained by dilution of Fordoche brines due to overpressuring in the region (Boles and Franks, 1979; Williams et al., 1995). The present investigation of brines and oils from the Fordoche Field does not reveal a mechanism for generating the regional B-trends (Fig. 2.1). An additional source of ^{10}B must be responsible for the high B-contents and low $\delta^{11}B$ values in the deep Gulf Coast basin. In the discussion below, the dissolution of other boron minerals, or degradation of organic matter at higher thermal grades is considered.

2.6.2a. Other Boron Minerals

Depending on the scale of fluid flow within the Gulf Coast sedimentary basin, the potential exists for B-rich minerals such as tourmaline or evaporite borate phases to contribute significant B to waters and modify the $\delta^{11}B$, particularly in reservoir sandstones. Detrital tourmaline grains have been found, for example, in the Wilcox Fm. However, tourmaline is extremely chemically and mechanically stable in clastic sedimentary environments (Henry and Dutrow, 1996). Boracite has been recovered from Jurassic

bittern salts beneath Eocene sediments (Macpherson and Land, 1989), but this sample (and other marine evaporites; Palmer and Swihart, 1996) have high $\delta^{11}B$ values, so that their effect on waters would not generate the observed regional decrease in $\delta^{11}B$.

2.6.2b. Organic Matter Boron

The general enrichment of ^{10}B in waters from deep clastic reservoirs of the Gulf Coast must be examined in light of the new isotopic data on B in kerogen. It is acknowledged that there is insufficient kerogen in the basin to provide all of the B in the clay minerals, and assumed that adsorbed and dissolved-B from breakdown of detrital clays provided most of the B incorporated into authigenic illite (Perry, 1972). However, illitization stops at ~5 km in the Gulf Coast (Perry and Hower, 1972), approaching depths equated with the later stages of organic maturation (Fig. 2.6). At this depth, clay minerals will no longer be a sink for boron. Their fixed-B is unlikely to be released until metamorphic recrystallization occurs (>350°C). Therefore clays should not play a significant role in the B mass balance as temperatures approach 150°C. The reactivity of organic matter becomes important at that stage however, as organic molecules release heteroatoms (i.e. boron) during late maturation of kerogen (Durand, 1985).

The source rock sample from the Wilcox Fm contained 5g kerogen out of a 50g sample of mudstone at ~4.3 km indicating a very high kerogen content (10%), which is not representative of the entire basin (2%). Nonetheless, the fact that the $\delta^{11}B$ of the kerogen is $-2\pm2‰$ (Table 2.3) indicates that B released from kerogen could still be a source of ^{10}B. The burial temperature of the extracted kerogen was ~125°C (vitrinite reflectance ~1.5 (Sassen, 1990)) indicating organic maturity in the wet gas zone (Fig. 2.6). At this

temperature, there is still a significant amount of B held in the kerogen (140 ppm). However, studies of B in graphite from metasedimentary rocks (slate) have indicated B-contents averaging <20 ppm (Douthitt, 1985). Therefore, at some temperature between 130°C and low grade metamorphism (~350°C), B will be released from kerogen. It is inferred that B is released from organic matter during the generation of dry gas (vitrinite reflectance >2.0).

Based on the $\delta^{11}B$ for B in kerogen, the amount of B potentially released during late thermal maturation can be estimated, and its influence on the isotopic composition of the water can be determined. In the Wilcox Fm the amount of shale is ~70% and sandstone comprises ~30%. A conservative estimate of the amount of kerogen in the source region of the Wilcox Fm is 2% (Tissot and Welte, 1984). Porosity is estimated at 20% in the sandstones and 10% for mudstones (including fracture porosity). Assuming the pores are 70% filled with water (the rest being oil and gas), then an isotopic mass balance for B can be calculated. Figure 2.7 shows the isotope changes expected if the water $\delta^{11}B$ was initially 28‰ (observed in Fordoche reservoir W-12), and all of the B from kerogen was released (with no isotopic fractionation). Calculations were made for a range of kerogen $\delta^{11}B$ values from +10 to -10‰, to show that even large variations in the kerogen $\delta^{11}B$ could achieve the range of $\delta^{11}B$ observed in the deep basin waters. Obviously, there could be isotopic fractionation during the release of B, especially if there is a gas phase involved. But the validity of this calculation is justified by the fact that negligible amounts of B are found in the oil and essentially all of the B is lost from kerogen during late maturation. This leaves the water as the primary host for released-B.

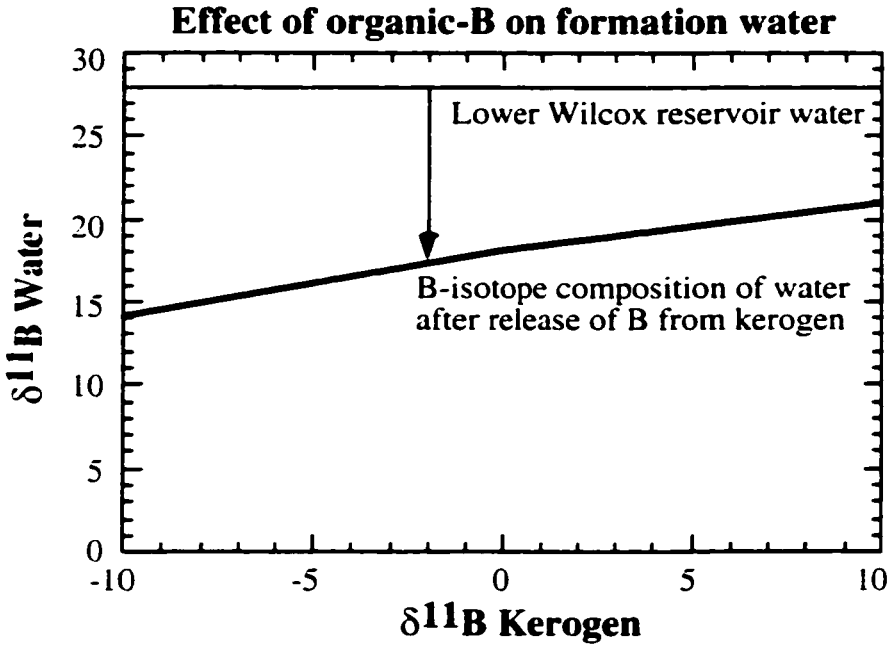

Figure 2.7 Plot showing results of isotope mass balance calculations between kerogen and water in the deep Gulf Coast sedimentary basin. If kerogen with a -2‰ $\delta^{11}B$ releases all of its B (>100 ppm), a 28‰ water from the lower Wilcox Fm would decrease in $\delta^{11}B$ to ~17‰, assuming no fractionation.

The typical Gulf Coast oilfield water could have a $\delta^{11}B$ reduced to ~17‰ by release of B from a -2‰ kerogen. This value approximates the low $\delta^{11}B$ waters in the Gulf Coast basin found at temperatures between 160-175°C (Land and Macpherson, 1992). The amount of B in kerogen could account for the increase in B-content and decrease in $\delta^{11}B$ of waters deep in the Gulf Coast basin. The mobility of B released from kerogen will depend on its interactions with minerals along the migration path. However, the importance of organic-B cannot be ignored in efforts to understand the B-geochemistry of sedimentary basins. Results from this research suggest that B is released during late stages of organic maturation with a distinctly negative $\delta^{11}B$ that could provide a means for tracing hydrocarbon migration paths.

2.7. CONCLUSION

The boron content and isotopic composition of oil field brines increases with increasing distance of fluid migration both upwards and laterally across Fordoche field. The isotopic composition of the oil varies similarly, however the amount of B in the oil is insignificant. One possibility for the high $\delta^{11}B$ of oil field waters is the preferential incorporation of ^{10}B into the tetrahedral layers of authigenic illite, leaving the water ^{11}B-enriched. The very low $\delta^{11}B$ of fixed-B in mudstone (-18‰) relative to sandstones (-2‰) at the same depth indicate that ^{10}B is retained in the mudstone clay minerals and is not released into the reservoir waters. The reservoir waters most likely contain fluids that migrated with the hydrocarbons. Illitization ceases at ~5 km of burial and therefore B ceases to exchange between clay minerals and pore waters.

This study has demonstrated that kerogen in the Gulf Coast basin contains a significant amount of organically-bound B (140 ppm), with a negative $\delta^{11}B$. After illitization has ceased (~150° C), B released from kerogen becomes a potential source of ^{10}B that could cause the low $\delta^{11}B$ in deep sedimentary brines. It was deduced that >100 ppm B can be released from organic matter during dry gas generation (vitrinite reflectance ~2.0). Although kerogen makes up only a small percentage of the sedimentary basin, its significance as a source of boron in deep sedimentary basins cannot be ignored when considering its reactivity compared to clay minerals.

CHAPTER THREE:

EXPERIMENTAL DETERMINATION OF BORON ISOTOPE FRACTIONATION DURING REACTION OF SMECTITE TO ILLITE: APPLICATION TO THE GULF OF MEXICO SEDIMENTARY BASIN

3.1 ABSTRACT

Experiments were performed to measure the isotopic fractionation of boron between illite/smectite (I/S) clay minerals and water as a function of temperature (300° and 350 °C) and degree of illitization. Corresponding changes in the oxygen isotopes were monitored as an indication of the approach to equilibrium. The kinetics of the B-isotope exchange follows the mineralogical restructuring of smectite as it recrystallizes to illite. An initial decline in $\delta^{11}B_{I/S}$ occurs when the I/S is randomly ordered (RO). The $\delta^{11}B_{I/S}$ values reach a plateau during R1 ordering of the I/S representing a metastable condition. The greatest change in $\delta^{11}B_{I/S}$ is observed during long-range (R3) ordering of the I/S when neoformation occurs.

Values of $\delta^{11}B_{I/S}$ measured on the equilibrium reaction products were used to construct a B-isotope fractionation curve. There is a linear correlation among data from these experiments, adsorption experiments at 25°C (Palmer et al., 1987), and 1100°C basaltic melt-fluid fractionation experiments (Hervig and Moore, 2000). Unlike other stable isotopic systems (e.g., oxygen) there is no mineral-specific fractionation of B-isotopes, but rather a coordination dependence of the fractionation. Under diagenetic conditions B is predominantly in trigonal coordination in fluids, but substitutes in tetrahedral sites of silicates. The preference of ^{10}B for tetrahedral bonds is the major fractionating factor of B in silicates.

Combining knowledge of the B-isotope fractionation with O-isotope fractionation the isotopic systems can be applied in tandem to sediments undergoing burial in the Gulf of Mexico sedimentary basin. The results show that illite and muscovite record

conditions of precipitation (temperature, fluid composition) throughout temperatures of burial diagenesis. The neoformation of illite at depths common to hydrocarbon generation make it a potential tracer of fluids related to organic maturation.

3.2. INTRODUCTION

Clay minerals are abundant and highly reactive minerals in clastic sedimentary basins. They adsorb boron on surface sites at low temperatures (<120°C: You et al., 1996) and substitute boron for tetrahedral silicon during diagenesis (Spivack et al., 1987). Boron is most abundant in the sedimentary clay minerals illite/smectite (I/S) (Harder, 1970) which contain orders of magnitude more boron than other common diagenetic minerals (e.g., quartz, carbonates, feldspar). Boron is a highly mobile element, preferring aqueous phases to that of most minerals (Levinson, 1980). Thus, by understanding how the aqueous boron is incorporated into typical clay minerals, important insights may be gained to the fluid and chemical dynamics of a sedimentary basin. To use this geochemical tool, one must be able to interpret the boron isotopic composition of paleofluids that were present in a basin at the time of clay mineral diagenesis. Late-stage or deep diagenesis of clay minerals (Eberl, 1993) coincides with the time/temperatures associated with organic maturation processes that lead to the expulsion and accumulation of hydrocarbons. The presence of anomalously high B-contents of many oil field brines (Collins, 1975) leads us to investigate whether there is an expulsion of organically bound-B that can be used to trace hydrocarbon migration paths. Thus the potential for the common authigenic clay mineral illite to incorporate boron and record isotopic ratios acquired during crystallization was examined. Lacking definitive information on the

fractionation between aqueous-B and B- substituted for Si in tetrahedral sites of illite. this research began with the simple goal of measuring the isotopic changes in boron during illitization of smectite.

The experiments address two fundamental questions. First, how is boron incorporated into tetrahedral sites of authigenic illite? Is it a gradual increase with burial, like the increase in illite layers in I/S, or does it occur in stages associated with the restructuring (ordering) of the I/S? Second, what is the equilibrium fractionation of $^{11}B/^{10}B$ between the tetrahedral layers of the silicate and the fluids as a function of temperature? It is important to distinguish between adsorbed-B on the surfaces of the clay, and 'fixed-B' that substitutes for Si. The adsorption of B on clay surfaces has been extensively studied (Schwarcz et al., 1969; Keren and Mezumen, 1981; Palmer et al., 1987), but since it can be easily exchanged (Bassett, 1976), it is not useful in determining paleofluid chemistries. However, fixed-B exchanges with pore fluid-B only when Si-O bonds are broken, therefore Si release is expected during this exchange. This may provide an important diagenetic marker if a significant change in $\delta^{11}B$ can be linked to the release of Si, which can potentially form quartz cements (Hower et al., 1976).

Oxygen isotope changes during the illitization of smectite should also be linked to the fixed-B isotope exchange. Concurrent changes in $\delta^{11}B$ and $\delta^{18}O$ of I/S were examined in the experiments performed. The reaction of smectite to illite was conducted at 300°C and 350°C therefore the kinetics will be fast compared to a basin undergoing burial. However, after 4-5 months the oxygen isotope fractionation between the I/S and water approximated that predicted for the experiment temperatures (Savin and Lee,

1988), indicating nearly 100% oxygen isotopic re-equilibration (Whitney and Northrup, 1988). It is assumed that the results of these experiments also establish isotopic equilibrium for boron, since B cannot exchange without a change in $\delta^{18}O$.

3.3. EXPERIMENTAL SETUP

Smectite was reacted to illite following the experimental method used by Whitney and Northrup (1988) for measuring the O-isotope changes coincident with illitization. The starting material was a smectite standard (SWy-1), which was size fractionated to select the <2 μm size-fraction, and K-saturated (Moore and Reynolds, 1989). Trace amounts of quartz and muscovite were included in this size fraction, which along with the added K promote the reaction of smectite to illite (Whitney and Northrup, 1988) at 300° and 350 °C, 100 MPa (1 kbar) pressure. A 1:1 ratio of mineral to water (by weight) was used (200 mg solid: 200 μl liquid). The aqueous solution contained the boron isotope standard NBS SRM 951 boric acid at an initial pH of 6.8. The samples were sealed in 5 cm long, 5 mm O.D. Au capsules. The capsules were placed in a hydrothermal bomb closed with a Bridgeman seal, using deionized water as the pressurizing medium (Fig. 3.1). Temperature was measured using an inconel-sheathed chromel/alumel thermocouple inside the pressure vessel, placed in the center of the long axis of the capsules. This allowed minimal uncertainties in temperature estimated at <5 °C. Pressure was measured using Bourdon-tube gauges and was monitored within ±5 MPa. The siliciclastic reaction buffers the pH (Hutcheon et al., 1993) during the experiment to low values (pH~6 after quench) thus the predominant aqueous boron species is trigonal $B(OH)_3$. This is also true

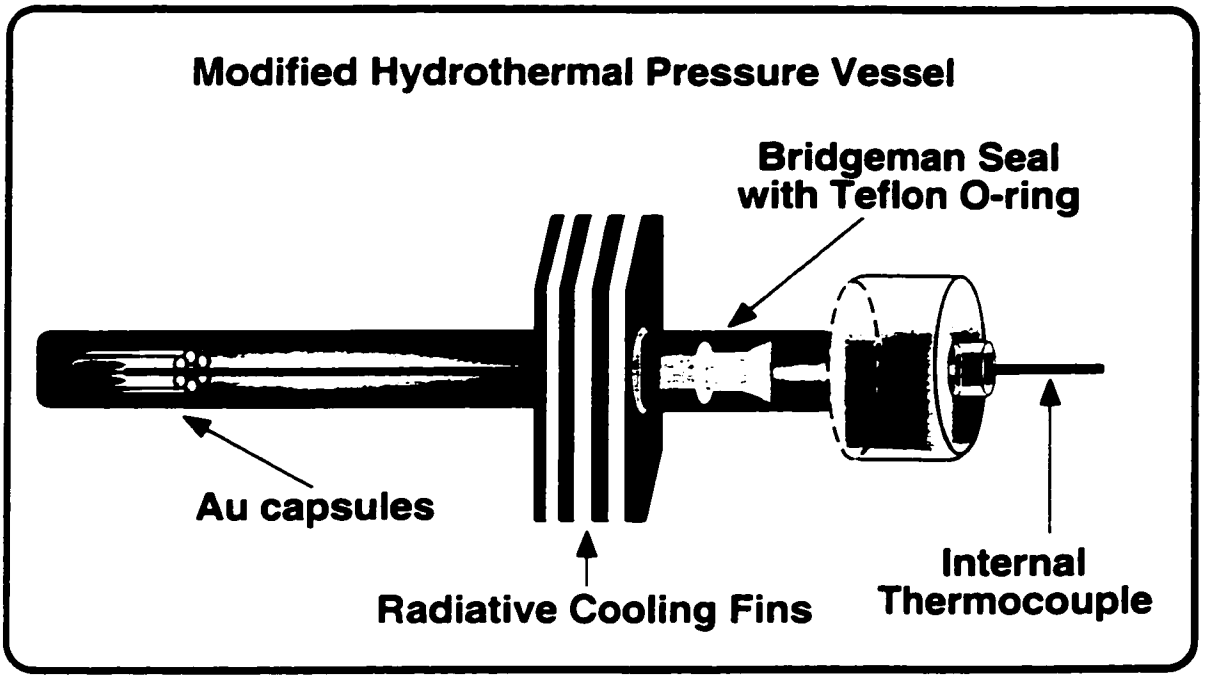

Figure 3.1. Schematic diagram of the hydrothermal reaction vessel. Starting materials used were smectite (SWy-1), <2 μm fraction, K-saturated, and NBS SRM 951 boric acid (aq). Experiments were run at 350° and 300° C, 100 MPa (1 kbar) pressure. Reactants included K-saturated smectite with traces of detrital minerals (quartz, mica) and the products included illite, quartz and chlorite.

for most oil field waters in deep sedimentary basins, although there is the possibility of formation of some polynuclear B-species when B concentrations are high (Bassett, 1976).

Three experiments were done in order to test the effect of B-concentration and temperature on B-substitution in illite. Experiment 1, run at 350°C, used a low aqueous B-concentration (20 ppm). These conditions limited the amount of B available for fixation in the mineral to two times the original B-content. This was intended to simulate conditions observed the Gulf of Mexico sedimentary basin where B-contents of I/S essentially doubles during progressive illitization (Perry, 1972). Experiments 2 and 3 used high concentrations of aqueous-B (1000 ppm) so that the B supply would not be limited. These two experiments differed only in temperature (and run time), with Experiment 2 at 350°C and Experiment 3 at 300°C.

3.4. METHODS

3.4.1. Sample Extraction and Preparation

The experiments at 350 °C (Exp.1 and 2) ran for 120 days, with samples collected at intervals in order to monitor the reaction progress. The 300°C experiment (Exp. 3) ran an extra month in an attempt to reach equilibrium conditions. Duplicate capsules were run in the first experiment in order to determine the reproducibility of results. The experiment was quenched on sampling days and the capsules were opened under vacuum on an extraction line. The aqueous contents were collected in a U-tube cold trap. Only samples that yielded 100% recovery (≥200 µl fluid) were analyzed for O-isotope ratios. Conventional analyses of O-isotopes (by Mountain Mass Spectrometry Inc.) required ~150 µl of solution.

The solid reaction product and Au-capsule were rinsed in 'B-free' water to remove adsorbed-B. The 'B-free' water is deionized water that has been filtered through a column of amberlite resin to remove traces of B. ICP analyses of this water show no detectable levels of B with a detection limit of 4 ppb. The solid was additionally washed for two hours in mannitol solution (Ishikawa and Nakamura, 1990; Xiao et al., 1997) to enhance removal of the adsorbed-B. The mannitol solution also contained no detectable levels of B. The samples were then rinsed three times in B-free water. The solution was kept for ICP analysis of the B-content. The solid sample was then split into two aliquots. About 100 mg was mounted as oriented clay slides for X-ray Diffraction (XRD). A small drop of clay slurry was dried onto a B-free glass slide. The clay standard (IMt-1 illite) was added to each clay mount so that sample changes were not required between analyses of sample and standard. The air-dried clay mounts were Au-coated for analysis by secondary ion mass spectrometry (SIMS).

3.4.2. X-Ray Diffraction

The solid experimental run products were ethylene-glycolated and examined by XRD in order to monitor the decrease in expandability of the mixed-layered I/S as illitization occurred. The characterization of mixed-layered clay minerals is described in Moore and Reynolds (1989). The analyses were performed using Siemens D500 and D5000 spectrophotometers with CuKα radiation. The D5000 instrument was set up with a position sensitive detector (PSD) for more rapid analysis of small quantities of material. Comparison of the results from each diffractometer indicates that the peaks are positioned correctly, but the relative intensities using PSD may be unreliable on oriented mounts

(Batchelder and Cressey, 1998). Since the goal was to monitor shifts in the major peak positions for the I/S, the intensity did not affect the interpretation. The percent illite in ethylene-glycolated I/S was estimated using the $\Delta 2\theta$ between the 001/002 and 002/003 peaks of I/S (Moore and Reynolds, 1989, p.251). Nearest neighbor (R1) ordering (ISIS) is indicated by a strong reflection at ~6.5° 2θ while a reflection near 5° 2θ indicates random (R0) interstratification. When this peak shifts to >7° 2θ a long-range (R3) ordering (ISII) is indicated.

3.4.3. Secondary Ion Mass Spectrometry

Secondary ion mass spectrometer (SIMS) measurements of B-isotopes do not yield the high precision results of thermal ionization mass spectrometry (TIMS; Swihart, 1996) but the analyses can be done directly on the solid products without digestion and the possibility of inducing isotope fractionation during ion exchange. The SIMS analyses (Cameca Ims 3f) used a primary beam of O^- defocused to approximately 50 μm in diameter. By defocusing the beam the sample was sputtered more uniformly with time yielding a more stable secondary ion current. The depth of the analytical crater after 30 minutes of ion bombardment was <5 microns. The general method for analysis of B-isotope ratios in silicates by SIMS can be found in Hervig, (1996) and Chaussidon et al.(1997). Modifications to allow analyses of B-isotopes in clay minerals are described below.

3.4.3a. Boron Isotope Analysis of Clay Minerals

Boron isotope ratios are reported as:

$$\delta^{11}B = [\{(^{11}B/^{10}B_{sample})/(^{11}B/^{10}B_{standard})-1\} * 1000] - IMF$$

where the standard is NBS SRM 951, boric acid, with a $^{11}B/^{10}B$ ratio of 4.0437. The IMF is instrumental mass fractionation determined by measuring a mineral standard on which the $\delta^{11}B$ is known. B-isotope analyses were calibrated by measuring a clay mineral standard IMt-1 (Silver Hill Illite) that had been characterized by bulk thermal ionization mass spectrometry (TIMS). The illite (IMt-1) was rinsed three times in B-free water, and centrifuged to select the <2μm fraction. Aliquots of this standard were analyzed by the method of Tonarini et al. (1997) using alkali carbonate fusion and ion-exchange separation for boron purification, and PTIMS using $Cs_2BO_2^+$ (Analyses done at Rice University by W.P. Leeman). Three replicate analyses averaged –8.66 ± 0.23 ‰. Another aliquot was analyzed by NTIMS (Analyses done at University of Calgary) with 2 replicates averaging –9.86 ± 0.65 ‰. An average $\delta^{11}B$ value of -9‰ was used for the IMt-1 illite. During each SIMS analytical session, the $^{11}B/^{10}B$ ratio was measured on IMt-1 before and after sample analyses. The difference between the measured ratio and the TIMS value determines the instrumental mass fractionation (IMF) factor. During our clay analysis sessions over three years, the IMF has varied between -44 and -51‰ (i.e., the raw $^{11}B/^{10}B$ ratio is ~5% lighter than the TIMS value), depending on the instrumental set up. The IMF remains constant (within error) during each analytical session, allowing the correction for $\delta^{11}B$ relative to NBS SRM 951. As noted by Chaussidon et al. (1997) there is not a significant matrix effect on B-isotope analyses, therefore it is assumed that the IMF for smectite and illite are not significantly different.

The primary current used for analyses was determined by the intensity of the $^{10}B^+$ secondary ion signal. In order to achieve a precision of <2‰, the primary current was

increased until there was stable emission of ~500 counts per second (cps) on $^{10}B^{+}$. Generally, this required 3-5 nA of primary current. The analyses were set up to count for 20 s on mass 10 and 5 s on mass 11 for 49 cycles. In order to eliminate $^{10}BH^{+}$ interference with $^{11}B^{+}$ counts, the entrance slits were closed down until the two peaks could be separated (Fig. 3.2). The magnetic field was adjusted to collect counts from the center of the $^{11}B^{+}$ peak, and this was checked every 10 cycles to correct for drift. These conditions resulted in combined $^{10}B^{+} + {}^{11}B^{+}$ signals of $\geq 5 \times 10^{5}$ integrated counts, indicating an error based on counting statistics of <2‰. The actual errors determined by the standard error of 49 measurements of $^{11}B/^{10}B$ in each analysis are equal to, or greater than, the predicted errors. Analyses that produced errors greater than two times the predicted error were eliminated. This condition usually indicates a problem such as charging, low counts due to sample aberrations (e.g., not flat), or that the primary ion beam has drifted out of alignment.

An analysis of B-isotope ratios in clay minerals by SIMS is burdened by two major problems. First, B occurs in two sites of clay minerals, surface-adsorbed and tetrahedral-layer sites, and the isotopic ratios of the B in each site is different (Spivack et al., 1987; Palmer et al., 1987). Second, the clay size fraction is by definition <2μm in diameter, and often the authigenic crystals are even smaller (<0.2μm), so a SIMS analysis samples numerous crystallites during a single analysis. In essence then, these are small volume bulk analyses that consume <3 ng of material (~10^{8} atoms). Since the proportion of adsorbed-B and fixed-B in any particular clay mineral cluster may be variable, it is impossible to know how much B in a SIMS analysis of bulk clay is fixed or adsorbed.

Furthermore, aqueous-B may not be effectively removed from the capsule during fluid extraction on the vacuum line. Xiao et al. (1997) showed that a significant portion of B stays in solution during evaporation, therefore it might precipitate on the surfaces of the clay (and capsule) during the vacuum extraction. This would confuse the results of B-analyses on the bulk clay. Since the 'fixed-B' substituted for Si in tetrahedral sites is of primary interest, the adsorbed-B was removed with mannitol, as described earlier, and analyses of the remaining B represents the fixed-B.

The measurement of fixed-B content in the product was determined by SIMS using a calibration curve based on the counts of B (mass 11) relative to Si (mass 30). The calibration curve (Fig. 3.3) was measured on borosilicate glasses with known B-content, using the same high mass resolution conditions used for the B-isotope analyses. Boron analyses of the clay standard IMt-1 (illite) were compared to measurements made by ICP-AES on an aliquot digested in HF-HCL. The ICP value for the B-content of IMt-1 was 240 ppm. Individual point analyses of B by SIMS, using the calibration curve, agreed within 5%.

3.4.3b. Oxygen Isotope Analysis of Clay Minerals

SIMS was also used to analyze O-isotope ratios of the solid run products. The analytical setup is significantly different and more complex than analyses for B-isotopes, due to the need for sample charge compensation. A primary beam of Cs^+ is used instead of O^-. Use of a positive primary beam adds significant charge buildup to a silicate sample (insulator) that results in unstable secondary ion signals unless it is neutralized by use of

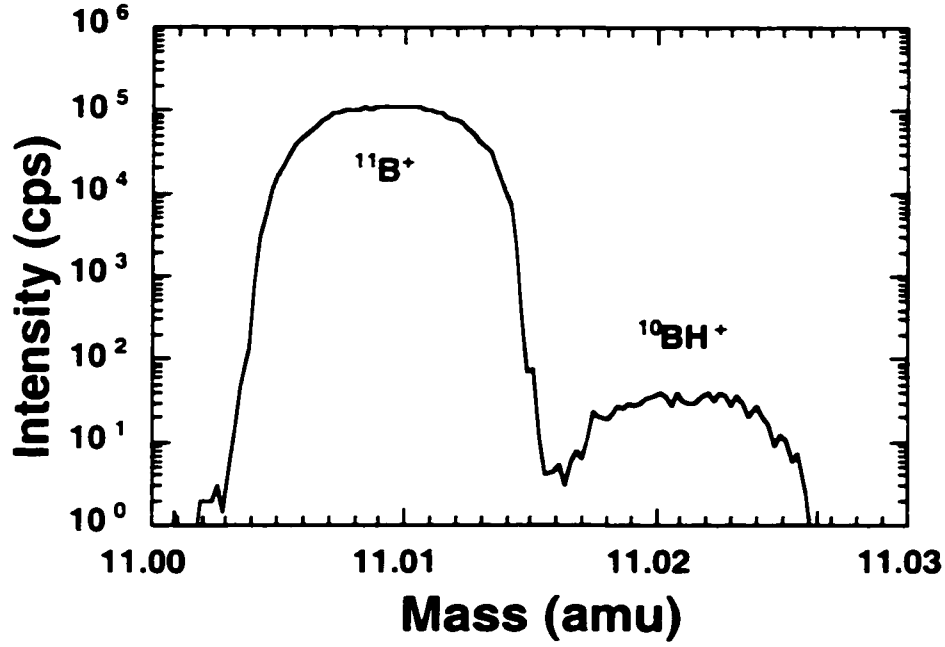

Figure 3.2. Example of the separation of $^{11}B^+$ from the molecular hydride $^{10}BH^+$ by high mass resolution. By closing down the entrance slits to the secondary ion mass spectrometer it is possible to resolve the two species.

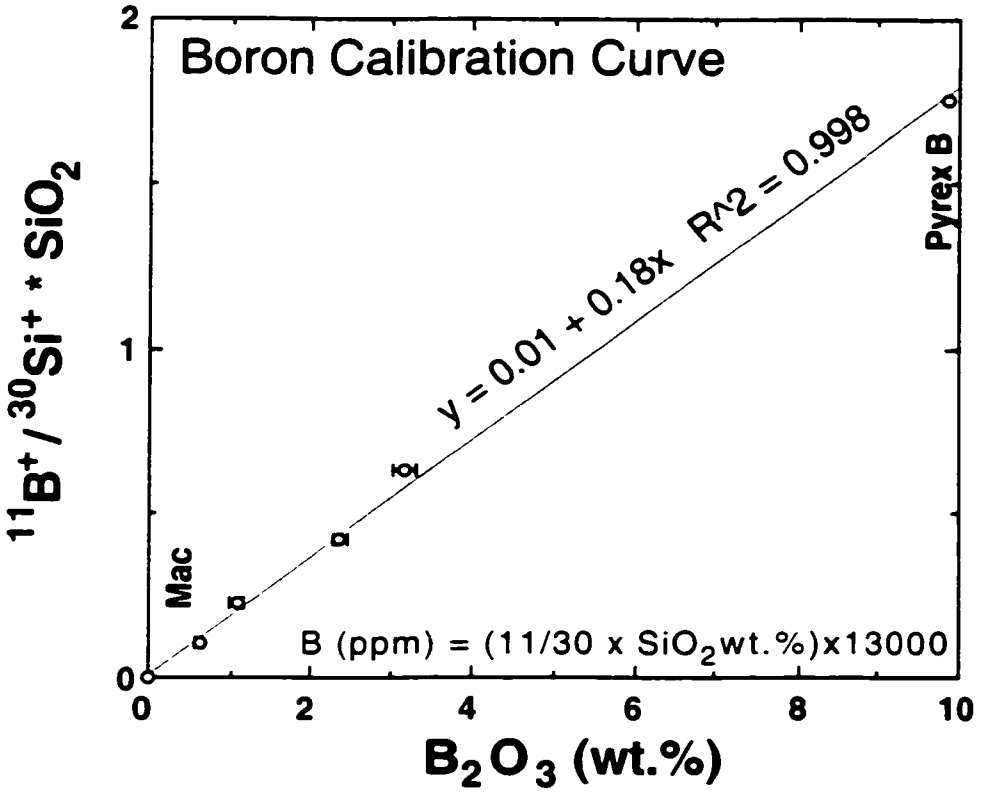

Figure 3.3. Calibration curve for estimation of B-content of silicates by secondary ion mass spectrometry if the silica content is known. Minerals and glasses of known B-content were used to construct the curve (see Hervig, 1996).

an electron gun. A normal incidence electron gun was used to compensate the charge during oxygen isotope analysis of the clays.

Extreme energy filtering was used to eliminate molecular interferences (Hervig et al., 1992). Several tests were made to determine how to calibrate different clay minerals. First, standards of kaolinite (KGa-1), smectite (SWy-1) and illite (IMt-1) were analyzed by conventional O-isotope methods (Analyses performed at University of Western Ontario by Fred Longstaffe) so that they could be used as SIMS standards. The instrumental mass fractionations (in the SIMS) for the illite and smectite standards were not significantly different, perhaps due to their common 2-layer structure. Raw oxygen isotope ratios on these two phases by SIMS were 65‰ lighter than nominal values (IMF = –65‰). This calibration varied little over multiple analytical sessions. The 1-layer kaolinite standard produces less instrumental fractionation with a reproducible average of –53‰ (Fig. 3.4).

To test the effect of oxygen from adsorbed interlayer water on the overall O-isotope composition of smectite, an aliquot of Swy-1 was soaked in ^{18}O-enriched water (Fig. 3.5) and then analyzed. The test showed that the effect of adsorbed water on the overall O-isotope ratio is small. The isotopic composition should be affected by no more than ~0.025‰, which is far less than the analytical precision of the SIMS measurements. There is still some question about the effect of mineral orientation on the secondary ion sputtering rate and IMF (e.g., Eiler et al., 1997). Sputtering rates were measured on a large muscovite crystal oriented to sputter on the c-axis (flat surface) or down the a-c plane (between the layers). Figure 3.6 shows a difference in sputtering rates depending on

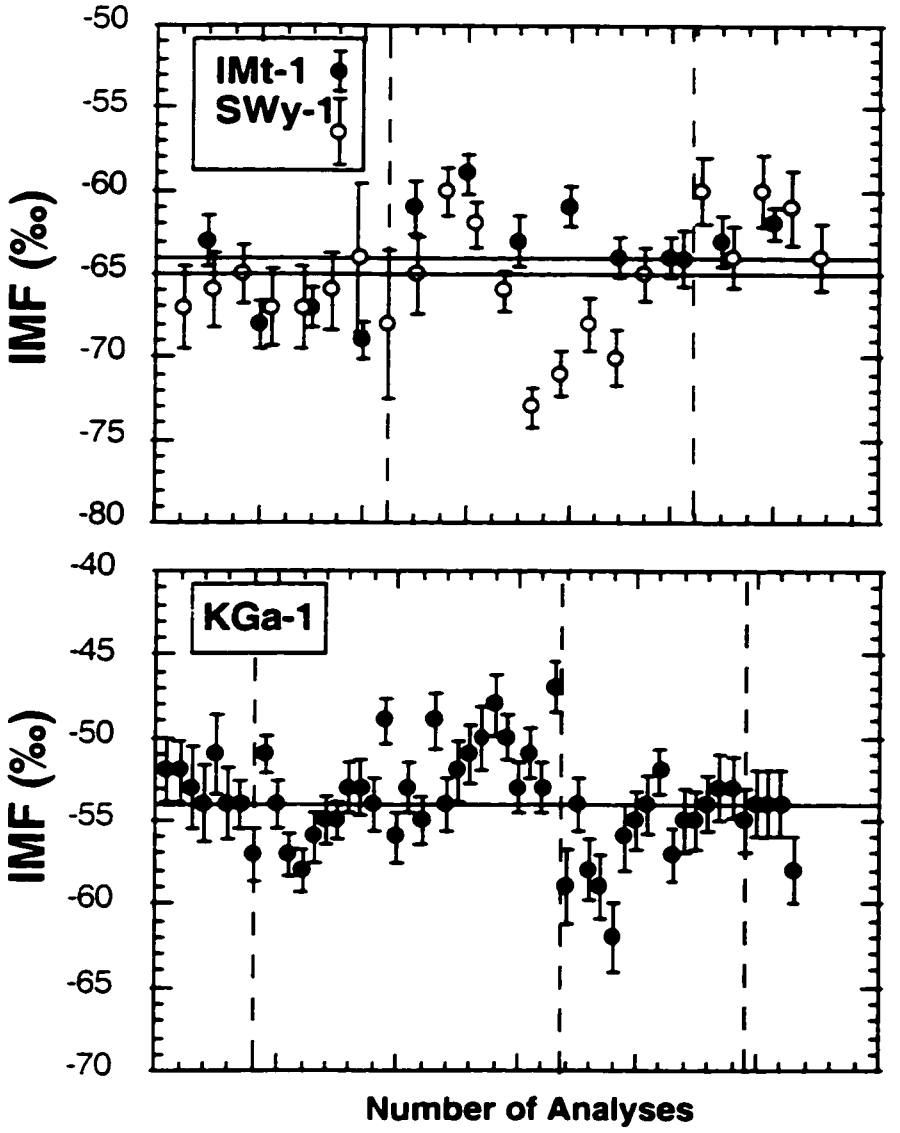

Figure 3.4. Variation in instrumental mass fractionation (IMF) of O-isotopes in clay mineral standards illite (IMt-1), smectite (SWy-1) and kaolinite (KGa-1). Dashed lines demark different analytical sessions over three years time. The clay standard is checked before and after each sample and results are adjusted for instrumental drift.

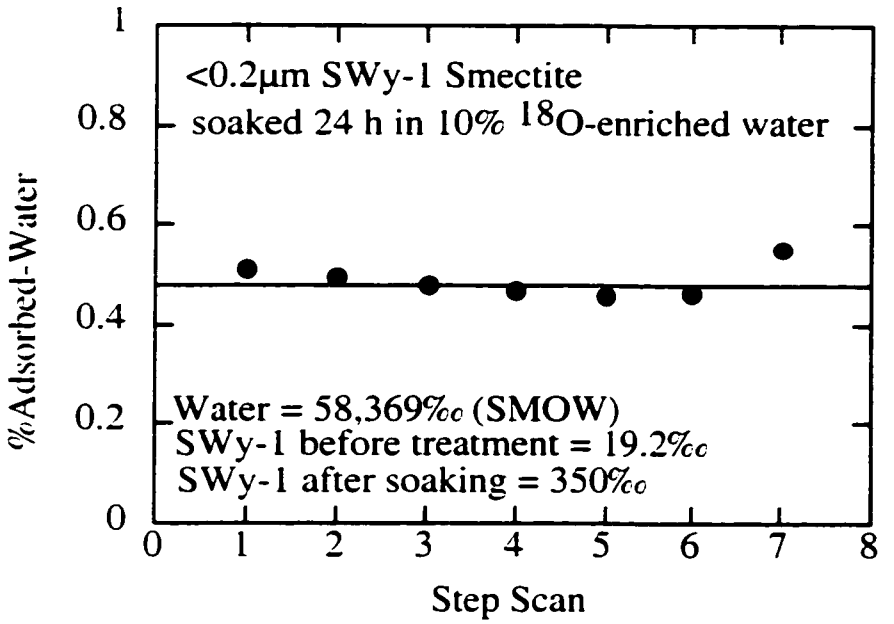

Figure 3.5. Results of the test for how much interlayer and adsorbed water influences the O-isotope ratio measured by secondary ion mass spectrometry. The amount of adsorbed water can be calculated:

$\%H_2O_{ads}$ = [(Spiked SWy-1(‰) - SWy-1(‰)) / Water ‰] * 100

These data show that for typical basinal fluids the effect would be on the order of 0.025‰ of the smectite $\delta^{18}O$.

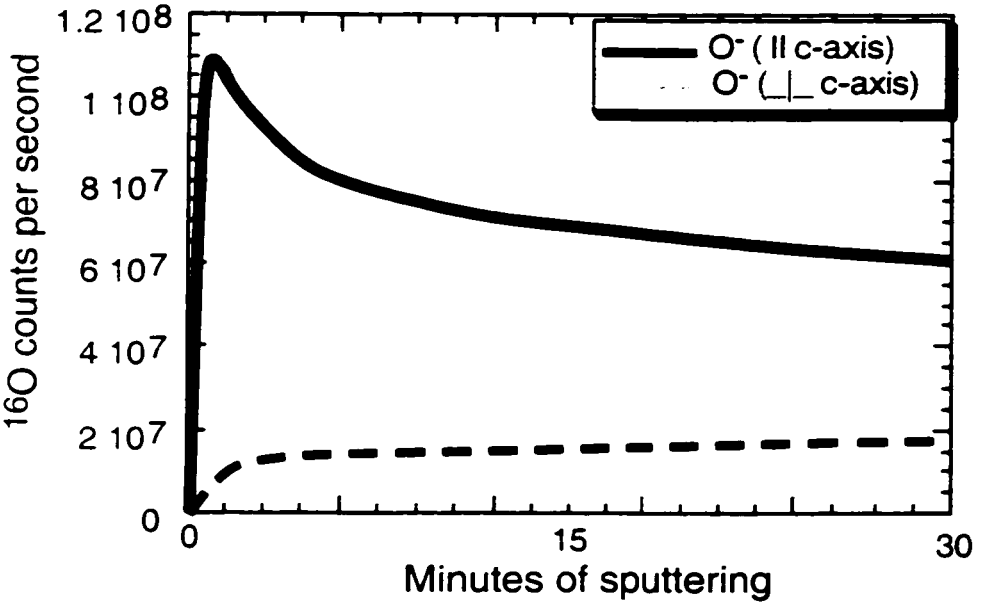

Figure 3.6. Test results for the effect of clay mineral orientation on the sputtering rate of secondary ions. The sample was a large crystal of muscovite mounted with the c-axis normal and perpendicular to the analyzed surface.

mineral orientation. Nonetheless, on the <2μm scale, analyses encompass many differently oriented clay crystallites so there is an averaging of this effect. For example, analyses of pore-filling kaolinite books in a thin section from North Sea reservoirs show O-isotope variations <4‰ (Fig. 3.7), which could reflect actual changes in the water chemistry as pore fluids evolved (Williams et al., 1997a; Williams and Hervig, 1997). Clay mineral standards mounted separately with each sample analyzed have shown consistent results over three years.

3.4.4. Thermal Ionization Mass Spectrometry

A thermal ionization mass spectrometer was used to detect negative ions for B-isotope ratio analysis. Negative thermal ionization mass spectrometry (NTIMS) is a common technique for analysis of solutions with very small amounts of B (Heumann and Zeininger, 1985; Vengosh et al., 1989; Klötzli, 1992) because the ionization efficiency for negative ions is greater than for positive ions. Analyses can be made on samples containing as little as 10 ng of B (Hemming and Hanson, 1994). The aqueous samples are loaded on a rhenium filament that has been outgassed to remove surface impurities. Generally, 1 to 3 μl of solution was used along with 3 μl of a $Ba(OH)_2$ solution (10 μg Ba) as an emission activator. The filament is heated in vacuum (~2 x 10^{-7} Torr) by a current of approximately 1800 mA. A stable emission current was generated at temperatures of 850° - 900° C.

The spectrometer is set up to measure BO_2^- emitted from the filament using a single Faraday cup collector. The masses measured are 42 ($^{10}B^{16}O_2^-$) and 43 ($^{11}B^{16}O_2^-$). Interference from ^{17}O (Klötzli, 1992) is negligible because the abundance of ^{17}O is far

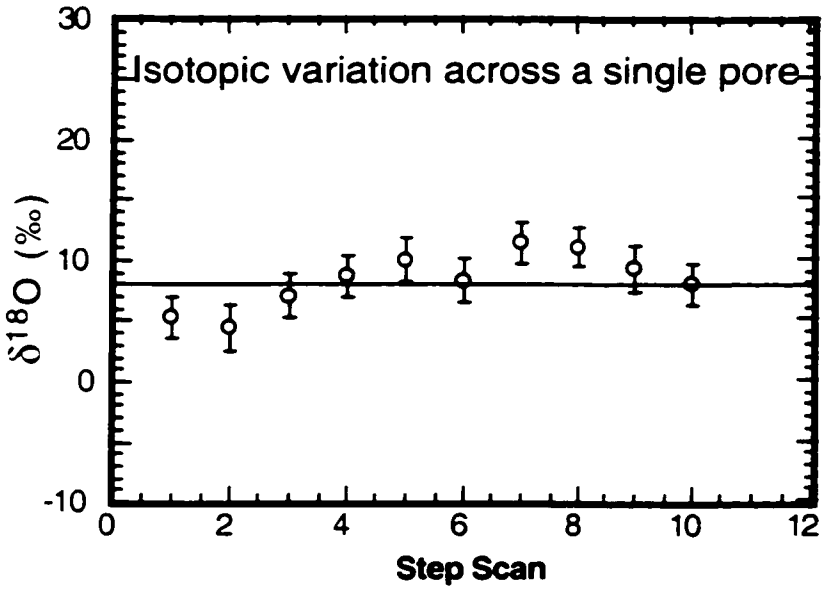

Figure 3.7. Step scan results from in situ analyses in thin section. Ten analyses at 50 μm spacing were made across randomly oriented kaolinite books in a reservoir sandstone. Results show reasonable scatter that could reflect changes in fluid composition during pore-filling.

less than the analytical errors (±2‰). The masses were alternately sampled in 10 cycles per block. At least 10 blocks of data are averaged to obtain an isotope ratio. Analyses yield errors on the order of 1-2‰. Measurements of the boron isotope standard NBS SRM 951 yielded a $^{11}B/^{10}B$ ratio of 4.0337±0.0041. Analyses of seawater collected from the Pacific ocean yield a $\delta^{11}B$ value of +39.8‰, which is in excellent agreement with that measured by others (Hemming and Hanson, 1994).

3.5. RESULTS

3.5.1. Mineralogical

The mineralogical changes that occurred during the reaction are indicated by XRD spectra of the experimental run products. Figure 3.8 shows the results from Experiment 1, which represent the mineralogical changes observed in all three experiments. The spectra show the extent of illitization and other minor products formed (quartz and chlorite) as the reaction progressed. During the first week of the reaction the smectite reacts to ~50% illite (Fig. 3.8). R1 ordering begins at least by day 10 as indicated by the appearance of a peak near 13Å (~6° 2θ). Figure 3.9 shows the variation in illitization progress for each experiment, all of which show illitization rates. Experiment 1, with low B-content, shows a gradual illitization similar to that reported by Whitney and Northrup (1988). After 30 days of reaction the I/S is 70% illite and it approaches 80% illite after 120 days. Experiment 2, with higher B in solution takes twice as long (two months) to reach 70%. It seems to reach a plateau at about 60% illite during the first 36 days, with a more sudden change to 75% illite at 60 days. All three experiments show a significant shift in the 13Å peak to 12Å between 30 and 60 days.

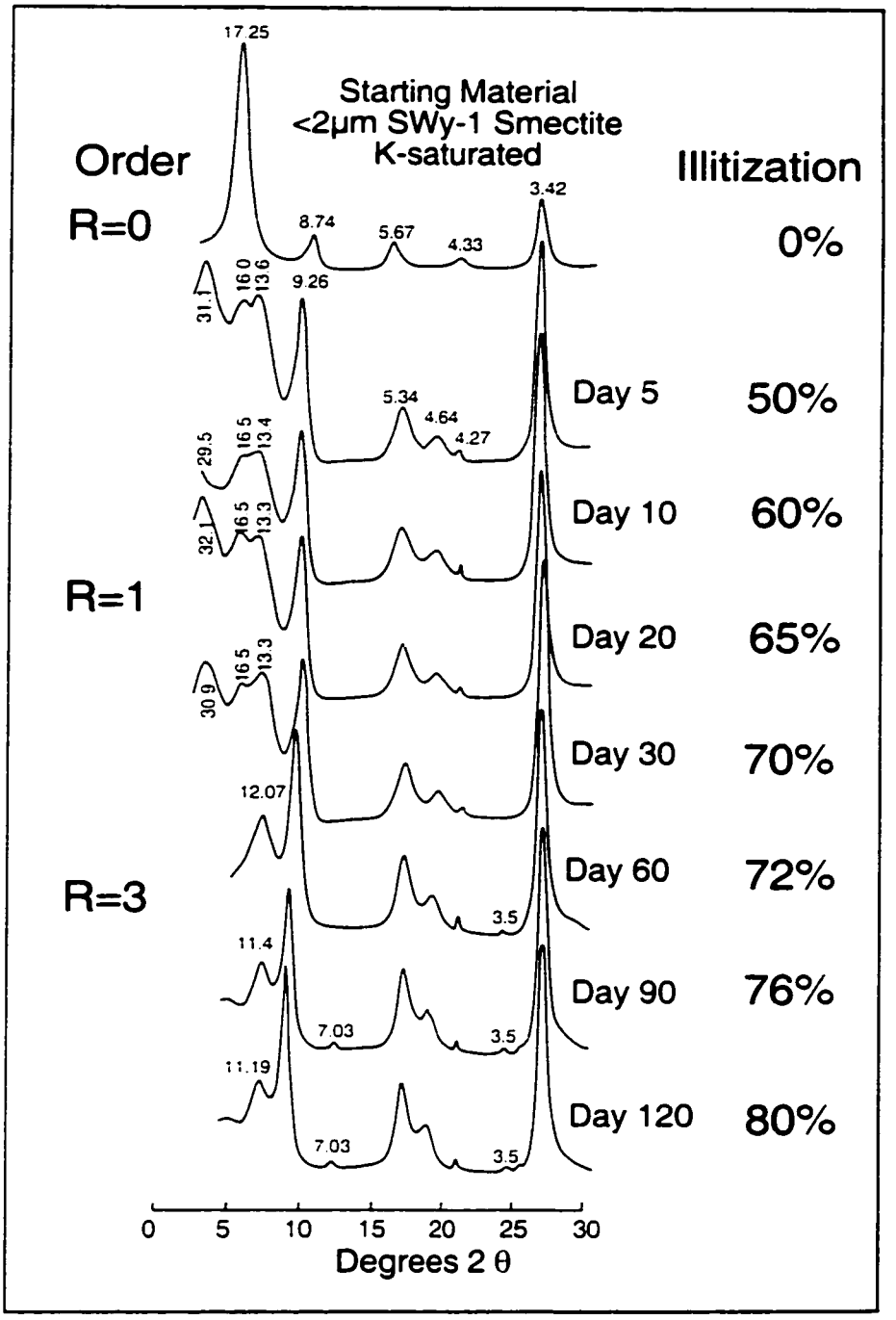

Figure 3.8. X-ray diffraction spectra of solid reaction products from Experiment 1. The mineralogical changes show increased ordering and illitization of smectite with time. Other products include chlorite and quartz during R3 ordering.

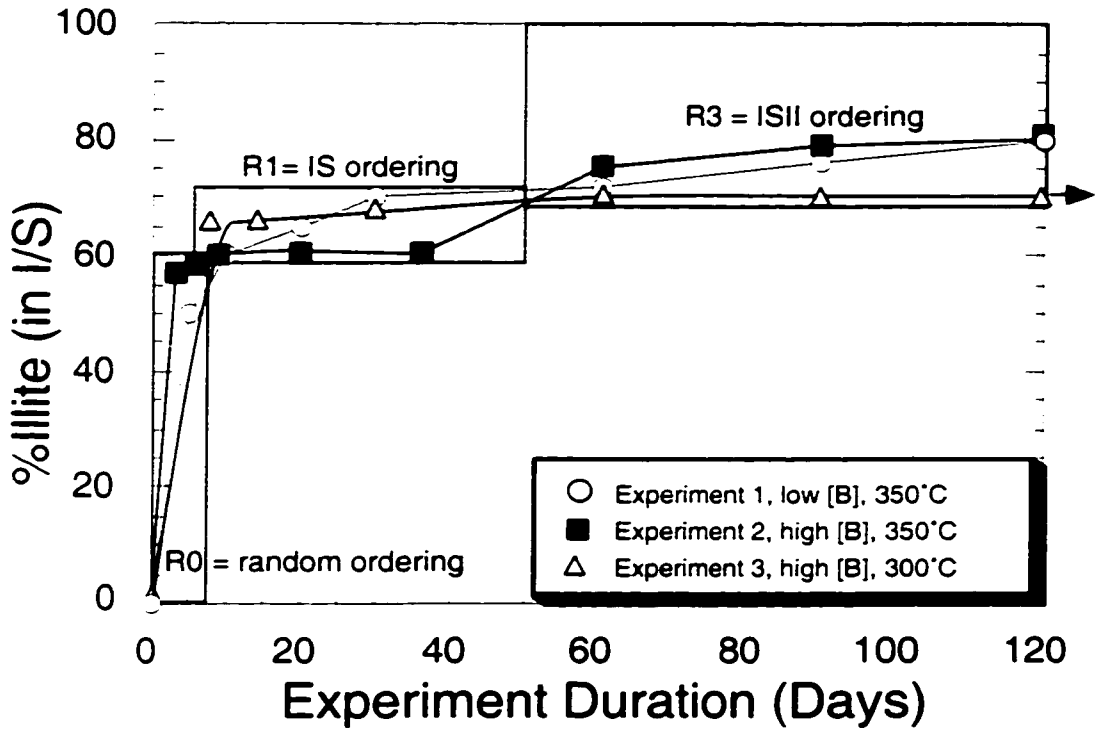

Figure 3.9. Plot of the ordering and illitization progress over time for all experiments.

indicating a long-range ordering sequence. This R3 ordering indicates that each smectite layer is surrounded by three illite layers (Srodon, 1980). Experiment 3, at 300 °C never progresses beyond ~70% illitization even after 150 days of reaction time. In fact, there is only a small increase in the illitization after the first week of reaction at 300 °C. The higher temperature experiments (Exp. 1 and 2) produced an 80/20 R3 ordered I/S after 120 days. A small peak appears at 3.5Å after 60 days (Fig. 3.8), indicating a small amount of chlorite produced. This is more obvious in the spectra from day 90 and day 120 when the chlorite 7Å peak appears. Production of chlorite was also observed in the illitization experiments of Whitney and Northrup (1988). The trace quantities of chlorite produced are not volumetrically important enough to influence the isotope ratio measurements, which average information from multiple (up to 59) individual analyses. Finally, the increasing intensity of the quartz peak at 26.6° 2θ after 60 days (Fig. 3.8) suggests that increasing amounts of Si is produced during long-range (R3) ordering associated with recrystallization of the I/S.

3.5.2. Isotope Exchange

3.5.2a. Oxygen

The O-isotope changes in the solid and liquid reaction products are shown as a function of time in Figure 3.10. Changes in the oxygen isotope ratio are most dramatic during the first 20 days of the experiment then equilibrium is approached gradually over the remaining 120 to 150 days. A decreased rate of change in the O-isotope re- equilibration occurs as R1 ordering of the I/S begins. The oxygen isotope composition of the clays reaches a plateau after about 60 days, coincident with R3 ordering. There is still a slight

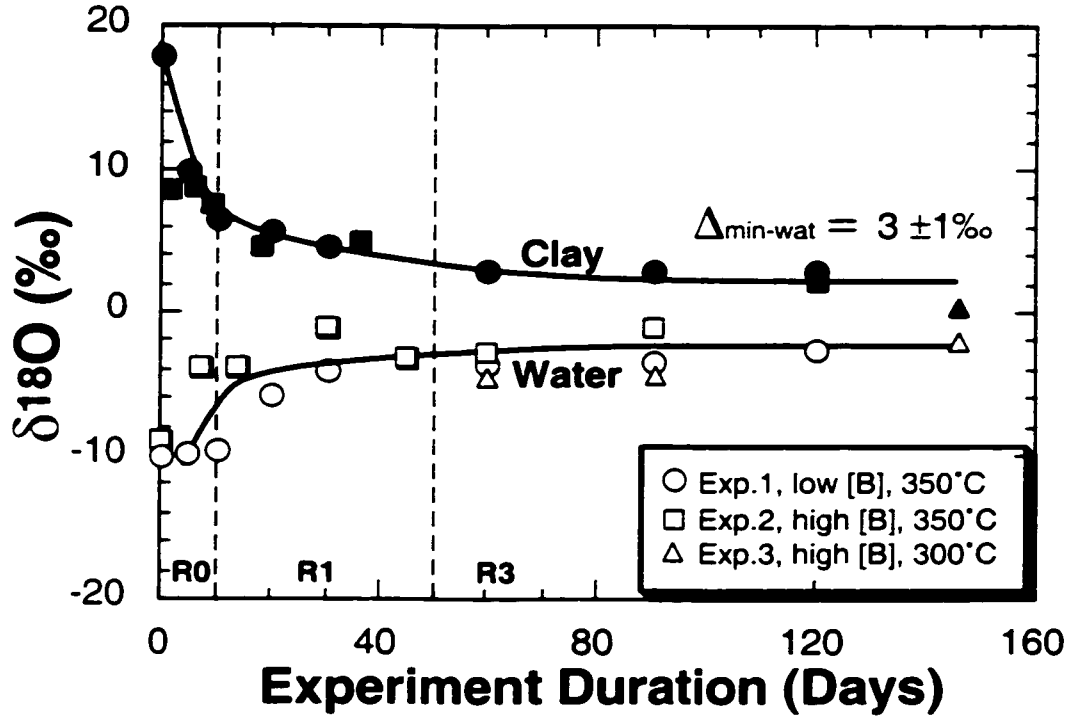

Figure 3.10. Results of the O-isotopic changes with time in experimental run products (clay = solid symbols; water = open symbols). The O-isotope $\Delta_{\text{I/S-water}}$ at 350°C is ~3‰ (Savin and Lee, 1988). Vertical dashed lines denote changes in ordering of the I/S.

increase in the $\delta^{18}O$ of the water, but the changes are not recognizable in the clays due to the large errors (±2‰) associated with clay analyses by SIMS. Nonetheless, the final Δ between the $\delta^{18}O$ of the I/S and $\delta^{18}O$ of the water is ~3 ± 2‰. The equilibrium isotope fractionation between I/S and water at 350° and 300° C is ~+2‰ and +3‰, respectively (Savin and Lee, 1988), therefore it appears that the end products of the experiment have nearly reached equilibrium with respect to oxygen (within analytical errors).

3.5.2b. Boron

Changes in the B-content (Fig. 3.11) and isotopic ratios (Fig. 3.12) of solid run products occur as the illitization reaction progresses. Table 3.1 summarizes the analytical results for boron in the solid run products. Temperature and aqueous B-content were different for each experiment, resulting in variable reaction paths. There are notable differences in the quantity of B incorporated into I/S during the reaction. The starting smectite (SWy-1) contained 12 ppm fixed-B after washing and K-saturation removed adsorbed-B. The $\delta^{11}B$ of the fixed-B in the starting material was -3 ± 1‰ (2σ). Experiment 1, with a low aqueous B-content showed insignificant changes in the fixed-B content of the clay over the first 30 days of reaction time. After 60 days, however, the fixed-B content doubled, coincident with long-range (R3) ordering of the I/S (Fig. 3.11). Experiment 2 differed from Experiment 1 only in the higher concentration of aqueous-B. The fixed-B content of the I/S increased to nearly 60 ppm during R1 ordering, but equilibrated at 50 ppm after R3 ordering. Similarly, the Experiment 3 results indicate an initially high fixed-B content of the I/S increasing to ~90 ppm during R1 ordering, with only 50 ppm fixed-B in the R3 ordered end-product.

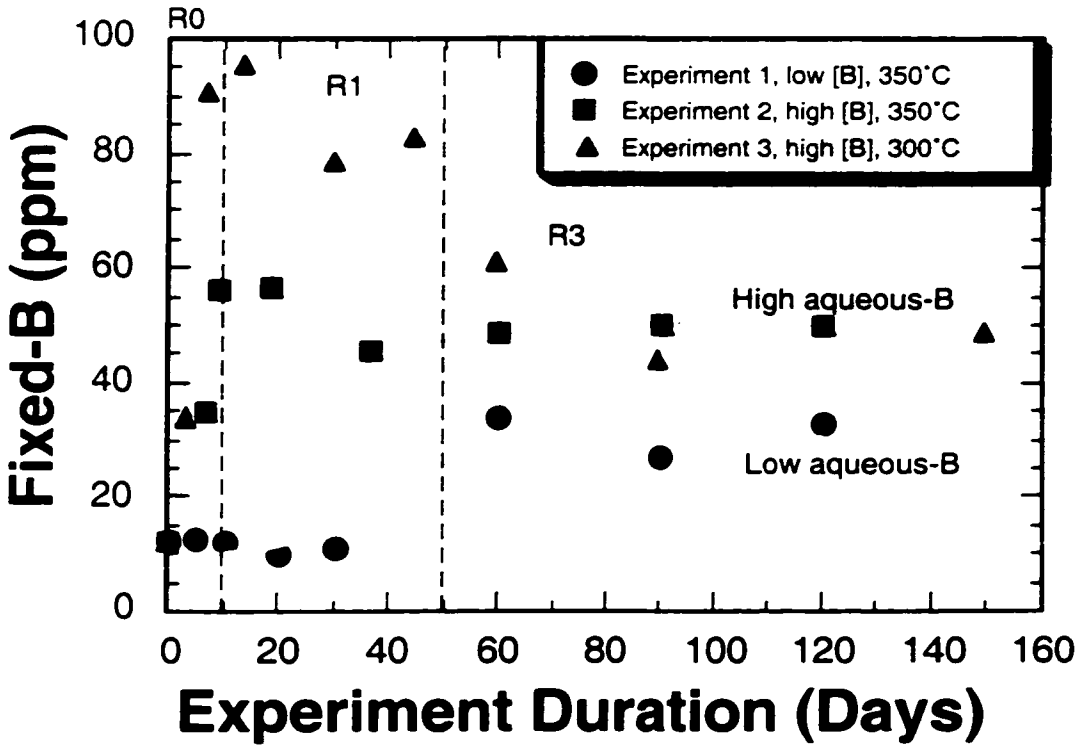

Figure 3.11. Changes in fixed-B content with time for all experiments. Gray lines denote general trends. Vertical dashed lines show changes in ordering of the I/S.

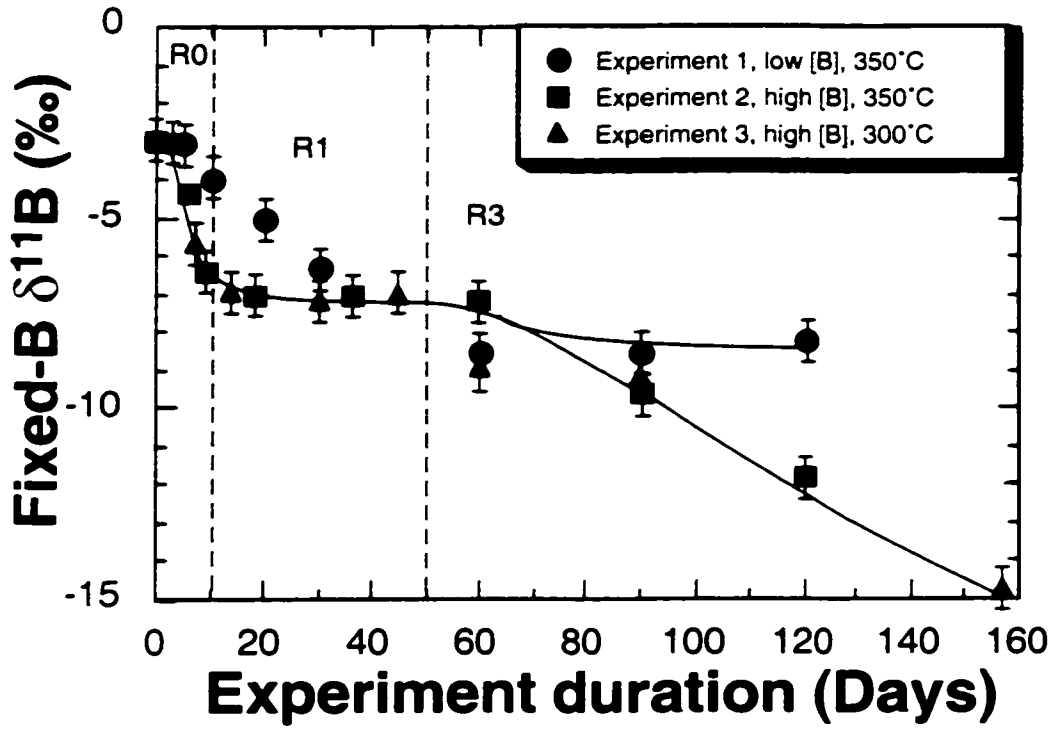

Figure 3.12. Changes in fixed-B $\delta^{11}B$ with time. Symbols as in previous figure.

Table 3.1. Summary of boron analytical results by secondary ion mass spectrometry.

Experiment 1

Sample	11/10	S.D.	error ‰	P.E.‰	IMF	$\delta^{11}B$	S.E. ‰	n	B (ppm)
Day 0	3.8254	0.0082	0.8	0.8	-50.9	-3.1	0.4	7	12
Day 5	3.8209	0.0147	1.5	1.3	-51.4	-3.7	0.4	14	13
Day 10	3.8519	0.0257	2.6	2.6	-43.0	-4.4	0.6	7	13
Day 20	3.8170	0.0223	1.7	1.5	-51.4	-4.7	0.1	6	10
Day 30	3.8279	0.0179	1.8	1.6	-46.0	-7.1	0.5	15	11
Day 60	3.7990	0.0150	1.5	1.5	-52.0	-8.5	0.3	4	34
Day 90	3.7974	0.0182	1.8	1.6	-52.0	-8.5	0.3	20	27
Day 120	3.8187	0.0175	1.8	1.4	-48.0	-7.6	0.5	20	33

Experiment 2

Sample	11/10	S.D.	error ‰	P.E.‰	IMF	$\delta^{11}B$	S.E. ‰	n	B (ppm)
Day 0	3.8213	0.0123	1.8	1.2	-52.0	-3.0	0.5	5	14
Day 3	3.8340	0.0087	0.9	0.9	-49.0	-2.9	0.7	4	34
Day 6	3.8159	0.0099	1.0	0.8	-52.0	-4.3	0.7	3	35
Day 9	3.8078	0.0079	0.8	0.7	-51.0	-6.4	0.2	32	56
Day 18	3.8323	0.0084	0.8	0.7	-45.0	-7.3	0.3	10	57
Day 36	3.8306	0.0071	1.0	0.9	-41.0	-11.7	0.4	19	45
Day 60	3.8938	0.0084	1.2	1.2	-30.0	-7.1	0.6	16	49
Day 90	3.8841	0.0101	1.4	1.3	-30.0	-9.6	0.3	8	50
Day 120	3.8686	0.0104	1.5	1.5	-31.0	-12.3	0.7	9	50

Experiment 3

Sample	11/10	S.D.	error ‰	P.E.‰	IMF	$\delta^{11}B$	S.E. ‰	n	B (ppm)
Day 0	3.8254	0.0082	0.8	0.8	-50.9	-3.1	0.4	7	12
Day 7	3.8144	0.0075	1.1	0.6	-51.0	-5.7	0.3	4	91
Day 14	3.8038	0.0051	0.7	0.5	-52.0	-6.9	0.7	4	96
Day 30	3.8028	0.0082	1.2	0.6	-52.0	-7.2	0.4	20	79
Day 45	3.8116	0.0072	0.9	0.6	-52.0	-5.7	0.8	5	91
Day 60	3.8405	0.0090	1.3	1.0	-41.0	-8.9	0.5	27	83
Day 90	3.8739	0.0083	1.2	1.1	-30.0	-12.0	0.8	6	74
Day 150	3.8723	0.0084	1.2	1.1	-31.0	-15.5	0.7	60	50

The mass 11/10 ratios reported are averages of n analyses on each sample. The standard deviation (S.D.) is based on 49 ratios averaged for each analysis. Errors were averaged for each sample. The predicted error (P.E.) is based on counting statistics and is a measure of the best possible error. Instrumental mass fractionation (IMF) varies for each analytical session. The $\delta^{11}B$ is calibrated by IMF. The standard error (S.E.) is the S.D. of all analyses (n) on each sample divided by n^0.5. Fixed-B content (ppm) is based on the ratio of mass 11/30 (see Fig. 3.3).

Changes in the isotopic composition of the fixed-B (Fig. 3.12) for each experiment show very similar trends. There is a rapid decline in $\delta^{11}B$ from the initial -3‰ $\delta^{11}B$ while the I/S is randomly ordered (R0). The experiments containing abundant aqueous-B (Exp. 2 and 3) both show a plateau in $\delta^{11}B$ at -7±1‰ during R1 ordering. When R3 ordering begins after 60 days of reaction, the isotope ratio of the fixed-B decreases further. Experiment 1 (low aqueous-B) decreased only slightly during R3 ordering, probably due to the limited B supply. The B supply in Experiments 2 and 3 was not similarly limited. During R3 ordering of the I/S the $\delta^{11}B$ reached -12 ±0.5‰ at 350 °C and -15 ± 0.9‰ at 300 °C. The B-isotopic exchange was complete after 120 days at 350 °C and 150 days at 300 °C, as indicated by O-isotope equilibrium.

Boron in solution was measured by ICP analysis of the B washed from the capsule walls and solid product (using mannitol). This fraction of B is representative of what was in solution at experimental temperatures, where the distribution coefficient is zero for adsorbed-B (You et al., 1996). This assumes that little B was removed from the capsules by volatilization during vacuum extraction of the solution. The amount of B measured in this wash varied from 75% to 100% of the B added. This variability indicates incomplete recovery of solution B, perhaps causing a fractionation during the extraction process. Due to the unreliability of these results, mass balance calculations were made for determining $\delta^{11}B_{water}$. Based on measurements of B-content and $\delta^{11}B$ of the solids, and calculating these values for the water by difference, the mass balance calculations determined the ideal fractionation ($\delta^{11}B_{mineral}$–$\delta^{11}B_{water}$) at the experimental temperatures. These calculations assume that no B was lost from the Au capsules by diffusion, which is unlikely at the low temperatures of the experiments. Analysis of the

pressurizing fluid used in the hydrothermal reaction vessel showed 11 ppm B, which would not effect the calculated fractionation factors and is likely from other contaminants (steel, and/or lubricants used to seal the vessel).

3.6. DISCUSSION

3.6.1. Background

Clay minerals generally concentrate the light isotopes of boron over the heavy isotope, which prefers the aqueous phase. This is contrary to what is observed in most stable isotopic systems. Heavy isotopes form bonds with a lower vibrational frequency than lighter isotopes of the same element and therefore should make stronger bonds (Faure, 1986). Thus, the light isotopes are more reactive, and are usually concentrated in more volatile phases. In the case of boron, however, the coordination state plays an important role in fractionation (Palmer and Swihart, 1996; Hervig et al., in review). In solution boron occurs predominantly as $B(OH)_3$ or $B(OH)_4^-$, although there may be polynuclear species and organic-B molecules as well (Bassett, 1976; Mackin, 1987). The light isotope, ^{10}B, prefers tetrahedral coordination, and the heavy isotope ^{11}B prefers trigonal coordination (Palmer and Swihart, 1996).

Spivack et al. (1987) showed that adsorbed-B in marine sediments has an average $\delta^{11}B$ of +15‰, but it accounts for only 10-20% of the total-B in the sediment. The rest is 'non-desorbable-B', meaning that portion that was not removed by sonifying in B-free water after 3 washings. The non-desorbable-B fraction of the marine sediment had $\delta^{11}B$ values ranging from 0 to −10‰ (Spivack et al., 1987). This covers the average range of $\delta^{11}B$ values found in granitic and basaltic source materials (Leeman and Sisson, 1996).

Spivack et al. (1987) found no evidence for fixation of B into clay minerals (substitution for Si) during early diagenesis. Therefore all of the isotopic variations observed in shallow marine sediments are interpreted to result from interactions between pore fluid B and surface adsorbed-B, and are consequently pH dependent.

The experimental results presented here address the isotopic behavior of B during late diagenesis when recrystallization of smectite to illite allows B-substitution for Si. In deep sedimentary basins undergoing siliciclastic diagenesis, the pH of pore fluids is buffered to values below 7 (Hutcheon et al., 1993) where $B(OH)_3$ is the predominant aqueous-B species (Palmer et al., 1987). As a result ^{11}B prefers the aqueous phase. Illite/smectite undergoes significant recrystallization during diagenesis and provides tetrahedral coordination sites preferred by ^{10}B (Spivack et al., 1987; Ishikawa and Nakamura, 1993). It is this coordination preference that causes ^{10}B-enrichment in clay minerals.

Whitney and Northrup (1988), and others (Eberl, 1993; Yates and Rosenburg, 1996) suggested that there may be more than one mechanism of illitization; initially a layer-by-layer transformation related to charge distribution of layers, and finally a complete dissolution-precipitation, or 'neoformation'. Only a partial isotopic equilibration occurs during the early reaction of smectite to illite, but neoformation requires complete breakdown and reassembly, resulting in ordered I/S. It is during this neoformation stage that the isotope ratios are 100% reset.

During early recrystallization of the smectite (~60°C), adsorbed and aqueous-B may be incorporated into some tetrahedral layers of the authigenic illite. Since it is the coordination change that causes the isotopic fractionation, the incorporation of surface-adsorbed-B (tetrahedral) into lattice structure tetrahedral sites should not significantly affect the magnitude of the fractionation (Palmer and Swihart, 1996). During the neoformation stage, at temperatures approaching ~120°C, the partition coefficient for adsorbed-B approaches zero (You et al., 1996), so the isotopic fractionations measured in experiments conducted at 300-350°C represent the fractionation between the aqueous-B (trigonal) and tetrahedral layers of the sheet silicate, not adsorption sites.

3.6.2. Interpretation

3.6.2a. Fixed-B Content

Different kinetic pathways for the incorporation of B into illite are expressed by the variable trends in the fixed-B content of the I/S over time (Fig. 3.11). Experiment 2 and 3 differed only in temperature, but each showed a maximum B-content during R1 ordering. Experiment 3 (300°C) incorporated more B initially (~90 ppm) than the Experiment 2 (~60 ppm at 350°C), perhaps reflecting a temperature dependence of the boron distribution coefficient between the fluid and B-sites in the illite. The peak in B-content during R1 ordering may result from the competition between B and Al for available tetrahedral sites. During early reaction progress the source of Al may be limited by decomposition of minor amounts of K-feldspar and detrital mica included in the starting material. Low Al availability might have allowed more B to substitute for Si during early stages of the reaction. Boles and Franks (1979) suggested that during later

stages of illitization some Al may be derived from the dissolution of smectite layers (see also Pollastro, 1985). Dissolution of the smectitic material over time might increase the Al availability thus increasing Al competition for the Si-sites. This could cause the decreased fixed-B content observed during long-range (R3) ordering of the I/S associated with neoformation.

The total amount of B incorporated in the authigenic illite (I/S) in these experiments (50 ppm at equilibrium) is a four-fold increase over the starting material. In nature the fixed-B content of illites is commonly much higher, on the order of hundreds of ppm (Harder, 1970). Early experiments on B-fixation in illite (Couch and Grim, 1968) showed that B-ion activity increases with salinity of the solution, especially in the presence of $CaCl_2$ (Schafer and Sieverts, 1941). The dissociation of boric acid:

$$B(OH)_3 + 2H_2O \leftrightarrow H_3O^+ + B(OH)_4^-$$

may be enhanced with increased ionic strength of solution (Couch and Grim, 1968).

Another possible limitation to B-uptake in the experiments could be the high aqueous B-concentrations used. Nies and Campbell (1964) showed that at boric acid concentrations above 0.5M (~5500 ppm B) there is an increase in the population of polynuclear borate ions. If $B(OH)_3$ is not the dominant aqueous species then B-uptake by illite may be limited. Nonetheless, the concentration of B in the experiment solution (1000 ppm B) and the concentrations found in oil field brines (100's –1000's ppm B; Collins, 1975) is well below that used by Nies and Campbell (1964). Couch and Grim (1968) found that the major factors contributing to boron fixation were salinity, aqueous B-concentration, and temperature. They suggest that the surface area of the clay mineral

may play a role in B-uptake, but they did not establish that equilibrium conditions were achieved in their experiments. The experiments described here showed no correlation between the amount of fixed-B and the equilibrium isotopic composition.

3.6.2b. B-isotopes

The isotope ratios of fixed-B in the I/S showed changes during reaction progress (Fig. 3.12) related to structural changes in the clay. The most rapid change in $\delta^{11}B$ occurs initially during the change from random R0 to R1 ordering. There is a plateau in the $\delta^{11}B$ value at –7‰, perhaps indicating a metastable condition. This occurs at the same time that the fixed-B content reaches a maximum. Nonetheless, it is important to understand that this is a kinetic effect of the high temperatures used in the experiment and cannot necessarily be extrapolated to the diagenetic environment. At this point in the time series, the reactants are not in equilibrium with the fluid. Equilibrium is indicated (according to 100% O-isotope resetting) after 120 days at 350°C and 150 days at 300°C. Therefore the final isotope ratio measured for fixed-B in the I/S can be used to calculate the equilibrium fractionation between the water and illitic clay minerals.

The O-isotopes (Fig. 3.10) show a more gradual change between R1 and R3 ordering than the results for B-isotopes. This indicates that B-substitution is not directly linked to each O-bond exchange. This is expected since oxygen is not only exchanging from the tetrahedral sites, but also from hydroxyl sites and interlayer water as dehydration of the smectite occurs. The oxygen isotope changes do not reflect one unique mechanism of exchange. However, the B exchange is related only to the breaking of tetrahedral Si-O bonds, and is therefore a unique diagenetic marker.

3.6.3. Boron Isotope Fractionation

The B-isotope fractionation curve (Fig. 3.13) was constructed from the results of the illitization experiments (300°C, 350°C; 1kbar), the fractionation between water and adsorbed-B on clay surfaces at 25°C, (Palmer et al., 1987) and a fluid-silicate melt fractionation measured at 1100°C (Hervig and Moore, 2000). Based on these data, a linear change in fractionation with reciprocal temperature is observed. All of these experiments determined that the isotope fractionation occurs as a result of the coordination change of B from trigonal in the fluid to tetrahedral in the minerals. It is expected that minerals containing trigonal sites (i.e. borates, carbonates) would not follow the same fractionation curve.

Mass balance calculations (Table 3.2) determined the B-isotope fractionation between I/S and water at 350°C and 300°C. During quenching of the experiment, and extraction of the fluid from the Au-capsules, B will adsorbed on the clay surfaces, but this fraction of adsorbed-B is not representative of the conditions at higher temperatures and is not representative of the fractionation of B incorporated into tetrahedral layers. It is removed prior to B-isotope ratio measurement. Experiment 1 results were not used in these calculations due to the limited B-content of the solution. Detection limitations and analytical errors on such low concentrations led to a propagation of large errors. Nonetheless, Experiments 2 and 3 contained an abundance of B in solution so that errors in the measurements of B-content and $\delta^{11}B$ did not significantly affect the fractionation factor determined. The B-contents were measured with less than 5% error. Errors in the B-isotope analyses of the run products were under 1‰, and the B-isotope fractionations

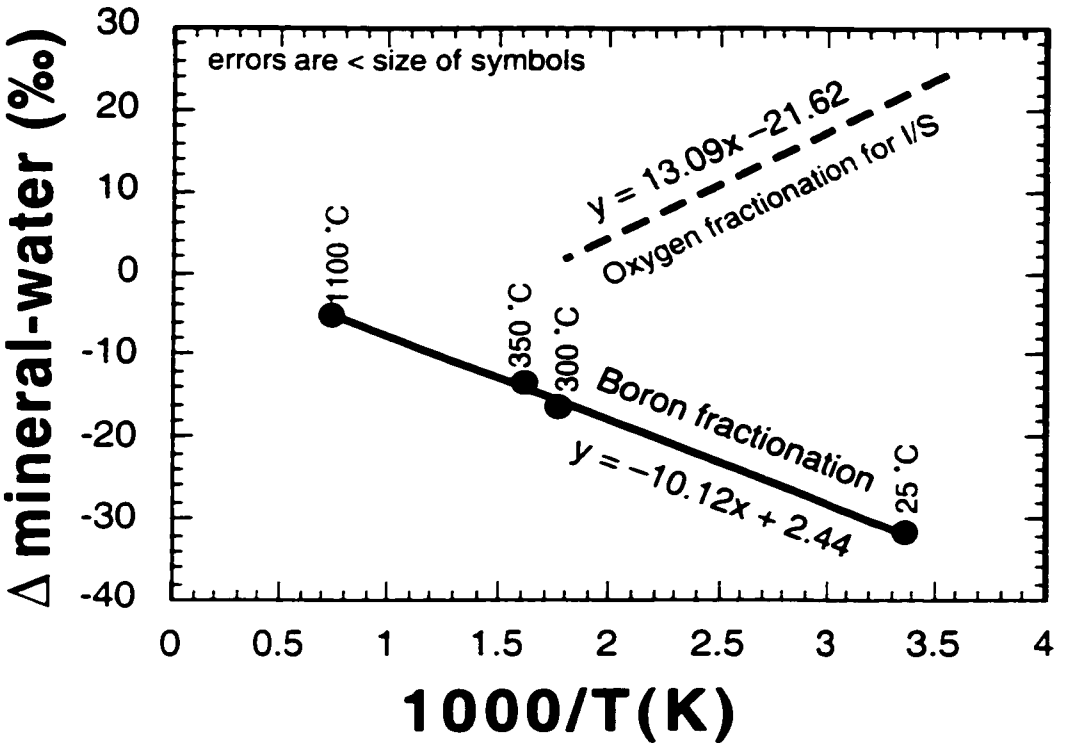

Figure 3.13. Boron isotope fractionation as a function of reciprocal temperature, compared to oxygen isotope fractionation (from Yeh and Savin, 1977) for I/S .

Table 3.2. Mass Balance for mineral-water B-isotope fractionation at 300° and 350° C.

Mass Balance Calculations for 350°C Experiment

INITIAL	fixed-B (ppm)	‰ fixed-B	mass 11/10	mass 10	mass 11
	10	0	4.0437	1.9827	8.0173
	water B (ppm)	‰water	mass 11/10	mass 10	mass 11
	1000	0	4.0437	198.2671	801.7329
FINAL	fixed-B (ppm)	‰ fixed-B	mass 11/10	mass 10	mass 11
	50	-12	3.9952	10.0097	39.9903
	water B (ppm)	‰water	mass 11/10	mass 10	mass 11
Calculated water	960	0.6	4.0463	190.2402	769.7598
$\Delta_{\text{mineral-water}}$		**-13**			

Mass Balance Calculations for 300°C Experiment

INITIAL	fixed-B (ppm)	‰ fixed-B	mass 11/10	mass 10	mass 11
	10	0	4.0437	1.9827	8.0173
	water B (ppm)	‰water	mass 11/10	mass 10	mass 11
	1000	0	4.0437	198.2671	801.7329
FINAL	fixed-B (ppm)	‰ fixed-B	mass 11/10	mass 10	mass 11
	45	-15	3.9830	9.0306	35.9694
	water B (ppm)	‰water	mass 11/10	mass 10	mass 11
Calculated water	965	0.7	4.0466	191.2192	773.7808
$\Delta_{\text{mineral-water}}$		**-16**			

were calculated assuming a closed system. Propagation of errors gave ~±1.5‰ (2σ) for each experimental fractionation determination.

The adsorbed-B fractionation measured by Palmer et al. (1987) for clay minerals at 25°C was used to anchor the fractionation curve at the low temperature end. At this temperature the fixed-B composition does not reflect equilibrium conditions with the aqueous fluid, but reflects the chemical environment of its source material. Boron is not fixed in the silicon tetrahedra until recrystallization of the I/S occurs at diagenetic temperatures above 60°C (Perry, 1972). Nonetheless, the fractionation measured at 25°C was based on the coordination change of B from trigonal (in solution) to tetrahedral sites on the clay surface.

The high temperature (1100°C) fractionation was measured on mid-ocean ridge basaltic glass doped with 2000 ppm B (NBS SRM 951, boric acid) and melted at 100 MPa (1 kbar) pressure over 24 hrs, with an equal mass of B-free water. The fractionation between the aqueous fluid and basaltic melt is again related to the coordination change from trigonal to tetrahedral sites in the melt. For other isotopic systems, such as oxygen, the mass fractionation between fluid and minerals is mineral specific due to bonding difference associate with local electrochemical variations in different mineral structures. Boron isotope fractionation does not appear to follow this mineral specificity. Under conditions where the dominant aqueous B-species is $B(OH)_3$ and the mineral sites prefer $B(OH)_4$, the B-isotope fractionation forms a single linear trend with reciprocal temperature, independent of mineral structure. One explanation for this is that the ionic radius of B is much smaller than that of Si or Al, thus the strength of B-O bonds within

tetrahedral sites of silicates are large enough to make the effect of neighboring sites insignificant (Hervig et al., in review).

3.6.4. Application to the Gulf of Mexico Sedimentary Basin

One common use of isotopes as a geothermometer in geologic environments is dependent on the differences in isotopic fractionation between water and different minerals that contain the same isotopes (e.g., oxygen). If the equilibrium fractionation curves have a significantly different slope, and the two minerals co-precipitated, then the equations can be used to calculate a specific temperature of crystallization. This technique is not simple to employ in a diagenetic environment where co-precipitation and equilibrium conditions are difficult to determine, and most authigenic phases have fractionation curves with similar slopes (Kyser, 1987).

It may be useful, however, to use two isotopic systems, i.e. B and O, that are geochemically linked by a single prograde mineral reaction of smectite to illite to predict equilibrium conditions. Figure 3.13 shows that the fractionation curves for the two different isotopic systems have a significantly different slope. In a closed system dominated by I/S (common in many sedimentary basins), there should be a unique temperature and water composition that satisfies the equilibrium of both B and O-isotopes in the I/S. Following is an example of the integrated use of B and O-isotopes for evaluating diagenetic changes in sediments from the Gulf of Mexico sedimentary basin.

3.6.5. Wilcox Fm

3.6.5a. Mudstones

According to Yeh and Savin (1977) the change in $\delta^{18}O$ of I/S within mudstones of the Eocene Wilcox Fm is nearly linear and decreases over a depth range of 2.5 to 5 km (68°-155°C). Here it is believed that the mudstones represent a closed system with respect to fluids, and that complete isotopic exchange resulted during the illitization of smectite (Savin and Lee, 1988). Bloch et al., (1998) have suggested that volcanic ash is a significant source of the detritus in the Gulf Coast basin. Therefore the smectite was probably of volcanic origin, with a $\delta^{18}O$ representing the volcanic source and the pore fluid $\delta^{18}O$ was approximately 0‰ (seawater).

Coinciding with the O-trend, there is an increase in the fixed-B content of I/S as temperatures exceed 60°C (Perry, 1972). The B increases from 100 to 200 ppm over depths from 1.5 to 6 km. Smectite from altered volcanic ash or weathered continental rocks would be expected to have an initial B-isotopic composition around 0‰ (Leeman and Sisson, 1996; Palmer and Swihart, 1996). Marine pore fluids would have an initial $\delta^{11}B$ near +39.5‰ (seawater), but the detrital minerals and fluid are not in isotopic equilibrium at surface temperatures. The isotopic fractionation curve cannot be applied to detrital marine sediments where the B in minerals is not in equilibrium with the fluids. However if one assumes that B-isotopic changes (toward equilibrium) accompany the observed increase in fixed-B (as shown in these experiments), and that the B-isotopic composition of the I/S is linked to isotopic changes in oxygen, then the two isotopic systems could be used as a predictive tool.

Samples were collected from cores penetrating the Wilcox Fm at ~4 km (~120°C) in south central Louisiana (Williams et al., 1995). Measurement of $\delta^{18}O_{I/S}$ and $\delta^{11}B_{I/S}$ indicated average values of +20±2 and −18.8±0.8‰, respectively. The burial history of the basin shows a linear trend over time (Boles and Franks, 1979) with a constant thermal gradient approximating 30°C/km based on corrected bottom-hole temperatures (Williams et al., 1995).

Information on the fluid chemistry of mudstones is difficult to obtain due to difficulty in extracting water from aquicludes. However, Suchecki and Land (1983) developed a model to calculate oxygen isotopic compositions of the authigenic illite/smectite and formation fluid in mudstones resulting from burial diagenesis. Their calculations take into account the initial temperature plus thermal gradient and the degree of illitization of the smectite. Their calculations indicate that the O-isotopic composition of water in equilibrium with I/S (>70% illite) at 4 km, under a geothermal gradient of 30°C/km, should be approximately +8‰. Using this information together with the measured $\delta^{18}O$ of the illitic mudstone (+20‰), the $\Delta_{mineral\text{-}water}$ for oxygen (+12‰) corresponds to a temperature of 116°C (Fig. 3.13). This is within the range of bottom-hole temperatures measured in the cores examined (Williams et al., 1995). The B-isotope fractionation curve predicts a $\Delta_{mineral\text{-}water}$ for boron at this temperature of −24‰. This information, together with measurements of $\delta^{11}B$ on the illitic mudstone (-18.8±0.8‰) indicates that the pore fluid in equilibrium with this mudstone should have a $\delta^{11}B$ around +6‰. This value is lower than reported measurements showing a minimum $\delta^{11}B$ of +12‰ (Fig. 3.14) in formation waters from the Gulf Coast (Macpherson and Land, 1989;

Land and Macpherson, 1992; Moldovanyi et al., 1994) but all those measurements were made on waters from carbonate and clastic reservoirs, not mudstones. The +6‰ $\delta^{11}B$ is not unreasonable in the context of waters associated with sedimentary rocks. Palmer and Sturchio (1990) reported $\delta^{11}B$ values for continental hydrothermal waters as low as –8‰.

3.6.5b. Sandstones

Sandstones are usually not closed systems in sedimentary basins. They are open to migration of hydrocarbons and related fluids, and they are not dominated by clay minerals, as are the surrounding mudstones. Formation waters from sandstone reservoirs will be influenced by other diagenetic sources of oxygen and boron therefore it is not possible to use the two isotopic systems to predict fluid compositions. However, understanding the general diagenetic framework for B- and O-isotopes related to I/S, one can begin to appreciate the mobility of B in the sedimentary basin. With some careful consideration of the various sources of B it may be possible to use B-isotopes as a tracer of fluid migration.

Formation waters were collected from hydrocarbon bearing sandstone reservoirs in the Wilcox Fm, adjacent to the mudstone samples discussed above. The temperature of the sandstones ranges from 100-125°C. The $\delta^{11}B$ value of the water determined by NTIMS ranges from +28‰ to +36‰ (Chapter 2), but the pore-filling (authigenic) clay minerals in the sandstones (mostly illite) have a consistent $\delta^{11}B$ value of –2±2‰. The fixed-B content of these clay minerals varied from 150-250 ppm B. If the pore-filling clay minerals precipitated under current reservoir conditions (~100°C), the B-isotope

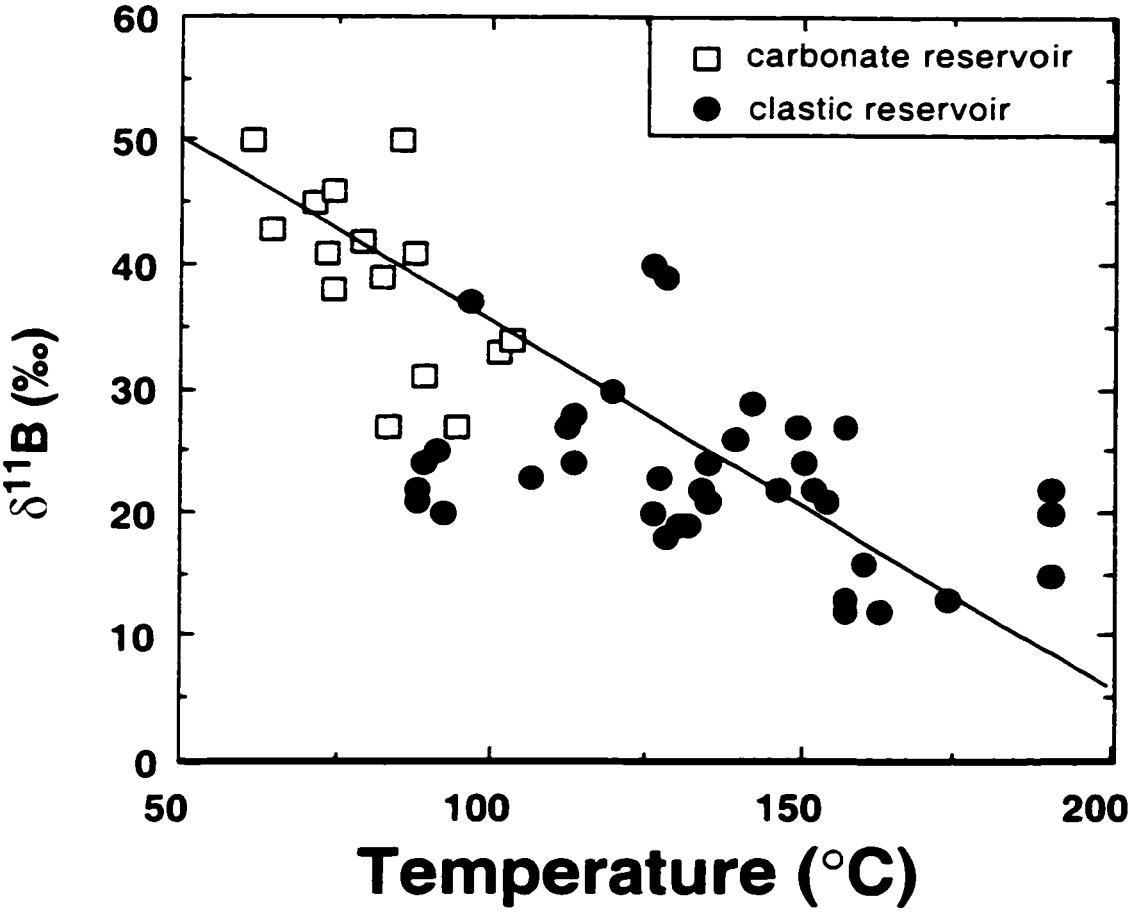

Figure 3.14. Trend in boron isotope compositions of formation waters from carbonate and clastic reservoirs in the Gulf of Mexico sedimentary basin. Data compiled from Land and Macpherson (1992) and Moldovanyi et al. (1994).

fractionation curve (Fig. 3.13), indicates that waters in equilibrium with the I/S should have an isotopic composition of +22±1‰. This indicates that the current reservoir is not in equilibrium with the clay cements. Either the clay formed at a much lower temperature (<60°C) or the isotopic composition of the reservoir fluid has been altered from that predicted.

The I/S in the Wilcox reservoirs consists of approximately 70% authigenic illite (Williams et al., 1995) and it would be difficult to achieve this degree of illitization at temperatures <80°C since the Late Eocene. It is more reasonable to assume that the oil-field brines represent influx of fluids containing B from a new source introduced after formation of the authigenic illite. A similar argument was made for these reservoirs on the basis of N-isotopes in authigenic illite (Williams et al., 1995). The enrichment of ^{11}B in the present waters may result from mixing with seawater, dissolution of evaporites containing positive $\delta^{11}B$ borates or a gas phase separation that concentrates ^{11}B in a more volatile fraction (Palmer and Sturchio, 1990). Certainly, the isotopic composition of the sandstone water is not at all similar to the mudstone pore fluids. However, water released from the mudstones, through compaction or smectite dehydration, may supply some B to the reservoir.

The mass balance considerations for the sedimentary basin as a whole indicate that there must be a significant source of ^{10}B at depth. Figure 3.15 shows estimates of the B-content and $\delta^{11}B$ of sediment and water in the Gulf of Mexico, from the surface (Spivack et al., 1987; Perry, 1972) to deep in the basin (this study). The Mississippi River sediment (<4μm fraction) contains ~100 ppm fixed-B with a $\delta^{11}B$ of 1.9±0.4‰ (Spivack

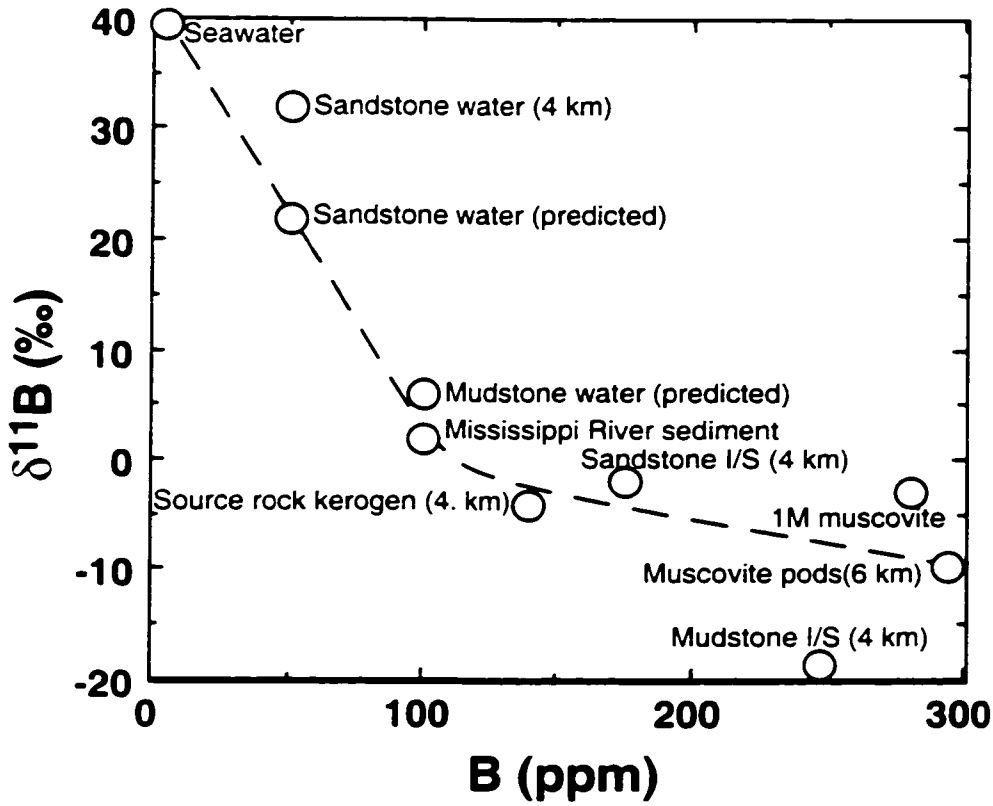

Figure 3.15. Summary of data discussed in the evaluation of B-isotope trends and fluid/rock interactions in the Gulf of Mexico sedimentary basin.

et al., 1987). The marine sediments contain seawater in the pore space upon deposition, thus the fluid has a B content of ~5 ppm B with 39.5‰ $\delta^{11}B$. At 4 km depth, the depositionally equivalent marine sandstones contain I/S that has increased in B-content (~150 ppm B) but decreased in $\delta^{11}B$ by as much as 6‰ from the originally deposited sediment. Similarly the formation water has increased in B-content by ~50 ppm with a decrease in $\delta^{11}B$ of about 12‰. This requires addition of ~100 ppm of isotopically light-B over the course of 4 km burial. More deeply buried sediments (Norphlet Fm. discussed below) indicate a continued increase in B-content of authigenic clay minerals, and decrease in the $\delta^{11}B$ with depth (and age).

It was shown that adsorbed-B will be released at temperatures less than 120°C (You et al., 1996). At ~120°C the partition coefficient for adsorbed-B (B_{clay}/B_{fluid}) approaches zero. The adsorbed fraction of the near surface sediment averages +15‰ (Spivack et al., 1987) and thus has the potential to lower the pore fluid $\delta^{11}B$ from the original 39.5‰ seawater $\delta^{11}B$. The effect of this desorption would depend on the temperature, fluid/rock ratio, degree of compaction, and would compete with other diagenetic reactions. Above 120°C there should be no adsorbed-B on the sediment, and the experiments have shown that at >70% illitization (similar to conditions at 4 km burial) recrystallization and long-range ordering of I/S allows significant substitution of B into illite. This process will deplete the pore fluid supply of ^{10}B and would be expected to leave the fluids ^{11}B-enriched. At the same time (temperature) however, organic matter matures to the point of hydrocarbon expulsion. It was shown (Chapter 2) that kerogen from the source rock for oil in these reservoirs (Sassen, 1990) has a B-isotopic

composition of –4‰ to –10‰ (Chapter 2). It is not known how much boron was in the organic matter before it was thermally mature, but at present temperature (>125°C) the B-content is 140 ppm. This is a potential source of ^{10}B for reservoir waters. The reservoir waters are certainly influenced by the introduction of hydrocarbons. If the B isotopic ratio of the reservoir fluids can be linked to the source rock it could be a useful tracer of hydrocarbon migration.

3.6.6. Norphlet Fm

Deeper in the Gulf Coast Basin (~22.000 ft; 6.7 km) the Jurassic Norphlet sandstone is host to significant gaseous hydrocarbon reserves. The unit has a number of stylolites with associated authigenic quartz and muscovite (1M) thought to have formed from pressure solution (Thomas et al., 1993). There are also pore-filling muscovites and muscovite pods in the formation. Thomas et al. (1993) have determined the timing of stylolitization by age dating of the large 1M muscovite crystals, indicating formation at 51±9 Ma (Fig. 3.16). The pore filling muscovite is 77±22 Ma and the pods are 86±16 Ma. From this it is deduced that the stylolites formed when the sandstone was buried to ~18.000 ft (5.5km). Thermal maturity indicators show that the muscovite grew at the end of wet gas generation and beginning of dry gas generation (Fig. 3.16; Thomas et al., 1993). It was proposed that the stylolites formed during methane leakage associated with fracture of the overlying Smackover Fm that seals the Norphlet reservoirs.

The utility of SIMS analyses of boron isotopes in the muscovites is notable in this case, where crystallization of muscovite occurred at different times, each representing different conditions of formation. Analyses of the $\delta^{11}B$ were done on the stylolite in thin

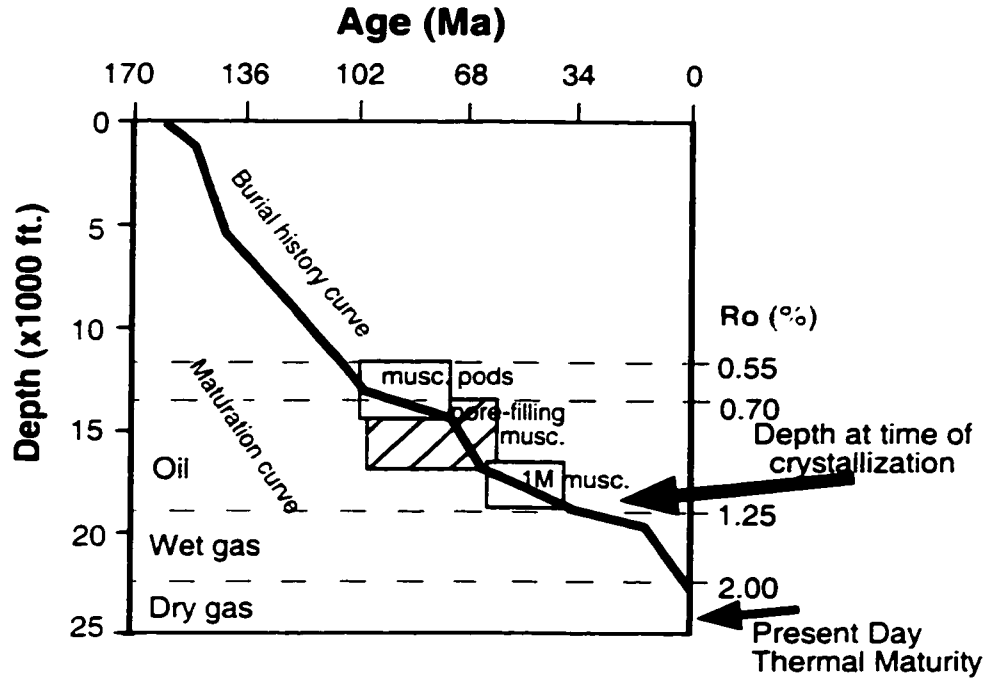

Figure 3.16. Burial history curve for the Norphlet Fm showing the interpreted timing of stylolite formation producing 1M muscovite and earlier pod and pore-filling muscovites (modified from Thomas et al., 1993). The thermal maturity curve estimates the stages of hydrocarbon generation during mineralization.

section (Fig. 3.17). The sample was measured before and after removal of adsorbed-B. Adsorbed-B was removed by ultrasonic washing of the thin section in mannitol solution (Chapter 2). Before removing the adsorbed-B the average $\delta^{11}B$ of the 1M muscovite was +11± 0.9‰ with a B-content of 483 ppm. After removal of surface adsorbed-B, the fixed-B analyses averaged –2.9 ± 0.3 ‰ with a B-content of 278 ppm. Using the burial history curve from Thomas et al. (1993; Fig. 3.17), one can estimate that the maximum temperature of crystallization of the muscovite was ~150°C. The B-fractionation ($\Delta_{mineral\text{-}water}$) at this temperature should be –21‰ (Fig. 3.13). This indicates precipitation of the muscovite in equilibrium with +19‰ water. According to the present day regional trend for $\delta^{11}B$ of Cenozoic formation waters (Fig. 3.14; Macpherson and Land, 1989; Land and Macpherson, 1992) this is a typical value for formation waters taken at 150°C. It is consistent with formation of the muscovite at a shallower depth than present day.

Analyses of the pore-filling muscovite show a $\delta^{11}B$ value of –2‰, overlapping values determined on the 1M muscovite, and similar to the pore-filling I/S in sandstone reservoirs currently at 4 km (as discussed above). The muscovite pods that have the oldest ages (86±16Ma; Thomas et al., 1993) have a $\delta^{11}B$ value of –10‰. These isotopically light muscovites are found in the insoluble residue of the stylolite, and appear to be intermixed with kerogen, again indicating that kerogen is isotopically light.

Using the B-fractionation curve, an interpretation can be made for the –10‰ muscovite pods. Based on the age and burial history curve, this oldest muscovite crystallized at ~100°C, in equilibrium with a +15‰ fluid. If that is true then the younger,

Figure 3.17. Photomicrographs of the 1M stylolite muscovite from the Jurassic Norphlet Fm, Gulf of Mexico sedimentary basin. SIMS analytical craters are ~20μm diameter.

(51±9 Ma) stylolite muscovite reflects a 4‰ *increase* in $\delta^{11}B$ of the pore fluid as the formation was more deeply buried. It is possible that there is preferential loss of ^{11}B to fluid associated with the evolution of B from kerogen during thermal maturation. The Norphlet Fm is a gas reservoir, and the stylolitization (1M muscovite crystallization) occurs during release of methane from the reservoir. This would indicate that the gaseous (light, or low molecular weight) hydrocarbons contain a ^{11}B-enriched component. Palmer and Sturchio (1990) found a similar, but small, fractionation due to phase separation. Another observation in support of this hypothesis is the high $\delta^{11}B$ (+37‰) of waters in the gas portion of the Wilcox Fm reservoirs (Chapter 2). Adjacent oil wells only a few hundred meters away contain +28‰ waters. It is possible that ^{11}B is concentrated in more volatile fractions of hydrocarbons.

Other possible mineral sources of B include tourmalines and borates. Detrital tourmalines in the Norphlet sandstone were analyzed and found not to be a likely source of ^{11}B-enrichment because of their low $\delta^{11}B$ (–6.7 ± 0.2‰), and because dissolution is unlikely at these reservoir conditions (Henry and Dutrow, 1996). Jurassic bittern salts, however, contain boracite with +31‰ $\delta^{11}B$ (Macpherson and Land, 1989). While they cannot be ruled out as a source of ^{11}B, their dissolution would be expected to have a more regional effect on the waters of the deep Gulf Coast basin. Instead a negative trend in $\delta^{11}B$ of waters with depth (Fig. 3.14) is observed, not a positive trend (Macpherson and Land, 1989).

Most importantly, the Norphlet Fm muscovites demonstrate that their B-isotope composition reflects the fluids present at the time of crystallization and retains that

signature at least through temperatures as high as the current burial depth (~250°C). The experimental work described here shows that B is not released from illitic clays but is incorporated in illite at 350°C. It is clear that authigenic clay minerals (illite and muscovite) precipitating at diagenetic temperatures can be useful monitors of changes in the fluid chemistry of hydrocarbon reservoirs. The equilibrium fractionation curve between aqueous-B and I/S may be refined through further experiments and field data, but the application demonstrated here indicates that it gives reasonable results in agreement with field observations.

3.7. CONCLUSIONS

The fractionation of boron isotopes depends mainly on the coordination state and temperature, and is independent of the mineral structure. The experiments reported here support a linear fractionation with reciprocal temperature, in accord with data from room temperature adsorption studies (Palmer et al., 1987) and high-temperature experiments of melt-fluid fractionation (Hervig and Moore, 2000). This relationship allows the application of B-isotopes to understanding fluid sources and migration during burial diagenesis. The study of authigenic illite and muscovite, the most common hosts of B in sedimentary basins may be critical to understanding important diagenetic events. The neoformation of illite and coincident changes in $\delta^{11}B$ at depths related to hydrocarbon generation, make boron a sensitive indicator of pore fluid changes related to organic maturation.

Boron substitutes in the tetrahedral layers of illite, with simultaneous exchange of oxygen. The results presented indicate a fractionation equation,

$$\Delta B_{mineral\text{-}water} = -10.12\ (1000/T(K) + 2.44$$

with a slope that opposes that established for O-isotopes (Yeh and Savin, 1977). In an ideal closed system dominated by I/S, one could predict equilibrium conditions using the geochemical link between B-isotopes and O-isotopes of I/S that change synchronously during illitization. Application to the Gulf of Mexico sediments indicates equilibrium conditions expected for I/S and fluid in the mudstones. The formation fluids in hydrocarbon reservoirs are distinctly different from that predicted. This reflects the introduction of reservoir fluids after precipitation of clay minerals, or diagenetic modification of the fluids. If the B-isotopic composition of these reservoir fluids can be linked to a specific source rock then the authigenic illite might record the presence of fluids related to hydrocarbons.

CHAPTER FOUR:

BORON ISOTOPES OF AUTHIGENIC ILLITE IN A CONTACT METAMORPOSED SHALE: IMPLICATIONS FOR B AS A TRACER OF FLUID/ROCK INTERACTIONS

4.1. ABSTRACT

Authigenic illite formed in the contact metamorphic aureole of a dike intruding shale, shows large isotopic fractionations of boron during progressive illitization that are retained up to 500°C. Incorporation of 500 ppm B in a sample closest to the intrusive indicates that illite is a host for B even under contact metamorphism. These results have implications for using authigenic illite in diagenetic environments as a tracer of fluids associated with hydrocarbons. Boron is commonly enriched in oilfield brines at temperatures where illitization occurs; thus authigenic illite may record a distinctive isotopic composition related to the presence of hydrocarbons and associated brines in potential reservoirs.

In order to determine the magnitude of B-isotope exchange as a function of temperature, samples were examined from a bentonite layer in organic-rich shale that was intruded by a dike. Vitrinite reflectance of the organic matter determined maximum temperatures across the contact aureole. Adsorbed-B is negligible at temperatures of contact metamorphism; therefore the isotopic changes observed are due to B-substitution for Si in tetrahedral layers of the illite/smectite (I/S).

Fixed-B in randomly ordered I/S retains the isotopic ratio of the original source material, but there is a 20‰ decline in $\delta^{11}B$ recorded during long-range ordering of the I/S. Application of the experimentally derived B-isotope fractionation curve for silicates (Chapter 3) allows the measured $\delta^{11}B$ values of I/S to be predicted using a Rayleigh volatilization model for isotopic fractionation. This application shows that the curve is a good assessment of the temperature dependence of B-isotope fractionations. Boron isotope

analyses of authigenic illite provide a valuable geochemical tracer of fluid/rock interactions in sedimentary and metamorphic terranes.

4.2. INTRODUCTION

Boron is enriched in shales and marine sediments (>100ppm) (Goldschmidt and Peters, 1932) because of preferential uptake of B by clay minerals. Recent studies of B-isotope systematics related to subduction of marine sediments shows that fluids derived from the subducted sediment have light $\delta^{11}B$ values compared to surficial waters (Bebout et al., 1993; You et al., 1995b; Peacock and Hervig, 1999). The large differences in $\delta^{11}B$ of fluids have made B-isotopes useful as an indicator of fluid sources. While B-isotopes have been explored on a tectonic-scale in subduction zones, it is possible that they can be useful for monitoring fluid flow in sedimentary basins as well because B is highly mobile in the aqueous phase (Levinson, 1980).

Studies of B in surficial sedimentary environments have focused primarily on adsorbed-B on clay surfaces (Schwarcz et al., 1969; Brumsack and Zulegar, 1992). Adsorption studies show a greater affinity of B for smectite and illite than for other clay minerals (Hingston, 1964; Couch and Grim, 1968; Keren and Mezuman, 1981). The enrichment of B in clay minerals does not occur during weathering of igneous rocks, nor during exposure to seawater (Spivack et al., 1987). Clay-rich marine sediments (<4μm fraction) have an average adsorbed-B content <20 ppm with $\delta^{11}B$ near +14‰, but the adsorbed-B accounts for only about 10% of the total-B in shales (Spivack et al., 1987). As temperatures approach 120°C, B-adsorption becomes negligible (You et al., 1995a). During diagenesis, substitution of B for Si occurs as smectite reacts to illite (Perry, 1972).

This tetrahedrally substituted-B in clay minerals accounts for the greater portion of B in marine sediments (>100 ppm B), and it has an average $\delta^{11}B$ of –5‰ (Palmer et al., 1987). This implies that pore fluids should become progressively ^{11}B-enriched as illitization proceeds, unless there is an additional source of B from hydrothermal fluids, organic material, or breakdown of other detrital minerals within the sedimentary basin. Identification of the sources of B and knowledge of the isotopic fractionation during illitization could provide a geochemical monitor of important diagenetic modifications to pore fluids during burial.

The purpose of this study was to compare the magnitude of B-isotope changes in a natural setting to that predicted by the experimental results for B-isotope fractionation during the illitization of smectite (Chapter 3). The temperature regime represented in the contact aureole overlaps with the temperatures of the experiments at 300°C and 350°C. Comparison of predicted and observed B-isotopic changes in this environment confirms the validity of the experimental measurements and utility of the fractionation equation.

4.3. GEOLOGIC SETTING

Samples were collected from an organic-rich portion of the Cretaceous Pierre shale near Walsenburg, Colorado where it is intruded normal to bedding by a 4 m thick composite lamprophyre dike of Eocene-Oligocene age (Johnson, 1964). The <2μm size fraction of the bentonite layer (altered volcanic ash) is dominated by smectite and illite, with minor kaolinite and chlorite (Table 4.1). The contact aureole of the dike extends for approximately 25m. Maximum temperatures affecting the sediment were determined by

Table 4.1. Mineralogical data for A) bulk powders, B) ≤2μm size fraction and C) organic matter. Ro % is vitrinite reflectance value.

A) Bulk Mineralogy

SAMPLE	DIST. (m)	%Carb	%qtz	%Ksp	%plag	%musc	%clay
WD-5	1.8	4.2	43.9	11.9	16.3	n.d.	23.7
WD-10	4.2	0.3	45.2	20.9	20.0	n.d.	13.5
WD-11	5.1	0.3	45.4	17.6	16.5	4.4	20.3
WD-12	6.2	5.7	46.6	7.9	12.0	4.6	24.3
WD-13	8.2	6.8	44.5	11.6	13.5	5.6	23.6
WD-14	10.4	5.8	51.9	9.1	9.4	7.4	23.7
WD-18	25.6	n.d.	35.6	21.8	15.1	7.4	24.8

B) Clay Mineralogy (<2μm size fraction)

SAMPLE	DIST. (m)	%Illite	%Smec	%I/S	%I (I/S)	%Kaol	%Chl
WD-5	1.8	25.4	3.2	55.3	100	0.0	16.1
WD-10	4.2	34.2	n.d.	40.3	96	16.7	8.8
WD-11	5.1	33.1	n.d.	47.3	89	19.6	0.0
WD-12	6.2	14.8	n.d.	66.1	79	9.6	9.5
WD-13	8.2	15.2	13.6	55.5	64	14.0	1.7
WD-14	10.4	9.1	6.0	61.5	40	21.9	1.6
WD-18	25.6	7.7	6.0	68.6	20	13.5	4.3

C) Organic Matter

SAMPLE	Temp °C	Ro %	TOC %
WD-5	500	3.80	0.38
WD-10	465	3.52	0.56
WD-11	430	2.75	0.69
WD-12	405	2.20	0.62
WD-13	350	1.40	0.57
WD-14	285	0.85	0.68
WD-18	200	0.50	0.51

vitrinite reflectance of the organic material in the shale to be between 200-500°C (Bostick and Pawlewicz, 1984). Thermal models based on the dike composition and thickness were tested by Pytte (1982), and found to be ~50°C lower than the estimated vitrinite temperatures. The duration of the thermal event was modeled to be on the order of 10's of years which is long enough to drive the illitization of smectite, but the kinetics of other mineralogical changes may preclude interpretations based on equilibrium assumptions.

Significant mineralogical changes observed in the shale near the dike contact include Na-metasomatism (albitization), an increase in quartz and a decrease in detrital mica and K-feldspar (Lynch and Reynolds, 1985). The increase in quartz near the dike may be due to excess SiO_2 produced during breakdown of detrital mica and feldspar. Lynch (1985) concluded that neoformation of authigenic illite occurred in a system closed with respect to major elements.

4.4. ANALYTICAL METHODS

4.4.1. Mineralogy

Bulk powder X-ray diffraction (XRD) was used to determine the mineralogy of the sediment. The <2 μm size fraction of the sediment was analyzed to identify the clay minerals (Moore and Reynolds, 1989) and degree of illitization of mixed-layered illite/smectite (I/S).

4.4.2. Isotope Geochemistry

Boron isotope analyses and B-content of the clay fraction was determined by secondary ion mass spectrometry (SIMS). Adsorbed-B was removed from these samples by multiple washings (5 or more) in de-ionized water to remove the marine pore fluid salts

and allow clay disaggregation. Samples were then washed in mannitol, a B-complexing agent that helps to remove surficial B contaminants (Hingston, 1964). A concentrated slurry of the clay fraction was dropped on a 1 inch round, B-free glass slide. After drying at 60°C, the samples were gold coated for charge compensation during SIMS analysis.

Analyses were done using a Cameca IMS 3f SIMS equipped with a standard duoplasmatron for generating a primary beam of O^- ions. In order to calibrate the SIMS for measuring the B-isotopic compositions of clay minerals, two natural samples were used as standards, that had been analyzed previously (You et al., 1995a) by thermal ionization mass spectrometry (TIMS). The samples were mineralogically similar to the bentonite, comprised of mainly illite/smectite with minor kaolinite, chlorite, and illite. The initial sample had a bulk $\delta^{11}B$ of –5‰. An aliquot was heated at 350°C and 80 MPa for 2 months producing complete recrystallization of the I/S to illite (You et al., 1995a) and a change in $\delta^{11}B$ to –10‰. SIMS analyses of the two samples also gave $^{11}B/^{10}B$ ratios that also changed by –5‰, indicating that the instrument calibration is independent of mineral matrix changes due to recrystallization. Chaussidon et al. (1997) also found matrix effects for analyses of B to be very small. Further details of the analytical technique can be found in Hervig (1996) and Chaussidon et al. (1997).

The isotope ratios are reported as delta values relative to boric acid standard NBS 951 ($^{11}B/^{10}B = 4.0437$).

$$\delta^{11}B = ((([\{^{11}B/^{10}B\}_{sample} / \{^{11}B/^{10}B\}_{standard}]-1) \times 1000) - IMF$$

where IMF is the instrumental mass fractionation, or correction factor. The IMF is measured on the standard before each analytical session and is rechecked after each sample.

The precision of the $\delta^{11}B$ values was 1-2‰ for each analysis, and each sample was analyzed more than 10 times producing analytical errors <1‰.

The B-content was determined from a calibration curve constructed from SIMS measurements of B-glass standards prepared with various B-concentrations. By measuring the ratio of $^{11}B^+$ to $^{30}Si^+$ (both measured with an electron multiplier) this curve can be used to determine the B-content of the sample if the SiO_2 content is known. Precision in measurement of B-concentration was <5%.

4.4.3. Organic Geochemistry

The vitrinite reflectance of organic matter in the Pierre Shale contact aureole of the Walsen Dike was examined by Pawlewicz and Bostick (1984) and their results were used as a measure of the maximum temperatures attained across the sampled region. Total organic carbon contents of the samples were determined using a CHN Elemental Analyzer (Perkin-Elmer Model 240C) on bulk rock powders (Williams and Ferrell, 1991).

4.5. RESULTS

The bulk mineralogy of the Pierre shale is presented as a function of distance from the dike/shale contact in Table 4.1. The clay mineral content of the shale is ~24%, with the exception of one sample ~4m from the contact with 14% clay. Other mineral modes show the following variations: quartz 36-52%, K-feldspar 8-22%, plagioclase 9-20%, carbonate ≤7%, and muscovite <7%. On a molar basis, Lynch and Reynolds (1985) found that albite replaces K-feldspar progressively as the dike is approached. Within the clay size fraction (≤2μm e.s.d.), the clay mineral assemblage is dominated by mixed-layered I/S. The most

apparent clay mineral reaction is the illitization of smectite with increasing temperature. The percentage of authigenic illite in the I/S (%I (I/S)) increases with proximity to the dike (Fig. 4.1, Table 4.1), with the sample >25 m from the dike contact showing 20% I (I/S) and the sample <2 m from the dike showing 100% illitization of the I/S.

The least illitized samples in the bentonite layer (>8 m from the contact) show a range in B-contents from ~200-300 ppm, and $\delta^{11}B$ values from +7.8 to +8.7‰. The $\delta^{11}B$ and B-contents decrease as temperatures increased with proximity to the dike (Fig. 4.2). The isotope ratios are not greatly affected however, until illitization has reached ~70% and R1 ordering (ISIS) of the mineral structure has begun (~350°C). The recrystallization of smectite to illite continues toward the dike as the temperatures reached a maximum of ~500°C near the contact. The sample taken <2 m from the dike shows a significant increase in B-content (~500 ppm) with a corresponding drop in the $\delta^{11}B$ to −12‰.

The total organic carbon (TOC) content across the contact aureole of the Pierre shale is between 0.5 and 1%. Table 4.1 lists the range of values for organic content and vitrinite reflectance values associated with that interval (Bostick and Pawlewicz, 1984). The range of temperatures interpreted from vitrinite reflectance is shown in Figure 4.1.

4.6. DISCUSSION

The B-content of the illite (Fig. 4.2), as well as other mineralogical differences within 2 m of the dike, indicates that fluids metasomatically altered this region closest to the dike intrusion (Lynch, 1985). For the rest of the bentonite samples bulk rock analyses show no indication of addition or subtraction of major elements during the metamorphic

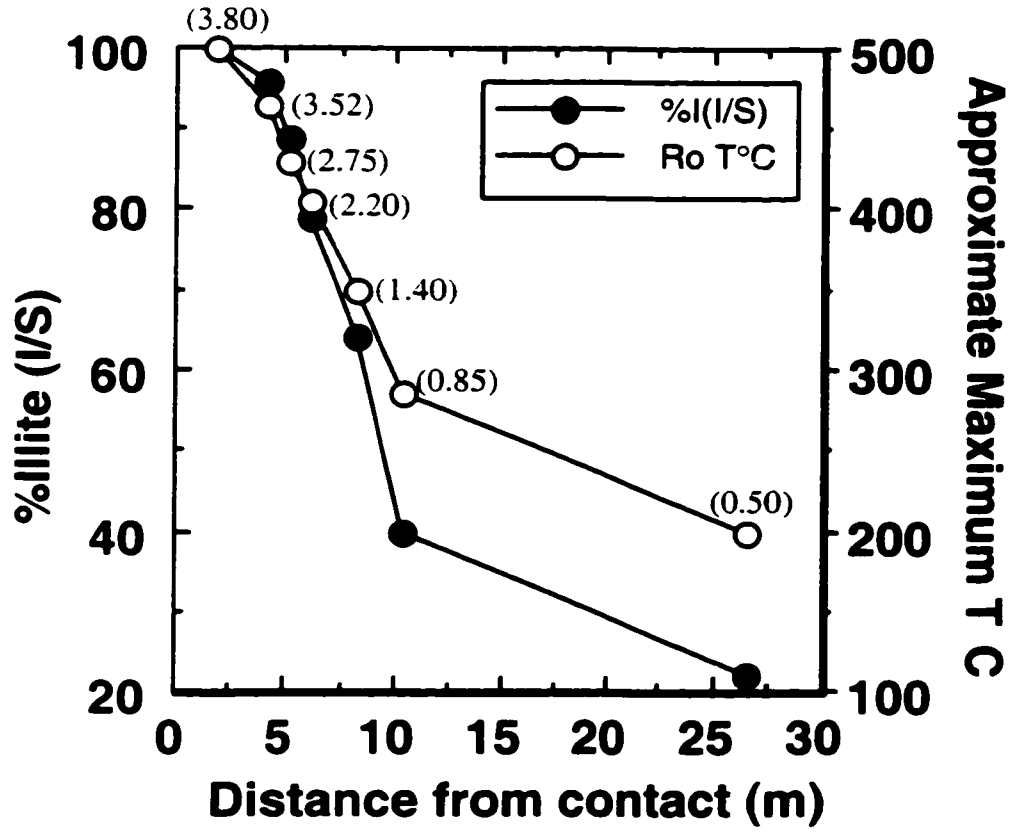

Figure 4.1. Plot showing the mineralogical changes in I/S as a function of temperature across a metamorphic contact aureole in the Pierre shale. Vitrinite reflectance values are indicated in parentheses (Bostick and Pawlewicz, 1984) and are the basis for the temperature scale. Long-range ordering of the I/S (R1 to R3) is found within ~8 m of the dike where temperatures exceeded 350°C.

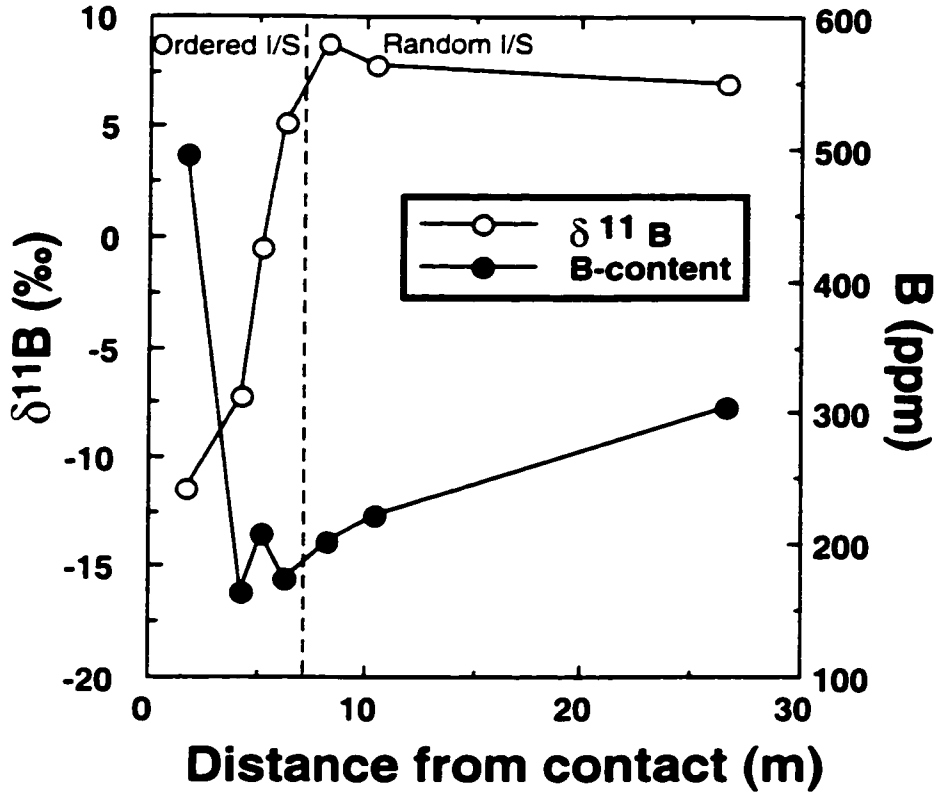

Figure 4.2. Trends in B-content and $\delta^{11}B$ across the contact aureole in the Pierre shale. Changes in the $\delta^{11}B$ do not begin until ordering of the I/S occurs at ~70% illitization.

event (Lynch, 1985). The major influence on the I/S across this layer was the short-lived thermal pulse associated with dike intrusion. Nonetheless, the system was not necessarily closed with respect to trace elements or pore fluid, and this hypothesis will be explored using the boron analyses of the dominant clay mineral I/S.

4.6.1. Boron trends

No significant change in the $\delta^{11}B$ is observed until the I/S is dominantly illitized (~70% at ~15m from the dike). Closer to the dike, the amount of authigenic illite increases to 100% and the $\delta^{11}B$ decreases by ~20‰. This observation is in close agreement with results from hydrothermal experiments on I/S (Williams et al., 1999; Chapter 3) that also show no significant change in B-isotope ratios until ~70% illitization. This suggests that major recrystallization of the mineral must occur before B isotopes begin to equilibrate with the fluid. For randomly ordered I/S the original boron isotopic composition of the source is apparently retained.

While mineralogical changes are important, another process that can influence boron is adsorption and desorption from clay mineral surfaces. This process is important in modifying low temperature pore fluids in marine and surface environments. At near surface temperatures (<60°C) the pH plays an important role in B-speciation. In aqueous fluids $B(OH)_4^-$ dominates at high pH while $B(OH)_3$ dominates at pH <8. The speciation will affect the isotopic fractionation of the adsorbed-B (Palmer and Swihart, 1996). However, You et al. (1995a) found that the amount of adsorbed-B becomes insignificant as temperatures approach 120°C. Under conditions of burial diagenesis, therefore, it is the fixed-B incorporated into the tetrahedral sheets in authigenic clay minerals, especially illite,

that will modify the $\delta^{11}B$ of the coexisting pore fluid. In the Pierre shale samples, high temperature (>200°C) contact metamorphism caused recrystallization of the smectitic sediment to illite, thus the changes in $\delta^{11}B$ observed in the clay minerals of the contact aureole do not reflect fractionation related to adsorption, but to tetrahedral B-substitution.

Under normal conditions of burial diagenesis, the B-content of authigenic I/S increases with illitization (Perry, 1972). This requires a source of B which could be other unstable detrital minerals such as micas, or perhaps organic matter (Chapter 2). In the case of the Pierre shale, there is an insufficient quantity of detrital mica and organic material to provide a significant source of B (Table 4.1). The metamorphosed Pierre shale samples show a slight decline in B-content of the clay with increasing temperature. This trend could be related to depositional variability, but it is more likely a result of the liberation of water during the reaction of smectite to illite. Boles and Franks (1979) wrote the general reaction for the illitization of smectite showing:

$$4.5\ K^{+} + 8\ Al^{3+} + \text{smectite} \rightarrow \text{illite} + 3\ Si^{4+} + (\text{cations} + \text{water})$$

The water released from the interlayer of smectite (~5-8 wt.%; Pytte, 1982) will cause dilution of the pore fluid in the immediate vicinity of the authigenic clay. A change in the B-concentration of the pore fluid requires re-equilibration of the B in the newly formed illite crystals; thus one would expect a lower B-content in the authigenic phase, reflecting the pore water dilution.

The very high B-content (500 ppm) of the 100% recrystallized illite near the dike contact (Fig. 4.2) suggests that metasomatic fluids introduced with the dike had a much higher B-content than the marine pore fluids trapped with the sediments. The fact that the

illite incorporates this much B in a samples that reached 500°C is evidence that authigenic illite is not a source of B during diagenesis or even moderate grades of metamorphism. Illite is a host for B at temperatures much higher than previously acknowledged. The illitization of smectite does not release B in sedimentary basins as has been suggested (e.g. Moldovanyi et al., 1994; Land and Macpherson, 1992).

4.6.2. Isotope Modeling

In a closed system, one would expect B-isotope ratios in I/S to track the fractionation between I/S and aqueous species of boron in the existing pore fluids (presumably seawater). The expected fractionation has been determined through experiments on I/S by Williams et al. (1999; Chapter 3) and the temperature dependence is shown in Figure 4.3. Assumptions required to apply this fractionation model include: 1) boron in authigenic illite is tetrahedral and 2) boron in pore water is trigonally coordinated. This is reasonable for a high-temperature, low pH environment (Palmer and Swihart, 1996) like a metamorphosed black shale. The predicted $\delta^{11}B$ composition of the pore water in equilibrium with I/S is given in Table 4.2, and shows a range of values from +27‰ for the low temperature I/S to −1‰ for the high temperature illite. Such a range is not possible to obtain in a closed system. To investigate the effect of open system metamorphism, that is, illitization accompanied by loss of water from the rock, two end-member models are presented: batch and Rayleigh volatilization (Valley, 1986).

The batch volatilization model (Nabelek et al., 1984) approximates a closed system where the liberated water is in equilibrium with the rock (Table 4.2). This model requires that the initial $\delta^{11}B$ of the rock is known and an approximation of the reaction progress

must be made in order to determine the fraction of reactant remaining. An initial $\delta^{11}B$ of +8‰ was assumed based on the average of the least altered samples analyzed (R0 I/S). In accordance with the observation that the $\delta^{11}B$ of I/S does not change until long-range (R1) ordering of the crystal structure ensues, the B-fixation reaction is defined as beginning at this point (f=1) and ending at 100% illite (f=0). The fraction of reactive material remaining (f) is proportional to the degree of illitization determined by XRD on samples with ≥R1 ordering (Table 4.2). The α used in each calculation was based on the maximum temperature indicated by vitrinite reflectance, and the corresponding fractionation ($\Delta_{mineral\text{-}water}$) predicted for that temperature (Table 4.2, Fig. 4.3).

Using the same parameters, a Rayleigh volatilization model was applied to the data. A Rayleigh model for isotopic fractionation results in large decreases in the $\delta^{11}B$ of I/S in a system where the water generated during illitization is immediately lost from the rock. The results of the predicted $\delta^{11}B$ of I/S compared to the measured $\delta^{11}B$ on I/S are shown in Figure 4.4. Neither end-member model accurately predicts the isotope data based on the measured parameters (vitrinite reflectance temperature, %illitization, $\delta^{11}B_{I/S}$), but the Rayleigh model shows a similar trend.

A good fit to the data can be made using a Rayleigh volatilization model based on higher temperatures of reaction (maximum 850°C instead of 500°C) but this is not reasonable considering the level of organic matter maturity and crystallinity of the sediment. Another important variable however is the value of f. By calculating the value of f that best fits the measured $\delta^{11}B$ of I/S (Table 4.2, f_{calc}), one finds that a change in f of only 10-20% is necessary to model the observed $\delta^{11}B$. At the highest temperature there is a 10%

Table 4.2. Isotope ratio predictions based on A) batch and B) Rayleigh volatilization models. The value for f fraction reactant) is defined to begin with R1 ordering of I/S (f=1). The % illitization was used as an estimate of the reaction progress (f*). The value $\delta^{11}B_{pred}$ is based on f*, however, the best fit to the data ($\delta^{11}B_{meas}$) is attained by using values of f_{calc}, which indicate a slower isotope exchange than estimated by % illitization. The difference between f* and f_{calc} indicates a 10-20 % difference in reaction rate.

A) Batch Volatilization Model $\delta f = \delta i - (1-f)*1000 \ln \alpha$

T°C	Temp. K	1000/T(K)	$\Delta_{min\ wat}$	α	%I(I/S)	% rxn.prog	f*	$\delta^{11}B_{pred}$	$\delta^{11}B_{meas}$	$\delta^{11}B_{water}$
25	298	3.36	-31.5	1.0315	10	0	1.00	8.0	8.0	39.5
200	473	2.11	-19.0	1.0190	20	0	1.00	8.0	7.8	26.8
285	558	1.79	-15.7	1.0157	40	0	1.00	8.0	7.8	23.5
350	623	1.61	-13.8	1.0138	64	0	1.00	8.0	8.7	22.5
405	678	1.47	-12.5	1.0125	79	42	0.58	2.8	5.2	17.7
430	703	1.42	-12.0	1.0120	89	69	0.31	-0.2	0.5	12.5
465	738	1.36	-11.3	1.0113	96	88	0.12	-1.9	-7.0	4.3
500	773	1.29	-10.7	1.0107	100	100	0.05	-2.1	-12.0	-1.3

B) Rayleigh Volatilization Model $\delta^{11}B\ (I/S) = (((\delta^{11}B)_{original} + 1000)*f^{(\alpha-1)}) - 1000$

T°C	α	%I(I/S)	% rxn.prog	f*	$\delta^{11}B_{pred}$	$\delta^{11}B_{meas}$	$\delta^{11}B_{in}$	f_{calc}	$f^* - f_{calc}$
25	1.0315	10	0	1.00	8.0	8.0	8.0	1.00	0.00
200	1.0190	20	0	1.00	8.0	7.8	8.0	1.00	0.00
285	1.0157	40	0	1.00	8.0	7.8	8.0	1.00	0.00
350	1.0138	64	0	1.00	8.0	8.7	8.0	1.00	0.00
405	1.0125	79	42	0.58	1.2	5.2	5.2	0.80	0.22
430	1.0120	89	69	0.31	-6.1	0.5	0.6	0.54	0.23
465	1.0113	96	88	0.12	-15.9	-7.0	-7.2	0.26	0.14
500	1.0107	100	100	0.05	-23.8	-12.0	-12.3	0.15	0.10

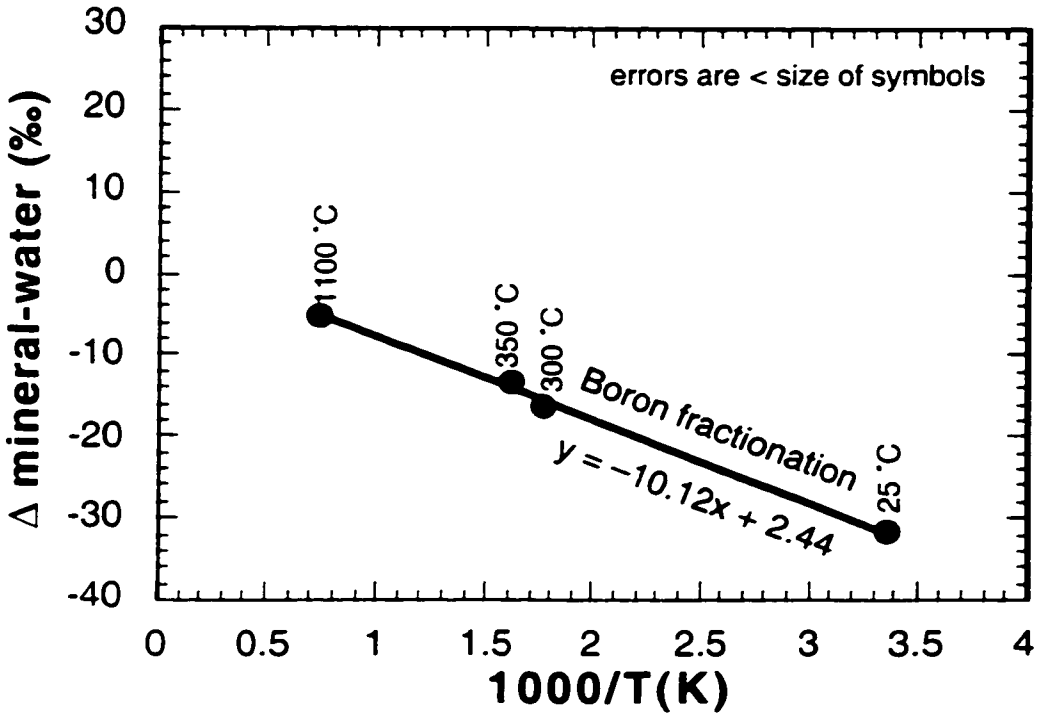

Figure 4.3. Boron isotope fractionation curve derived from experimental data of Palmer et al., (1987), Chapter 3 and Hervig and Moore (2000). Details can be found in Hervig et al., (in review).

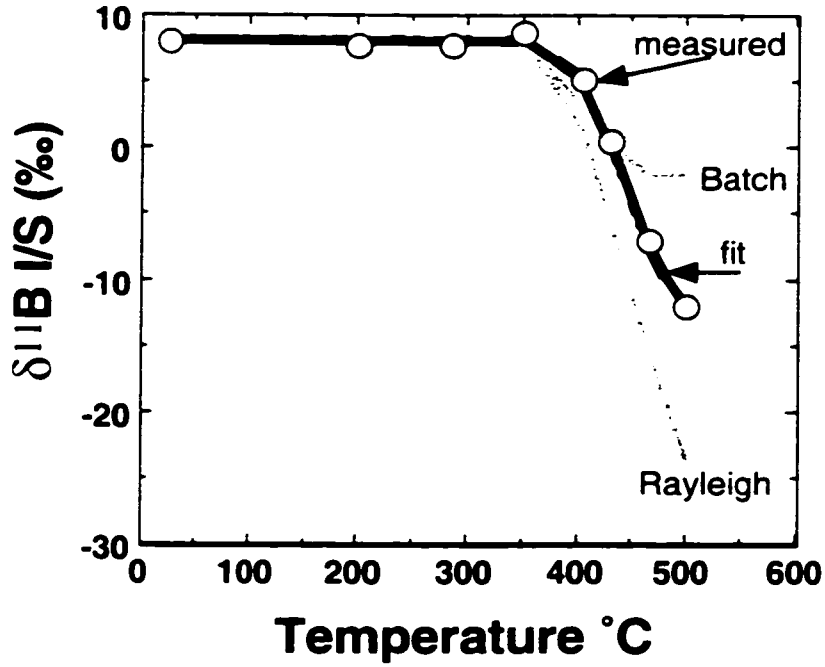

Figure 4.4. Volatilization models for predicting the changes in $\delta^{11}B$ expected in a contact metamorphic aureole. Two end-member models, batch and Rayleigh, show limits for the predicted $\delta^{11}B$ values (gray curves). Circles indicate the $\delta^{11}B$ measured on I/S, with errors indicated by the symbol size. The best fit to the data is shown by the dark curve which requires modification of the f parameter by 10-20% (See Table 4.2).

difference between the f based on illitization and f that best fits the isotope data. This difference increases at lower temperatures to ~20%, indicating that the reaction progress (isotope exchange) is 10-20% slower than estimated based on % illitization. One explanation for this could be differences in the fluid/rock ratio induced by the contact metamorphism. During dike emplacement, a greater volume of water would be expected immediately in samples that experience higher temperatures, due to more extensive dehydration and also from the introduction of metasomatic fluids. The amount of fluid that has infiltrated and exchanged with the bentonite can be calculated from isotopic mass balance (Taylor, 1977) for closed and open isotopic systems (Table 4.3). The calculations indicate that near the dike there was a three-fold increase in fluid content of bentonite during recrystallization that could cause dilution of the B-content.

The small adjustment (10-20%) to the reaction rate necessary to fit a Rayleigh model to the data can be explained by reaction kinetics. The assumption that the dominant exchange reaction began with R1 ordering of the I/S is validated by experimental results (Chapter 3), however the recrystallization depends on the reaction kinetics, as a function of temperature, time and fluid/rock ratio. It has been assumed that the recrystallization of each sample occurred at the maximum temperature that affected that sample, but it is possible that isotopic exchange occurred at a lower temperature, yet was retained in the authigenic illite as temperatures increased to the degree indicated by vitrinite reflectance.

Table 4.3. Mass balance calculations for fluid/rock ratios based on isotope ratios (Taylor, 1977).

				Fluid / Rock Ratios	
T °C	Δ min-wat	$\delta^{11}B$ (I/S)	$\delta^{11}B$ water	F/R_{closed}	F/R_{open}
25	-31.5	8.0	39.5	0.03	0.03
200	-19.0	7.8	26.8	0.04	0.04
285	-15.7	7.8	23.5	0.05	0.05
350	-13.8	8.7	22.5	0.03	0.03
405	-12.5	5.2	17.7	0.10	0.10
430	-12.0	0.5	12.5	0.19	0.17
465	-11.3	-7.0	4.3	0.29	0.26
500	-10.7	-12.0	-1.3	0.35	0.30

Δ min-wat is taken from the experimental fractionation equation (Fig. 3).

$\delta^{11}B$ water = $\delta^{11}B$ (I/S) - Δ

$F/R_{closed} = |(\delta \text{ final rock} - \delta \text{ initial rock})/(\delta \text{ initial fluid} - (\delta \text{ final rock} + \Delta))|$

$F/R_{open} = \ln (F/R \text{ closed} + 1)$

The relatively close agreement of the Rayleigh volatilization model with the measured $\delta^{11}B$ of I/S in this contact metamorphosed shale demonstrates the utility of B-isotopes for evaluating fluid/rock interactions. The results show that illite is an important mineral host for B, and that it retains the equilibrium $\delta^{11}B$ even in samples that have sustained temperatures of 500°C. Most importantly this establishes that authigenic illite will retain the isotope ratio acquired during recrystallization at lower diagenetic temperatures.

4.6.3. Application

Large accumulations of organic-rich mudstones in sedimentary basins produce significant quantities of hydrocarbons, and there is evidence that organic matter can be a source of B (Gulyayeva et al., 1963; Williams et al., 1997b, Chapter 2). It is known that some organic matter contains several hundred ppm B (eg., Gulyayeva et al., 1966; Goodarzi and Swain, 1994), which appears to be released during thermal maturation since metasedimentary graphite contains negligible B (Douthitt, 1985). Boron may be released from organic matter, similar to the release of H and O as C-O-H bonds are broken during thermal maturation. Many oilfields contain B-enriched brines associated with hydrocarbon accumulations (Sivan, T.P., 1972; Collins, 1975; Vengosh et al., 1994; Moldovanyi et al., 1992). Since B is not adsorbed by clay minerals at temperatures of hydrocarbon generation (You et al., 1995a), it partitions preferentially into the aqueous phase, and may be trapped along with hydrocarbons in sandstone reservoirs. The recrystallization of I/S to form R1 ordered structures commonly occurs at temperatures of hydrocarbon generation (100-150°C) over the long time periods of burial diagenesis (Tissot and Welte, 1984), thus fixation of B in the authigenic illite should record the chemistry of the oil-related waters.

The fixed B-isotope composition of authigenic illite could therefore be used to trace hydrocarbon migration paths.

4.7. CONCLUSIONS

The results of this work demonstrate that illite is a reservoir for ^{10}B, even at metamorphic temperatures as high as 500°C. Boron is incorporated into illite in isotopic proportions reflecting the coordination change between water (trigonal) and illite (tetrahedral). Measured $\delta^{11}B$ values of I/S generally match values predicted by a Rayleigh distillation model for isotopic fractionation, indicating that the shale is not closed with respect to pore fluids during contact metamorphism. There is good agreement between the field results and theoretical calculations based on the experimentally derived B-isotope fractionation curve (Chapter 3), indicating that it is a fair assessment of the temperature dependence of B-isotope fractionations between silicates and water. These fractionations are large compared to oxygen isotope fractionation at the same temperature (Savin and Lee, 1988) and may provide an important marker for diagenetic processes in hydrocarbon reservoirs.

In the contact metamorphosed black shale, the fixed-B of randomly ordered I/S retains the isotopic ratio of the original source material, but there is a 20‰ decline in $\delta^{11}B$ recorded when I/S undergoes long-range ordering. R1 ordering of I/S commonly occurs at depths similar to that of hydrocarbon maturation in sedimentary basins around the world, thus re-equilibration of $\delta^{11}B$ can be an important diagenetic marker of fluid changes associated with hydrocarbon maturation. If organically-bound B is released from kerogen

with a distinctive isotopic composition, then the B-chemistry of oil-related waters should be recorded by authigenic illite allowing hydrocarbon migration paths to be traced.

CHAPTER FIVE:

APPLICATION OF BORON ISOTOPES TO UNDERSTANDING FLUID/ROCK INTERACTIONS IN A HYDROTHERMALLY STIMULATED OIL-RESERVOIR IN THE ALBERTA BASIN, CANADA

5.1. ABSTRACT

Boron isotope ratios of minerals and fluids involved in diagenetic reactions may be useful as a geothermometer and monitor of fluid/rock interactions. In the steam-injected Cold Lake oil sands of northern Alberta, there is a notably large variation in the $\delta^{11}B$ of produced waters from the steam recovery project (Wieser, 1998). The higher temperature waters (~200°C) have isotopically light $\delta^{11}B$ values (+3‰) and high B-contents (~150 ppm). The range of $\delta^{11}B$ values observed is +3 to +14‰. This variation cannot be ascribed to fluid mixing because there are no fluid reservoirs in the region with a significant component of B. It is inferred that the hydrothermal fluids have interacted with the reservoir rock, causing a release of ^{10}B that lowers the $\delta^{11}B$ of the fluid.

Examination of the B-isotope ratios of reservoir minerals before and after steam injection, allows evaluation of the sources of B in the reservoir. The only significant phase containing B is pumice. It shows generally positive $\delta^{11}B$ values before steam injection and negative values after steam, with $\delta^{11}B$ as low as –28‰. Other possibly reactive phases include clay minerals and organic matter, but their abundance is not great enough for them to impact the isotopic composition of the produced waters.

This information makes it possible to evaluate the boron isotope fractionation equation derived from experimental data (Chapter 3). The results show that the fractionation curve accurately predicts the observed fractionation of B between pumice and hydrothermal fluids in the Cold Lake reservoir. This not only indicates that that the fluid and pumice have approached isotopic equilibrium, but also shows that B-isotopes potentially provide a useful geothermometer for hydrothermally stimulated oil-reservoirs.

5.2. INTRODUCTION

The application of boron isotope systematics to understanding fluid migration in hydrocarbon reservoirs has been proposed (Chapter 3), and an experimental fractionation curve was derived (Hervig et al., in review) in order to predict the relative changes of B-isotopes as a function of temperature. The dominant control on the large isotopic fractionations of B in nature result from the coordination change in B between aqueous $^{11}B(OH)_3$ and tetrahedral $^{10}B(OH)_4^-$ which prefers silicate minerals (Hervig et al., in review). Other factors that could affect isotope ratios include changes in the water chemistry brought about by decomposition of organic matter or other mineral sources of boron (Chapter 2), and mixing of waters from diverse origins.

In order to test the relative influence of these factors, and to apply the results of the experimental work to a larger scale experiment that may simulate a natural diagenetic environment, samples were studied from a thermal recovery project in oil sands from the Western Canada sedimentary basin. Recovery of high viscosity bitumen (API gravity~10°C) from reservoirs in the Cold Lake region of Alberta requires steam injection. The steam is injected at the rate of several hundred m^3/day, at temperatures as high as 300°C and pressures up to 12 MPa (Hutcheon and Abercrombie, 1990). The interaction of the fluid with reservoir rock is variable depending on the relative degree of fluid mixing and corresponding temperatures of fluid/rock interaction. Using an aqueous silica geothermometer (Gunter et al., 1997) on the recovered hydrothermal fluids, the temperatures sustained by the reservoir minerals range from 80-200°C, similar to temperatures of diagenesis (Hutcheon and Abercrombie, 1990).

Produced waters, meaning hydrothermal fluids that are recovered along with the mobilized bitumen, were examined for B-isotope ratios as a method of monitoring fluid mixing between the thermal recovery waters and formation waters (Wieser, 1998). The rock samples examined in this study were collected from cores that were near the recovery wells for the fluids. The cores were sampled before and after steam injection, so that mineralogical changes related to the steam injection could be evaluated. Using the experimental data on B-isotope fractionation (Chapter 3), we can predict the equilibrium chemistry expected for minerals in contact with fluids of known $\delta^{11}B$. A comparison of the predicted values to those measured helps to define which mineralogical changes most influence the B-isotopes, and how B can be used as a geochemical tracer of fluid/rock interactions in hydrocarbon reservoirs.

5.3. SAMPLES AND METHODS

Samples were collected from three production pads (B5, D11 and D23) in the vicinity of the produced waters (Fig. 5.1). Two samples were selected from each pad at approximately the same depth, for a total of six samples representing the pre and post-steam reservoir minerals. The samples were largely unconsolidated, so they were impregnated with epoxy for preparation as doubly polished thin sections. The previously described petrology and sedimentology of the samples (e.g. Hutcheon et al., 1989) documented extensive dissolution of framework grains (largely volcanic clasts) at the depth of the selected samples. Non-lithic fragments are predominantly quartz and feldspar, and lithic fragments include polycrystalline chert, pumice and shale

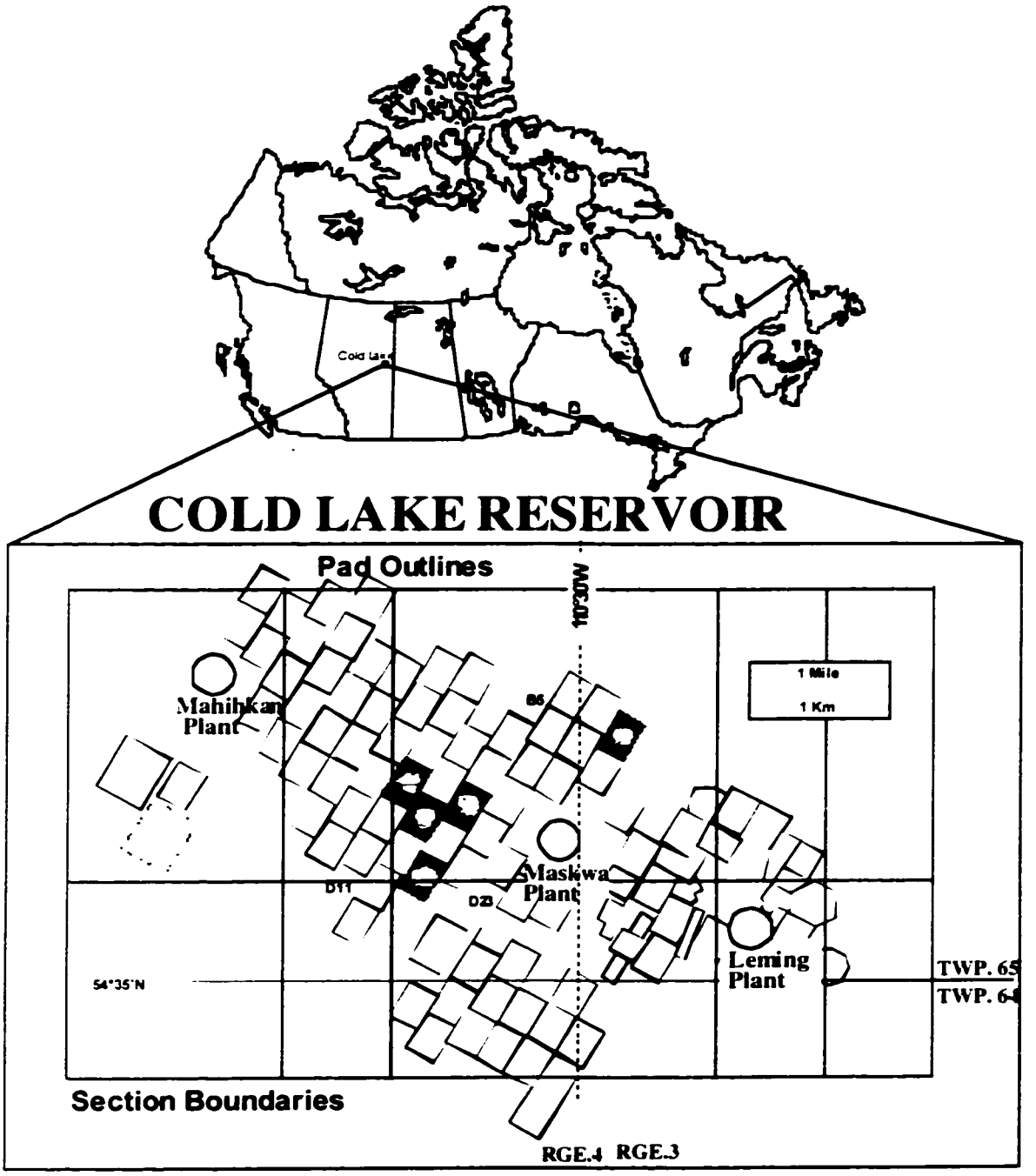

Figure 5.1 Location map of Cold Lake, Alberta basin. Enlargement shows core locations (Pads B5, D11 and D23) and locations of produced waters (Pads A4, C4, D3, D5, D7).

(Sedimentology Research Group, 1981). The abundance of clay minerals (smectite, chlorite, kaolinite and illite) is generally <6% (Hutcheon et al., 1989).

The process of drilling, coring, thin sectioning and polishing of the samples all combine to contaminate the surface of the minerals with B from fluids associated with each of these processes (e.g. Shaw et al., 1988). In order to remove B from the samples before isotopic analysis, thin sections were soaked in mannitol solution, which complexes with surface adsorbed-B. The mannitol is then washed from the samples by ultra-sonifying them in B-free distilled-deionized water. The samples were dried at 60°C then gold coated for isotopic analysis by secondary ion mass spectrometry (SIMS).

The method for SIMS analyses is described elsewhere (Chapter 3). The isotope ratios are reported as delta values relative to boric acid standard NBS SRM 951 ($^{11}B/^{10}B$ = 4.0437).

$$\delta^{11}B = ((([\{^{11}B/^{10}B\}_{sample} / \{^{11}B/^{10}B\}_{standard}] - 1) \times 1000) - IMF$$

where IMF is the instrumental mass fractionation, or calibration. The analyses were performed over a period of two years, during which the IMF varied from –35 to –46‰, but remained constant (within error) during each analytical session. The IMF is determined on a standard (IMt-1 illite), and must be known for each analytical session in order to correct the measured $^{11}B/^{10}B$ ratio for instrument bias. Most analyses were collected in stepping mode where the sample is moved in a line with analyses taken every 50 to 100μm. This allows a random sampling of the minerals in the thin section, so that results can be used to estimate the statistical variations in $\delta^{11}B$ of the entire sample. Normally multiple step scans were performed on each sample with the IMF rechecked on

standards between scans. This mode of operation produces results that are often unreliable, due to the analytical crater overlapping two phases, or hitting epoxy, or encountering a mineral (e.g. feldspar) with B-contents too low to produce a statistically significant isotope ratio.

Such analyses, however, are easy to identify based on the standard error of the individual analysis compared with the predicted error based on counting statistics. Repeated measurements of secondary ion intensity shows variation about a mean due to the random nature of the sputtering process. The predicted error can be described by a Poisson distribution for which the standard error (σ) is defined as the square root of the average of the total counts (Long, 1995). Analyses of areas that contain very little B will produce higher predicted errors. If the actual error of analysis (based on 49 cycles of measurement of mass 11 and mass 10) is more than twice the predicted error, the analysis is discarded as invalid. This condition usually indicates problems with instrumental stability or a non-ideal sample surface (charging or uneven). Analyses used for statistical compilation were based on this evaluation of the step-scanned data. The unfiltered data can be found in Appendix A.

Once the analyses were done, the analytical craters can be found as holes in the Au coat that can be observed in the petrographic microscope (Fig. 5.2). It is necessary to leave the Au coat on the sample for petrographic analysis because the analytical craters are less than a few microns deep and cannot be easily seen without the contrast provided by the Au layer. Petrographic study is required to identify the minerals encountered in

each analysis. There are often multiple analyses within one grain, allowing the assessment of intracrystalline chemical variability.

5.4. RESULTS

Table 5.1 is a summary of results based on 142 analyses that displayed acceptable statistical errors. The errors were high (>3‰) in minerals that contained little B (quartz and feldspar), but most of the analyses on lithic fragments yielded errors <2‰. Because the summary of results excludes analyses with high $\delta^{11}B$ errors, it is biased and is not an indication that lithic fragments dominate the sample. The pumice fragments contain highly variable quantities of B, ranging from tens to hundreds of ppm B in both pre- and post-steam samples. Since they display the most significant alteration between pre-steam and post-steam samples, their results are summarized separately from the other phases (Table 5.1). The small number of analyses of clay minerals in these samples limits the statistical significance of the results, however, on the basis of 3 analyses the pre-steam core from Pad B5 had B-contents averaging 50 ppm and the post steam core from Pad D11 showed a slight decline in B-content of clay (36 ppm). Other minerals (e.g. quartz, feldspar) displayed low B counts indicating that the B-content was very low (<10 ppm), so they were not analyzed.

There is considerable overlap of $\delta^{11}B$ values when comparing the pre- and post-steam samples from each production pad as a whole, however when the data are selected on the basis of mineralogy important differences are observed. The pumice fragments appear to be the most reactive constituent of the reservoir during steam injection, because they show the greatest difference in $\delta^{11}B$ between the pre and post-steam cores. Selecting

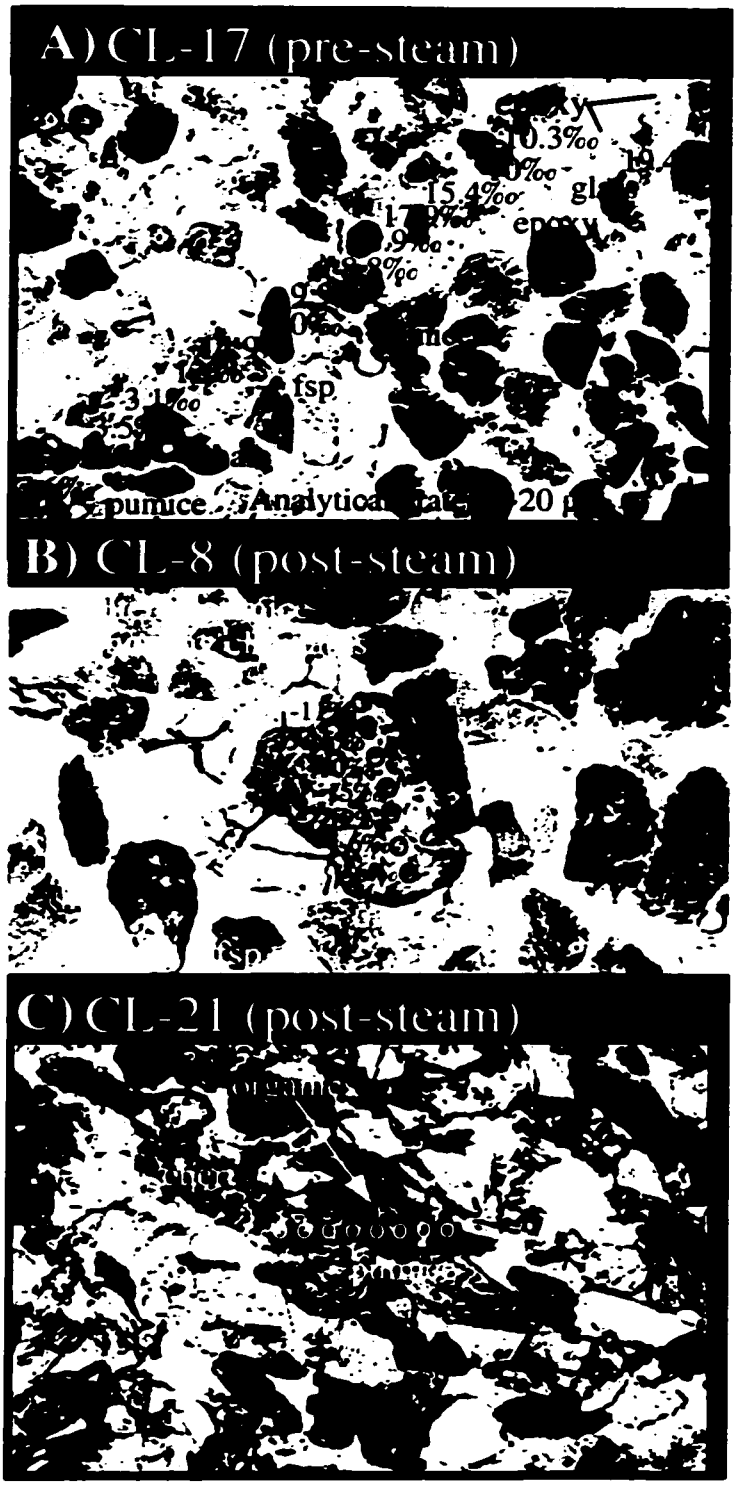

Figure 5.2 Photomicrographs of pre-steam and post-steam samples from Cold Lake showing A) step scan, B) altered pumice, and C) analyses in organic matter.

Table 5.1. Summary of boron data on minerals from the Cold Lake reservoir, Alberta basin.

Summary of pumice $\delta^{11}B$ values					
(n=142 analyses)		$\delta^{11}B$ ‰	$\delta^{11}B$ ‰	B (ppm)	B (ppm)
Sample Name	*Sample #*	*Pre-Steam*	*Post-Steam*	*Pre-Steam*	*Post-Steam*
B5-8 (460m)	1	-4 to +5		41-59	
B5-28P (460m)	8		0 to -28		*n.a.
D11-8 (461m)	17	-3 to +19		43-61	
D11-8P (461.3m)	21		+5 to -13		36-89
D23-6A(468.2m)	23	-2 to +12		25-575	
D23-8 (467.5m)	26		+7 to -16		13-107
	Other minerals				
	clay	+1 to -4	-4 to -10	50	36
	shale		-1 to -22		
	organics		-11 to -28		
	fsp	+10 to +15	+6 to +15		
	chert	+12 to +20			
	epoxy		+10 to +50	(low B, high errors)	

those data only, a histogram of the $\delta^{11}B$ values measured in pre- and post-steam pumice from each pad was compiled (Fig. 5.3). These data show that in general the pre-steam samples have a more positive $\delta^{11}B$ than the post steam samples. The greatest overlap of values is in the core from Pad D23. The greatest range of $\delta^{11}B$ values (0 to –28‰) is found in the post-steam sample from Pad B5, where the pumice was oil-stained. It is difficult to determine if the low $\delta^{11}B$ values were from the organic material or the pumice.

Clay minerals were rare in the sections analyzed. This may be due to loss during sample preparation. The few clay-rich areas analyzed appeared to be replacement of a framework grain (Fig. 5.2). Three clay analyses from the pre-steam core of Pad B5 had $\delta^{11}B$ values of +1 to –4‰. One post-steam core from Pad D11 had four analyses of replacement clay with values of –4 to –10‰. The clay mineral type was not determined. Other minerals analyzed did not contain a significant amount of B. Their range of $\delta^{11}B$ values is indicated in Table 5.1.

To aid the discussion, the B-isotopic composition and B-content of the produced waters (Wieser, 1998) is presented (Table 5.2), along with the temperature measured upon recovery, and temperatures interpreted for fluid/rock interaction (Gunter et al., 1997).

5.5. DISCUSSION

In order to understand factors influencing the B-isotope equilibrium between minerals and waters in the Cold Lake reservoir, it is necessary to evaluate the relative influence of various reactive phases in the rock. The discussion can be limited to three

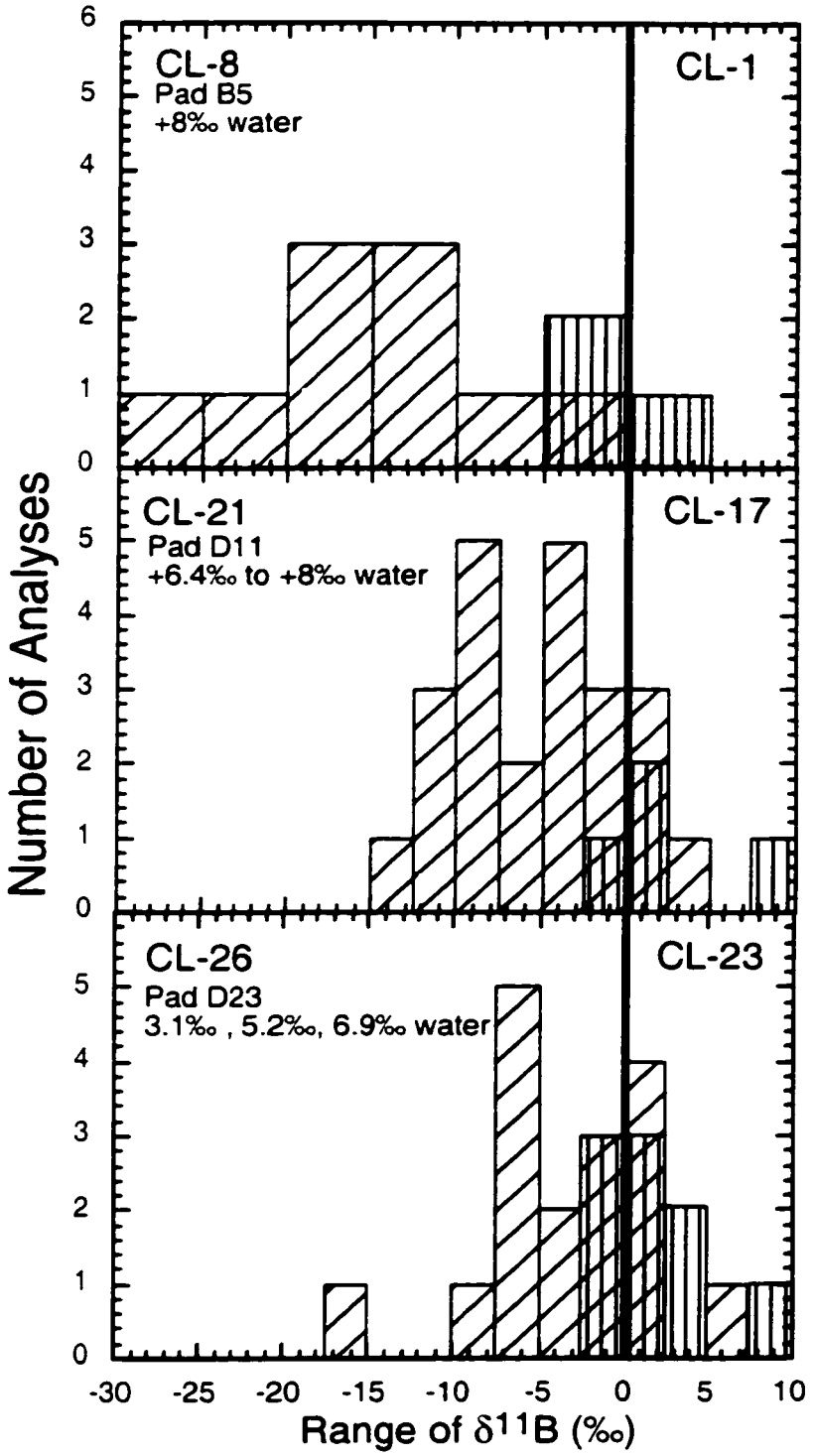

Figure 5.3. Histograms showing the range of $\delta^{11}B$ values measured on pumice in the pre-steam (vertical lines) and post-steam (diagonal lines) samples.

Table 5.2. Summary of boron data on produced waters from the Cold Lake reservoir

Sample	$\delta^{11}B$	B ppm	PW T °C	*Reservoir T °C	Near Pad
PW 1	+11.0	76.6	107	124	unknown
PW2	+8.0	95.4	80	96	B5
PW3	+3.1	148	182	190	D23
PW4	+6.9	154	159	185	D23
PW5	+5.2	159	177	182	D23
PW6	+8.0	169	142	167	D11
PW7	+6.4	196	151	177	D11
PW8	+14.1	85.7	unknown	unknown	unknown

* Reservoir temperatures were estimated based on the silica geothermometer
T (°C) = 1201 / (5.01 - log $aqSiO_2$ (ppm))-273

phases that were identified in this study as containing the greatest quantities of B: pumice, clay minerals, and organic matter. This evaluation lends credibility to the utility of the experimentally derived B-isotope fractionation curve in predicting fluid/rock interactions in a hydrocarbon reservoir.

5.5.1. Pumice

Volcanic rock fragments (pumice) provide the major mineralogical source of B in the samples studied. Volcanic glass is the most reactive mineral in the reservoir because it is the most unstable under reservoir conditions. In general, hydrothermal alteration breaks down volcanic ash to form various clay minerals and silica (Nesbitt and Young, 1984), and the Cold Lake post-steam core samples have several grains that show such alteration to clay laths (Fig. 5.2). During the recrystallization of the pumice, one would expect exchange of B with the hydrothermal fluids. The $\delta^{11}B$ values of the recrystallized pumice should reflect the range of $\delta^{11}B$ values measured on the fluid (at equilibrium) thus providing a predictive tool. This depends on the assumptions that pumice is the source of B and the isotopic fractionation curve is valid for the temperatures and minerals under investigation.

For pumice with $\delta^{11}B$ values in the range indicated (Table 5.1), the $\delta^{11}B$ predicted for water is shown as a function of temperature (Fig. 5.4). The three curves plotted for water $\delta^{11}B$ span the range of values measured on the produced waters. The $\delta^{11}B$ for pre-steam pumice is shown at T <50 °C. It plots above the range of water $\delta^{11}B$ values that were measured on produced waters. This indicates that if pre-steam minerals were in equilibrium with the original pore fluids, then the pore-fluids' $\delta^{11}B$ was between

35‰ and 39.5‰ (seawater). This is the range of values observed in the formation waters (Wieser, 1998). The temperatures measured for the produced waters range from 80° - 182°C, but these are the cooled temperatures measured after interaction with the rock. The temperatures of the water during rock interaction have been estimated based on the silica geothermometer defined by Gunter et al. (1997), where

$$T\ (^{\circ}C) = 1201/(5.01 - \log SiO_{2\ (aq)}ppm) - 273.$$

This relation indicates temperatures of fluid/rock interaction in the range of 96°-190°C. The most common analyses of post-steam pumice range from –5 to –20‰ (Fig. 5.3). Using this range of mineral $\delta^{11}B$ and the indicated temperatures, the fluid/mineral fractionation of B generates water chemistries precisely in the range of $\delta^{11}B$ values measured for the produced waters (Fig. 5.4). This indicates that the $\delta^{11}B$ of the produced waters result from equilibration with the reactive pumice.

5.5.2. Clay Minerals

The clay minerals are not a significant influence on the B-isotope composition of the waters in this reservoir, because of the high water/rock ratio and because they are not volumetrically significant (<6%) compared to the volcanic clasts. Furthermore, experimental studies (Chapter 3) show that smectite and illite incorporate B at diagenetic temperatures. There is evidence that the clay minerals do not release fixed-B at temperatures <500°C (Chapter 4). This has also been found to be true for fixed-NH_4 in the interlayer sites of illite (Williams and Ferrell, 1991). Adsorbed-B, on the other hand, will be de-sorbed as temperatures approach 120°C, because the distribution coefficient for adsorbed-B approaches zero above that temperature (You et al., 1995a). The average

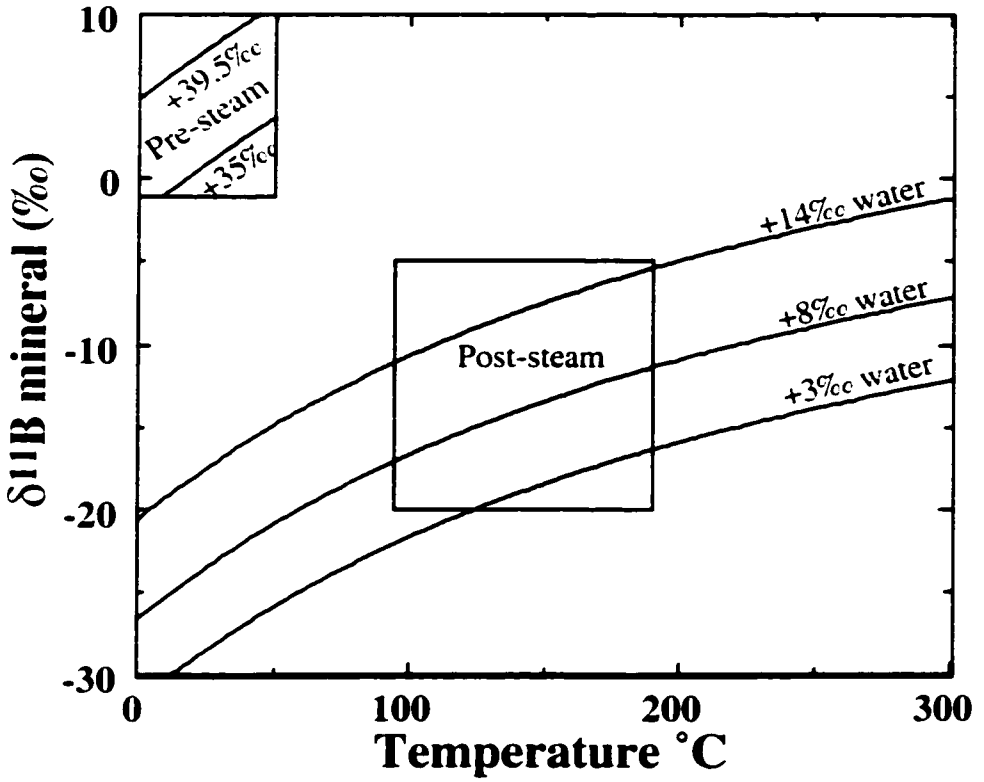

Figure 5.4. Plot showing the predicted equilibrium conditions for $\delta^{11}B$ in minerals and water as a function of temperature. The curves reflecting the water $\delta^{11}B$ were calculated from the experimental fractionation data (Chapter 3).

$\delta^{11}B$ of adsorbed-B for marine sediments is +14‰, but it was shown to be a minor fraction (<20%) of the total-B (Spivack et al., 1987). Since the clay minerals in the Cold Lake samples showed relatively low B-contents (50 ppm), the contribution from the adsorbed-B component would be <10 ppm. Mass balance precludes this as a significant source of B in the produced waters. The fact that clay minerals in the post-steam samples have a lower $\delta^{11}B$ (-4 to –10‰) than pre-steam samples (+1 to –4‰) indicates that they are re-equilibrating with the hydrothermal fluid. The temperature of nearby waters (PW 6 and PW 7) was 167-177°C. If the clays have reached equilibrium at this temperature (indicated by long-range ordering; Chapter 3) then the fluid composition should be +10 to +15‰.

5.5.3. Organic Matter

Some organic-rich areas of the post-steam sample from pad B-5 showed very light $\delta^{11}B$ values (-11 to –28‰). It has been shown that kerogen from the U.S. Gulf Coast basin contains isotopically light B (Chapter 2) and it was suggested that release of this B might occur during thermal maturation. To test this hypothesis, we examined samples from a coal seam that was transected by a dike in Wolcott, Colorado. Vitrinite reflectance of the samples (provided by Dr. Neeley Bostick, USGS, Denver) was used to determine the maximum temperatures that had affected the coal samples. Eighteen samples were analyzed that spanned a temperature range of 200-650°C (Clayton and Bostick, 1986). B-contents were determined by SIMS using a calibration curve based on the $^{11}B/^{12}C$ ratio. Details of the calibration can be found in Appendix B. This particular coal contained very little B, with a maximum of 32 ppm found in the lowest temperature sample (200°C).

Values declined to <10 ppm between 200 and 300°C and at higher temperatures there was no detectable B. Isotope ratio measurements of the coal samples yielded very high errors (3-7‰) but the average of the analyses was −15±2.8‰. These results indicate that organically-bound B is a potential source of B in hydrocarbon reservoirs, but somewhat higher temperatures than those affecting the Cold Lake reservoir may be necessary to release it. It would be necessary to know the amount of organic-B in the bitumen, in conjunction with the water/oil ratio, in order to determine the significance of organic-B liberation on the chemistry of the produced waters. Still, considering the greater abundance of pumice than bitumen, it is clear that the dominant influence on the B-chemistry of produced waters is the recrystallization of volcanic material at elevated temperatures.

5.5.4. Equilibrium Fractionation

The successful application of the experimentally derived B-isotope fractionation curve to predicting the isotope ratios of waters observed in this natural environment, lends credibility to the derived equation ($\Delta_{mineral\text{-}water} = -10.12(1000/T(K))+2.44$). Previously published fractionation data (Kotaka et al., 1973; Kakihana et al., 1977; Oi et al., 1989; Oi et al., 1991), based on theoretical calculations of reduced partition function ratios (RPFR), indicated a fractionation curve ($\Delta_{mineral\text{-}water} = -5.85\ (1000/T\ (K))+0.33$) with a much lower slope and intercept. This approximation does not explain the field data measured on Cold Lake samples. It would require waters to have much lower $\delta^{11}B$ values than observed, approaching 0‰.

The experimental data presented (Chapter 3) allow accurate prediction of the $\delta^{11}B$ of minerals and water as a function of temperature. This indicates that the dominant reactive phase (pumice) in the Cold Lake reservoir approaches equilibrium with the hydrothermal waters, even though steam injection has occurred over a time period of only a few years. The changes in water $\delta^{11}B$ appear to be a function of reaction with the rock rather than fluid mixing. This means that the $\delta^{11}B$ of the waters and pumice fragments could be monitored to evaluate the extent of thermal disturbances in the reservoir. The large fractionation of B-isotopes makes it an excellent geothermometer. The fact that the fractionation is not mineral dependent makes it even more valuable as a geochemical tool in a variety of geological environments.

5.6. CONCLUSIONS

The major source of B in the Cold Lake reservoirs is pumice, with B-contents ranging from 25-575 ppm. During steam injection, the increased temperatures cause recrystallization of the pumice, which reaches equilibrium with the hydrothermal fluid by releasing B. The isotopic composition of the fluid decreases with increasing temperature due to the equilibration with the rock, as predicted by the experimentally derived B-isotope fractionation curve.

The influence of other minerals on the B-isotope composition of produced waters is negligible at Cold Lake. Other reservoirs with significant amount of B-rich minerals (e.g. borates) would have to be evaluated for the relative reactivity of those minerals under the diagenetic conditions. Clay minerals are not expected to be a source of B at any diagenetic temperature (Chapter 3), but may be a significant sink for B during

recrystallization. At low temperatures (<120°C) adsorbed-B may alter the $\delta^{11}B$ of waters if the volume of clay minerals in the reservoir is significant. Organic matter is probably not a significant source of B on the scale of a single reservoir, because of the relatively low volume compared to the mass of rock. Furthermore, studies of B in coal indicate that B is not completely released until temperatures exceed ~300°C.

The magnitude of isotopic fractionation of B is large over the range of diagenetic temperatures represented (96-190°C). The fact that the fractionation is independent of mineralogy (at least for silicates), makes B a very good geothermometer for hydrothermally stimulated oil-reservoirs.

CHAPTER SIX: CONCLUSIONS

The results presented in these four papers (Chapters 2-5) have met the three main goals of the proposed research: to determine the B-isotope fractionation between I/S and water as a function of temperature, to explore the various sources of B in clastic sedimentary basins, and to apply the knowledge to understanding fluid/rock interactions in hydrocarbon reservoirs. A summary of the most important conclusions of the thesis is compiled below.

1. The B-content and isotopic composition of oil field brines in the U.S. Gulf Coast reservoirs showed changes both laterally across the reservoir and vertically among stacked reservoirs. There appears to be a ^{11}B enrichment of waters with distance of migration, that could result from the ^{10}B preference for clay minerals. However, this trend might also reflect a separation of gaseous or light hydrocarbons with a higher $\delta^{11}B$.
2. Kerogen from the source rock contains >100 ppm B, similar to the quantities observed in the pore-filling clay minerals of the reservoir. The isotopic composition is light (0 to −10‰), therefore organic matter is a potential source of ^{10}B during thermal maturation. This research has deduced that B is released by processes of late hydrocarbon maturation, possibly during dry gas generation. Although kerogen makes up only a small percentage of any sedimentary basin, its significance as a source of boron in deep sedimentary basins cannot be ignored when considering its reactivity compared to clay minerals.

3. The isotopic fractionation of B determined by the experimental reaction of smectite to illite allowed construction of a linear fractionation curve as a function of the reciprocal temperature. The best fit to the data from these experiments and other experiments at higher and lower temperature produced the following relationship:

$$\Delta_{\text{mineral-water}} = -10.12\ (1000/T\ (K))+2.44$$

4. The kinetics of the illitization reaction was demonstrated by a time-series of samples analyzed during the reaction progress. The results showed that metastable equilibrium is attained with respect to B-isotopes during R1 ordering of the I/S, but that equilibrium conditions require long range ordering (R3), indicative of neoformation of authigenic illite. In general, there was a 5-fold increase in the B-content of the illite during recrystallization. This indicates that illite is a sink for B, not a source of B during burial diagenesis.

5. The neoformation of illite at depths similar to those of hydrocarbon generation, makes boron a sensitive monitor of pore fluid changes related to organic maturation. If the B-isotopic composition of reservoir fluids can be linked to a specific source rock, then authigenic illite might record the presence of fluids related to hydrocarbons.

6. Authigenic illite is a reservoir for ^{10}B, even at high temperatures (~ 500°C). This was demonstrated by the very high B-content (500 ppm) of a bentonite sample taken near a dike in the presence of metasomatic fluids. Other samples in the bentonite showed a 20‰ decline in $\delta^{11}B$ of the I/S during long-range ordering. The isotopic fractionation

data derived from experiments was used in a Rayleigh distillation model to predict that isotopic compositions observed.

7. Application of the isotopic fractionation curve to a steam-injected reservoir in the Alberta basin demonstrated that the $\delta^{11}B$ of the hydrothermal fluids could be predicted by the isotopic composition of the pumice in the reservoir as a function of temperature. The pumice contained the highest concentrations of B and was the most reactive constituent of the reservoir because it was the most unstable at the temperatures of the hydrothermal perturbation.
8. The successful application of the new B-isotope fractionation curve to prediction of the pumice-water fractionation indicates that the curve is not limited to clay minerals, but can be used on a variety of silicate minerals that incorporate B in tetrahedral sites. It is the change of B between trigonal (aqueous) and tetrahedral (mineral) coordination that has the greatest affect on the isotopic fractionation. This makes B-isotopes a useful geothermometer in hydrothermally stimulated oil-reservoirs and potentially other high temperature environments such as geothermal wells.

CHAPTER SEVEN: RECOMMENDATIONS FOR FUTURE RESEARCH

The new B-isotope fractionation curve has tremendous potential for future research applications in sedimentary, igneous, and metamorphic research (Hervig et al., in review). Certainly, more experimental data measuring the isotopic fractionations at a variety of temperatures will be needed to confirm and refine the fractionation equation. The curve is only applicable in situations where B is dominantly in trigonal coordination in fluids, and where minerals provide only tetrahedral coordination sites for the substituted B. This precludes the application to carbonates and borates that have trigonal sites for B, and metamorphic minerals (e.g. some tourmalines and borosilicates) that contain a mixture of tetrahedral and trigonal sites. It also precludes application to surficial environments where the pH and temperature variations of water will affect the distribution of $B(OH)_3$ and $B(OH)_4$ aqueous species. Further work is needed on ways of predicting the B-isotopic fractionation under those types of conditions and in those types of minerals.

While the I/S experiments showed a significant increase in the amount of B substituted in authigenic illite, they did not produce the high B-contents of illite observed in nature. Experiments should be conducted with saline solutions in order to determine if the activity of B changes with ionic strength, allowing more to be fixed in authigenic minerals. It should also be confirmed that the isotopic fractionation is not a function of the amount of B incorporated at equilibrium conditions.

Future applications of B-isotope research in hydrocarbon-bearing sedimentary basins should focus on a variety of source rocks with different types of organic matter.

The variation in B-content of oil field brines is great and it may correlate with the type of oil present, or the degree of thermal or bio-degradation.

Much more research is needed on understanding the B-content of organic matter and how it may be released as a function of thermal maturation. It is not known what organic-B compounds exist in nature, and how they are bound in complex organic mixtures. It is not known if B is expelled from kerogen at once at a given temperature, or if it is gradually released, just as O is released from maturing organic matter. These types of studies should be combined with examination of the isotopic changes that take place. It should be determined if ^{11}B partitions into a gaseous hydrocarbon phase, that could explain the observed $\delta^{11}B$ increase found in the gaseous portion of the U.S. Gulf Coast reservoirs. This might also provide a unique method of correlating gas with source horizons.

In relation to sediments being subducted at continental margins, it may be profitable to examine the isotopic composition of hydrous silicates as an indicator of the temperature of fluids generated in the subduction zone. The temperatures reported have been in the range of 350°C: therefore this experimental work should be directly applicable. However, the pressures are much greater in that environment and the effect of pressure on the isotopic fractionation should be tested.

In summary, future applications of B-isotope systematics to natural geologic environments are as varied as the applications of other stable isotopic systems. Although B is a minor constituent of the earth's crust, its fractionation is simpler than the major element isotopic systems (e.g. oxygen) due to its high bond strength and small ionic

radius in minerals. It can be applied as a geothermometer and tracer of fluid compositions in a variety of field applications.

REFERENCES

Banerjee. I. and Goodarzi. F. (1990) Paleoenvironment and sulfur-boron contents of the Mannville (Lower Cretaceous) coals of southern Alberta. Canada. Sed. Geol. 67. 297-310.

Bassett. R. L.. (1980) Critical evaluation of thermodynamic data for boron ions. ion pairs. complexes. and polyanions in aqueous solution at 298.15 K and 1 bar. Geochim. Cosmochim. Acta. **44**. 1151-1160.

Bassett. R. L. (1976) The geochemistry of boron in geothermal waters. Ph.D. Dissertation. Stanford University. California. 220p.

Batchelder. M. and Cressey. G. (1998) Rapid. accurate phase quantification of clay bearing samples using a position-sensitive X-ray detector. Clays and Clay Mins. **46**. 183–194.

Bebout. G.E.. Ryan. J.G.. and Leeman. W.P. (1993) B-Be systematics in a subduction zone hydrothermal system: Catalina Schist terrane. California: Geology. **17**. 976-980.

Bloch. J.. Hutcheon. I. E. and de Caritat. P. (1998) Tertiary volcanic rocks and the potassium content of Gulf Coast shales-The smoking gun. Geology **26**. 527-530.

Boles. J. R. and Franks. S. G. (1979) Clay diagenesis in Wilcox Sandstones of southwest Texas: Implications of smectite diagenesis on sandstone cementation. J. Sed. Pet. **49**. 55-70.

Bostick. N.H. and Pawlewicz. M.J. (1984) Paleotemperatures based on vitrinite reflectance of shales and limestones in igneous dike aureoles in the Upper

Cretaceous Pierre shale. Walsenburg. Colorado. In: (J.G.Woodward. F.F. Meissner. and J.L. Clayton. eds.) Hydrocarbon source rocks of the Greater Rocky Mountain Region: Denver. Rocky Mtn. Asso. Geol.. 387-392.

Bruce. C.H. (1984) Smectite dehydration-Its relation to structural development and hydrocarbon accumulation in northern Gulf of Mexico Basin. Am. Assoc. Pet. Geol. Bull. **68**. 673-683.

Brumsack. H. J. and Zulegar. E. (1992) Boron and boron isotopes in pore waters from ODP Leg 127. Sea of Japan. Earth and Planet. Sci. Lett. **113**. 427-433.

Catanzaro. E.J.. Champion. C.E.. Garner. E.L.. Malinenko. G.. Sappenfield. K.M.. and Shields. W.R. (1970) Boric acid: isotopic and assay standard reference materials. U.S. Natl. Bur. Stand. Spec. Publ. 260-17. U.S. Gov. Printing Office. Washington. D.C.. 60 p.

Chaussidon. M.. Robert. F.. Mangin. D.. Hanon. P. and Rose. E. (1997) Analytical procedures for the measurement of boron isotope compositions by ion microprobe in meteorites and mantle rocks. Geostandard Newsletter **21**. 7-17.

Clayton. J.L. and Bostick. N.H. (1986) Temperature effects on kerogen and on molecular and isotopic composition of organic matter in Pierre Shale near an igneous dike. Organic Geochem. **10**. 135-143.

Collins. A. G. (1975). Geochemistry of Oilfield Waters. New York. Elsevier. pp. 496.

Couch. E. L. and Grim. R.E. (1968) Boron fixation by illites. Clays and Clay Mins. **16**. 249-256.

Douthitt. C. B. (1985) Boron in graphite: content speciation and significance. Chem.

Geol. **53**. 129-133.

Durand, B. (1980) Kerogen, insoluble organic matter from sedimentary rocks. Paris, Graham and Troman. 519p.

Durand, B. (1985) Diagenetic modifications of kerogens. Phil. Trans. Roy. Soc. London. **135**. 107-117.

Eberl, D. D. (1993) Three zones for illite formation during burial diagenesis and metamorphism. Clays and Clay Mins. **41**, 26-37.

Eiler, J. M., Graham, C. and Valley, J. W. (1997) SIMS analysis of oxygen isotopes: matrix effects in complex minerals and glasses. Chem. Geol. **138**, 221-244

Faure, G. (1986) Principles of isotope geology. Second edition. John Wiley and Sons, 589 p.

Goldschmidt, V. M. und Peters C. (1932) Geochemie des Bors: I Nachr. Ges. Wiss. Math-physik K1(Gottingen), 402-407.

Goodarzi, F. and Swain, D. J. (1994) Paleoenvironmental and environmental implications of the boron content of coals. Geol. Sur. Can. Bull. **471**, 76p.

Gulyayeva, I.A. Kaplun, V.B. and Shishenina, E.P. (1966) Distribution of boron among the components of petroleum. Geochem. Intn'l. **3**, 636-641.

Gunter, W.D., Wiwichar, B. and Holloway, L. (1997) Geothermometers for predicting temperatures during steam-assisted oil recovery in the oil sands reservoirs of the Mannville Group, Alberta. In: . (S.G. Pemberton and D.P. James eds.), Petroleum geology of the Cretaceous Mannville Group, Western Canada. Canadian Society of Petroleum Geologists Memoir **18**, 413-427.

Harder, H. (1970) Boron content of sediments as a tool in facies analysis. Sed. Geol. **4**, 153-175.

Hawthorne, F.C., Burns, P.C. and Grice, J.D. (1996) The crystal chemistry of boron. In: (E.S. Grew and L.M. Anovitz, eds.). Boron mineralogy, petrology and geochemistry. Min. Soc. Am. Rev. **33**, 41-115.

Hemming, K. G., Hanson, G. N. (1994) A procedure for the isotopic analysis of boron by negative thermal ionization mass spectrometry. Chem. Geol. **114**, 147-156.

Henry, D. J. and Dutrow, B. L. (1996) Metamorphic tourmaline and its petrologic applications. Boron mineralogy, petrology and geochemistry. In: (E.S. Grew, L.M. Anovitz, eds.) Boron mineralogy, petrology and geochemistry, Min. Soc. Am., Reviews in Mineralogy **33**, 503-557.

Hervig, R. and Moore, G. (2000) Experimental determination of the partitioning and isotopic fractionation of boron between mafic melts and vapor. State of the Arc 2000 Workshop, Auckland, NZ (abst).

Hervig, R.L. (1996) Analyses of geological materials for boron by secondary ion mass spectrometry. (In: E.S. Grew and L.M. Anovitz, eds.) Boron mineralogy, petrology and geochemistry, Min. Soc. Am. Reviews in Mineralogy **33**, 789-800.

Hervig, R.L., Williams, L.B., Moore, G.R., Peacock, S.M., Holloway, J.R. and Roggensack, K. (in review) Large, coordination-dependent isotope fraction of boron. Am. Min. Letts., February, 2000.

Hervig, R.L., Williams, P., Thomas, R.M., Schauer, S.N. and Steele, I.M. (1992) Microanalysis of oxygen isotopes in insulators by secondary ion mass spectrometry. Intl. J. Mass. Spec. Ion Proc. **120**, 45-63.

Heumann, K. G. and Zeininger, H. (1985) Boron trace determination in metals and alloys by isotope dilution mass spectrometry with negative thermal ionization. Intern. J. Mass Spec. Ion Proc. **67**, 237-252.

Hingston, F.J. (1964) Reactions between boron and clays: Australian Journal of Soil Research. **2**, 83-95.

Hower, J., Eslinger, E.V., Hower, M., and Perry, E.A. (1976) Mechanism of burial metamorphism of argillaceous sediment: 1. Mineralogical and chemical evidence. Geol. Soc. Amer. Bull. **87**, 725-737.

Hutcheon, I., Shevalier, M. and Abercrombie, H.J. (1993) pH buffering by metastable mineral-fluid equilibria and evolution of carbon dioxide fugacity during burial diagenesis. Geochim. Cosmochim. Acta **57**, 1017-1027.

Hutcheon, I. and Abercrombie, H.J. (1990) Fluid-rock interactions in thermal recovery of bitumen, Tucker Lake pilot, Cold Lake, Alberta. In: (I.E. Meshri and P.J. Ortoleva eds.) Prediction of Reservoir Quality Through Chemical Modeling. Am. Assoc. Pet. Geol. Memoir **49**, 161-170.

Hutcheon, I., Abercrombie, H.J., Putnam, P., Gardner, R. and Krouse, H.R. (1989) Diagenesis and sedimentology of the Clearwater Formation at Tucker Lake. Bull. Canadian. Petroleum. Geol. **37**, 83-97.

Ishikawa, T., and Nakamura, E. (1993) Boron isotope systematics of marine sediments. Earth and Planetary Science Letters **117**, 567-580.

Ishikawa, T. and Nakamura E. (1990) Suppression of boron volatilization from a hydrofluoric acid solution using a boron-mannitol complex. Anal. Chem. **62**, 2612-2616.

Johnson, R.B. (1964) Walsen composite dike near Walsenburg, Colorado: U.S. Geological Survey Professional Paper **501-B**, B69-B73.

Kakihana, H., Kotaka, M., Satoh, S., Nomura, M. and Okamoto, M. (1977) Fundamental studies on the ion exchange separation of boron isotopes. Bull. Chem. Soc. Japan **50**, 158-163.

Keren, R. and Mezuman, V. (1981) Boron adsorption by clay minerals using a phenomenological equation. Clays and Clay Mins. **29**, 198-204.

Klötzli, U. S. (1992) Negative thermal ionisation mass spectrometry: a new approach to boron isotope geochemistry. Chem. Geol. **101**, 111-122.

Kotaka, M. (1973) Chromatographic separation of boron and nitrogen isotopes using pure water as eluent. [Ph.D. Thesis]: Tokyo Institute of Technology, 163 p.

Kyser, T.K. (1987) Equilibrium fractionation factors for stable isotopes. In (Kyser, T.K., ed.) Stable isotope geochemistry of low temperature processes. Min. Soc. Can. Short Course **13**, 1-84.

Land, L. S. and Macpherson, G. L. (1992) Origin of saline formation waters, Cenozoic Section, Gulf of Mexico Sedimentary Basin. Geochim. Cosmochim. Acta **76**, 1344-1362.

Leeman, W.P. and Sisson, V.B. (1996) Geochemistry of boron and its implications for crustal and mantle processes. In (Grew, E.S. and Anovitz, L.M., eds.) Boron Mineralogy, Petrology and Geochemistry, Min. Soc. Am., Reviews in Mineralogy **33**, 645-697.

Leeman, W.P., Vocke, R.D., and McKibben, M.A. (1992) Boron isotopic fractionation between coexisting vapor and liquid in natural geothermal systems. In: (Y.K. Kharaka and A.S. Maest, eds.) Proceedings of the 7th International symposium on water-rock interaction. Rotterdam, A.A. Balkema. **7**, 1007-1010.

Leeman, W.P. Vocke, R.D., Jr., Beary, E.S. and Paulsen, P.J. (1991) Precise boron isotopic analysis of aqueous samples: Ion exchange extraction and mass spectrometry. Geochim. Cosmochim. Acta **55**, 3901-3907.

Levinson, A.A., (1980) Introduction to Exploration Geochemistry, Second Edition, Applied Publishing Ltd., Wilmette, Illinois. 924 p.

Long, J.V.P. (1995) Microanalysis from 1950-the 1990s In: (P.J. Potts, J.F.W. Bowles, S.J.B. Reed and M.R. Cave, eds) Microprobe techniques in the earth sciences. Chapman and Hall, Min. Soc. Series **6**, 1-46.

Lynch, F.L. III (1985) The stoichiometry of the smectite to illite reaction in a contact metamorphic environment. M.S Thesis, Dartmouth College, 84 p.

Lynch, F. L. and Reynolds, R.C. (1985) The stoichiometry of the smectite-illite reaction: The Clay Minerals Society 33rd annual clay minerals conference. Program with Abstracts p. 84.

Mackin, J.E. (1987) Boron and silica behavior in salt-marsh sediments: Implications for paleo-boron distributions and the early diagenesis of silica. Am. J. Sci. **287**, 197-241.

Macpherson, G.L. and Land, L.S. (1989) Boron in saline brines, Gulf of Mexico sedimentary basin, USA. In: (D.L. Miles ed.) 6th International symposium on water-rock interaction proceedings. A.A. Balkema. Rotterdam. **6**, 453-456.

Moldovanyi, E. P. and Walter, L. M. (1992) Regional trends in water chemistry, Smackover Formation, Southwest Arkansas: Geochemical and physical controls. Am. Asso. Pet. Geol. Bull. **76**, 864-894.

Moldovanyi, E.P., Walter, L.M. and Land, L.S. (1994) Strontium, boron , oxygen, and hydrogen isotope geochemistry of brines from basal strata of the Gulf Coast sedimentary basin, USA. Geochim. Cosmochim. Acta **57**, 2083-2099.

Moore, D.M. and Reynolds, R.C., Jr. (1989) X-ray diffraction and the identification and analysis of clay minerals. Oxford University Press, New York. 332 p.

Nabelek, P.I., Labotka, T.C., O'Neil, J.R. and Papike, J.J. (1984) Contrasting fluid/rock interaction between the Notch Peak granitic intrusion and argillites and limestones in western Utah: evidence from stable isotopes and phase assemblages. Contrib. Mineral. Petrol. **86**, 25-34.

Nakamura, E., Ishikawa, T., Birck, J-L. and Allegre, C.J. (1992) Precise boron isotopic analysis of natural rock samples using a boron-mannitol complex. Chem.Geol. **94**, 193-204.

Nesbitt, H.W. and Young, G.M. (1984) Prediction of some weathering trends of plutonic and volcanic rocks based on thermodynamic and kinetic considerations. Geochim. Cosmochim. Acta **48**, 1523-1534.

Nies, N.P. and Campbell, G.W. (1964) Inorganic boron-oxygen chemistry: Boron, Metallo-Boron Compounds, and Boranes. Interscience **1**, 53-232.

Oi, T., Kato, J., Ossaka, T., and Kakihana, H. (1991) Boron isotope fractionation accompanying boron mineral formation from aqueous boric acid-sodium hydroxide solutions at 25°C. Geochem. Jour. **25**, 377-385.

Oi, T., Nomura, M., Musashi, M.,Ossaka, T., Okamoto, M., and Kakihana, H. (1989) Boron isotopic compositions of some boron minerals. Geochim. Cosmochim. Acta **53**, 3189-3197.

Palmer, M.R., and Swihart, G.H. (1996) Boron isotope geochemistry: an overview. Boron mineralogy, petrology and geochemistry. In: (E.S. Grew and L.M. Anovitz, eds.). Min. Soc. Am., Reviews in Mineralogy **33**, 709-744.

Palmer, M. R. and Sturchio, N. C. (1990) The boron isotope systematics of the Yellowstone National Park (Wyoming) hydrothermal system: A reconnaissance. Geochim. Cosmochim. Acta **54**, 2811-2816.

Palmer, M.R., Spivack, A.G. and Edmond, J.M. (1987) Temperature and pH controls over isotopic fractionation during adsorption of boron on marine clay. Geochim. Cosmochim. Acta **51**, 2319-2323.

Peacock, S.M. and Hervig, R.L. (1999) Boron isotopic composition of subduction-related metamorphic rocks: Chem. Geol. **160**, 281-290.

Perry, E. A. (1972) Diagenesis and the validity of the boron paleosalinity technique. Am. J. Sci. **272**, 150-160.

Perry, E.A., Hower, J. (1972) Late-stage dehydration in deeply buried pelitic sediments. Am. Asso. Pet. Geol. Bull. **56**, 2013-2021.

Pollastro, R.M. (1985) Mineralogical and morphological evidence for the formation of illite at the expense of illite/smectite. Clays and Clay Mins. **33**, 265-274.

Pytte, A.M. (1982) The kinetics of the smectite to illite reaction in contact metamorphic shales. M.A. Thesis, Dartmouth College, 78 p.

Sassen, R. (1990) Lower Tertiary and Upper Cretaceous source rocks in Louisiana and Mississippi: Implications to Gulf of Mexico crude oil. Am. Asso. Pet. Geol. Bull. **74**, 857-878.

Savin S.M. and Lee, M. (1988) Isotopic studies of phyllosilicates. In (S.W. Bailey, ed.) Hydrous phyllosilicates (exclusive of micas). Reviews in Mineralogy **19**, 189-223.

Schafer, H. and Sieverts, A. (1941) Steigerung der Aziditat der Borsaure durch Zustatz von Neutralsalzen. Zeit. Anorg. Chem. **246**, 149-157.

Schwarcz, H.P., Agyei, E.K. and McMullen, C.C. (1969) Boron isotopic fractionation during clay adsorption from seawater. Earth and Planet.Sci. Lett. **6**, 1-5.

Sedimentology Research Group (1981) The effects of in situ steam injection on Cold Lake oil sands. Bull. Can. Pet. Geol. **29**, 447-478.

Shaw, D.M., Higgins, M.D., Truscott, M.G. and Middleton, T.A. (1988) Boron contamination in polished thin sections of meteorites: implications for other trace element studies by alpha-track images or ion microprobe. Am. Min. **73**, 894-900.

Sivan, T.P. (1972) Statistical substantiation of the significance of boron dissolved in underground waters of the Crimea for oil and gas exploration: Soviet Geology **10**, p. 148-151.

Spivack, A. J., Palmer, M. R. and Edmond, J.M. (1987) The sedimentary cycle of the boron isotopes. Geochim. Cosmochim. Acta **51**, 1939-1949.

Srodon, J. (1980) Precise identification of illite/smectite interstratifications by X-ray powder diffraction. Clays and Clay Mins. **28**, 410-411.

Suchecki, R.E. and Land, L.S. (1983) Isotopic geochemistry of burial-metamorphosed volcanogenic sediments, Great Valley sequence, Northern California, Geochim. Cosmochim Acta **47**, 1487-1499.

Swihart, G. H. (1996) Instrumental techniques for boron isotope analysis. In: (Grew, E.S. and Anovitz, L.M., eds.) Boron Mineralogy, Petrology and Geochemistry, Min. Soc. Am., Reviews in Mineralogy **33**, 845-862.

Taylor, H.P. Jr. (1977) Water/rock interactions and the origin of H_2O in granitic batholiths. J. Geol. Soc. London **133**, 509-558.

Thomas, A.R., Dahl, W.M., Hall, C.M. and York, D. (1993) $^{40}Ar/^{39}Ar$ analyses of authigenic muscovite, timing of stylolitization, and implications for pressure solution mechanisms: Jurassic Norphlet formation, offshore Alabama. Clays and Clay Mins. **41**, 269-279.

Tissot, B. P. and Welte, D. H. (1984) Petroleum Formation and Occurrence. New York, Springer-Verlag. 699 p.

Tonarini, S., Pennisis, M. and Leeman, W.P. (1997) Precise boron isotopic analysis of complex silicate (rock) samples using alkali carbonate fusion and ion-exchange separation. Chem. Geol. **142**, 129-137.

Valley, J.W. (1986) Stable isotope geochemistry of metamorphic rocks. In (J.W. Valley, H.P. Taylor Jr. and J.R. O'Neil, eds.) Stable isotopes in high temperature geological processes. Min. Soc. Am., Reviews in Mineralogy **16**, 445-486.

Vengosh, A., Starinsky, A., and Chivas, A.R. (1994) Boron isotopes in Heletz-Kokhav oilfield brines, the Coastal Plain Israel: Israeli Jour. Earth Sci. **43**, 231-237.

Vengosh, A., Starinsky, A., Kolodny, Y. and Chivas, A.R. (1991) Boron isotope geochemistry as a tracer for the evolution of brines and associated hot springs from the Dead Sea, Israel. Geochim. Cosmochim. Acta **55**, 1689-1695.

Vengosh, A., Chivas, A.R., and McCulloch, M.T. (1989) Direct determination of boron and chlorine isotopic compositions in geological materials by negative thermal-ionization mass spectrometry. Chem. Geol. **79**, 333-343.

Whitney, G. and Northrup, H.R. (1988) Experimental investigation of the smectite to illite reaction: Dual reaction mechanisms and oxygen-isotope systematics. Am. Min. **73**, 77-90.

Wieser, M.E. (1998) Stable isotope ratio mass spectrometry of nanogram quantities of boron and sulfur. Ph.D. Dissertation. The University of Calgary, Alberta, Canada. 127p.

Williams, L.B., and R.L. Hervig (1997) Potential for in-situ measurements of O-isotopic ratios in clay minerals using Secondary Ion Mass Spectrometry (SIMS). 11th International Clay Conference, Program with Abstracts, p. A80.

Williams, L.B. and Ferrell, R.E. (1991) Ammonium substitution in illite during maturation of organic matter: Clays and Clay Mins. **39**, 400-408.

Williams, L.B., Hervig, R.L. and Holloway, J.R. (1999) Experiments on the boron isotope fractionation of illite. Geol. Soc. Am. Annual Meeting, Denver, Colorado. Abstracts with Programs. **31**, A344.

Williams, L.B., Hervig, R.L., and Bjørlykke, K. (1997a) New evidence for the origin of quartz cements in hydrocarbon reservoirs revealed by oxygen isotope microanalyses. Geochim. Cosmochim. Acta **61**, 2529-2538.

Williams, L.B., Hervig, R.L., Wieser, M.E., and Hutcheon, I. (1997b) The influence of organic matter on the boron isotope geochemistry of the Gulf Coast Sedimentary Basin: The International Association of Geochemistry and Cosmochemistry Second International Applied Isotope Geochemistry Symposium, Lake Louise, Alberta, Canada, Abstract.

Williams, L.B. Ferrell, R.E., Hutcheon, I., Bakel, A.J., Walsh, M.M. and Krouse, H.R. (1995) Nitrogen isotope geochemistry of organic matter and minerals during diagenesis and hydrocarbon migration. Geochim. Cosmochim. Acta **59**, 765-779.

Xiao, Y.K., Vocke, R.D., Swihart, G.H. and Xiao, Y. (1997) Boron volatilization and its isotope fractionation during evaporation of boron solution. Anal. Chem. **69**, 5203-5207.

Yates, D.M. and Rosenberg, P.E. (1996) Formation and stability of end member illite: I. Solution equilibration experiments at 100 – 250 °C and $P_{v.soln}$ Geochim. Cosmochim. Acta **60**, 1873-1883.

Yeh H. and Savin, S.M. (1977) Mechanism of burial metamorphism of argillaceous sediment. 3. O-isotope evidence. Geol. Soc. Am. Bull. **88**, 1321-1330.

You C.F., Spivack, A.J., Gieskes, J.M., Martin, J.B. and Davisson, M.L. (1996) Boron contents and isotopic compositions in pore waters: a new approach to determine temperature induced artifacts- geochemical implications. Marine Geol. **129**, 351-361.

You, C.-F, Spivack, A.J., Gieskes, J.M., Rosenbauer, R., and Bischoff, J.L. (1995a) Experimental study of boron geochemistry: Implications for fluid processes in subduction zones: Geochim. Cosmochim. Acta **59**, 2435-2442.

You, C.-F., Chan, L.H., Spivack, A.J. and Gieskes, J.M. (1995b) Lithium, boron, and their isotopes in sediments and pore waters of Ocean Drilling Program Site 808, Nankai Trough: Implications for fluid expulsion in accretionary prisms. Geology **23**, 37-40.

You, C.F., Spivack, A.J., Smith, J.H., Gieskes, J.M. (1993) Mobilization of boron in convergent margins: Implications for the boron geochemical cycle. Geology **21**, 207-210.

APPENDIX A:

Compilation of Analytical Data on Cold Lake Reservoir Samples

Sample	$^{11}B/^{10}B$	S.D.	error ‰	P.E. ‰	$\delta^{11}B$	Grain type	$^{11}B/^{30}Si$	B ppm
CL-23	3.8651	0.01841	2.6	1.9	1.8	pumice		
Pre-steam	3.8815	0.01158	1.7	1.1	5.9	pumice	2.93E-03	24
IMF = -46	3.8315	0.01403	2.0	1.8	-6.5	pumice	1.17E-02	95.7
	3.8979	0.03140	4.5	2.8	9.9	plag		
	3.7919	0.00791	1.1	0.8	-16.3	pumice	2.79E-03	25
	3.8395	0.01783	2.5	1.1	-4.5	pumice		
	3.8827	0.01051	1.5	0.7	6.2	epoxy		
	3.8604	0.00969	1.4	0.8	0.7	pumice		
	3.8312	0.00869	1.2	0.9	-6.6	pumice		
	3.8339	0.00612	0.9	0.6	-5.9	pumice		
	3.8532	0.01333	1.9	0.5	-1.1	pumice		
	3.8668	0.01045	1.5	1.2	2.3	epoxy		
	3.9083	0.01833	2.6	2.8	12.5	chert		
	3.9402	0.02202	3.1	3.5	20.4	chert		
	3.9206	0.03168	4.5	4.0	15.6	chert		
	3.8534	0.00593	0.8	0.8	-1.1	pumice		
	3.8568	0.00622	0.9	0.8	-0.2	pumice		
	3.8625	0.00760	1.1	0.7	1.2	pumice		
	3.8793	0.01885	2.7	1.6	5.3	epoxy		
	3.8861	0.01470	2.1	2.2	7.0	Fe -stain		
	3.8740	0.00778	1.1	0.6	4.0	Fe -stain		
	3.8639	0.05277	7.5	1.8	1.5	epoxy		
	3.8383	0.03739	5.3	5.3	-4.8	pumice		
	3.8817	0.05730	8.2	8.4	5.9	epoxy		
	3.8599	0.01478	2.1	1.7	0.5	pumice	5.16E-03	47
	3.8340	0.01805	2.6	2.4	-5.9	pumice	6.32E-02	575
	3.8434	0.03167	4.5	2.2	-3.5	pumice		
	3.8260	0.02748	3.9	4.8	-7.8	pumice		
	3.8354	0.03870	5.5	5.5	-5.5	pumice		
	3.8462	0.02500	3.6	3.8	-2.8	pumice		
	3.8455	0.04800	6.9	4.4	-3.0	pumice		
	3.9233	0.04390	6.3	6.9	16.2	epoxy		
	3.8329	0.00958	1.4	1.3	-6.1	pumice	3.75E-03	34

Sample	$^{11}B/^{10}B$	S.D.	error ‰	P.E. ‰	$\delta^{11}B$	Grain type	$^{11}B/^{30}Si$	B ppm
CL-26	3.8759	0.00576	0.8	0.7	4.5	altered		
post steam	3.8655	0.04000	5.7	3.3	1.9	altered		
IMF =-46	3.8618	0.01276	1.8	2.1	1.0	pumice		
	3.8641	0.01495	2.1	1.6	1.6	pumice		
	3.8328	0.02282	3.3	1.5	-6.2	edge of clast		
	3.8756	0.03814	5.4	4.4	4.4	epoxy		
	3.8428	0.01170	1.7	1.7	-3.7	shale		
	3.8531	0.00828	1.2	1.1	-1.1	shale		
	3.7693	0.02195	3.1	3.3	-21.9	shale		
	3.8542	0.02481	3.5	2.7	-0.9	edge of clast		

Sample	$^{11}B/^{10}B$	S.D.	error ‰	P.E. ‰	$\delta^{11}B$	Grain type	$^{11}B/^{30}Si$	B ppm
CL-26	3.8598	0.04792	6.8	8.1	0.5	epoxy		
post steam	3.9158	0.03751	5.4	5.4	14.4	fsp		
IMF =-46	3.8989	0.04834	6.9	7.5	10.2	fsp		
	3.9179	0.03126	4.5	5.0	14.9	fsp		
	3.8693	0.02435	3.5	3.0	2.9	quartz		
	3.8718	0.04000	5.7	4.5	3.5	quartz		
	3.8497	0.01961	2.8	2.3	-2.0	pumice		
	3.9056	0.03439	4.9	4.2	11.8	glass?		
	3.8621	0.01083	1.5	0.7	1.1	pumice		
	3.8517	0.00751	1.1	0.9	-1.5	pumice		
	3.8646	0.00736	1.1	0.9	1.7	pumice		
	3.8644	0.01156	1.7	1.3	1.7	pumice	1.40E-03	13

Sample	$^{11}B/^{10}B$	S.D.	error ‰	P.E. ‰	$\delta^{11}B$	Grain type	$^{11}B/^{30}Si$	B ppm
CL-26	3.8484	0.01160	1.7	1.0	-2.3	pumice	1.17E-02	107
post steam	3.8756	0.01573	2.2	1.8	4.4	pumice		
IMF =-46	3.8536	0.00891	1.3	1.1	-1.0	edge of clast		
	3.8842	0.06362	9.1	8.9	6.6	epoxy		

Sample	$^{11}B/^{10}B$	S.D.	error ‰	P.E. ‰	$\delta^{11}B$	Grain type	$^{11}B/^{30}Si$	B ppm
CL-26	3.8569	0.00982	1.4	1.1	-11.2	pumice		
IMF = -35	3.8402	0.04000	5.7	6.0	-15.3	pumice		
	3.8628	0.00799	1.1	0.7	-9.7	pumice		
	3.8432	0.00686	1.0	0.9	-14.6	pumice		
	3.8519	0.02378	3.4	3.4	-12.4	pumice		
	3.8789	0.00800	1.1	1.1	-5.8	pumice		
	3.8774	0.02590	3.7	3.7	-6.1	pumice		

Sample	$^{11}B/^{10}B$	S.D.	error ‰	P.E. ‰	$\delta^{11}B$	Grain type	$^{11}B/^{30}Si$	B ppm
CL-1	3.8585	0.04302	6.1	1.5	-3.8	clays	4.49E-03	41
Pre-steam	3.8790	0.00584	0.8	0.7	1.3	clays	6.53E-03	59
IMF = -42	3.8575	0.01060	1.5	1.2	-4.0	clays		

Sample	$^{11}B/^{10}B$	S.D.	error ‰	P.E. ‰	$\delta^{11}B$	Grain type	$^{11}B/^{30}Si$	B ppm
CL-8	3.8648	0.01106	1.6	1.5	-9.2	pumice		
Post-steam	3.8403	0.01031	1.5	1.4	-15.3	pumice		
IMF = -35	3.9276	0.02617	3.7	3.8	6.3	fsp		
	3.8827	0.01068	1.5	1.5	-4.8	pumice		
	3.7892	0.01579	2.3	1.7	-27.9	organic		
	3.8482	0.01282	1.8	1.7	-13.3	organic		
	3.8025	0.02273	3.2	3.3	-24.6	organic		
	3.8563	0.02876	4.1	3.9	-11.3	glass?		
	3.8680	0.01152	1.6	2.0	-8.5	glass?		
	3.8567	0.01563	2.2	1.7	-11.2	organic		

Sample	$^{11}B/^{10}B$	S.D.	error ‰	P.E. ‰	$\delta^{11}B$	Grain type	$^{11}B/^{30}Si$	B ppm
CL-8	3.8548	0.01094	1.6	1.5	-11.7	organic		
Post-steam	3.8275	0.00903	1.3	1.4	-18.5	organic		
IMF = -35	3.8297	0.01301	1.9	1.6	-17.9	organic		
	3.9029	0.03588	5.1	5.1	0.2	quartz		
	3.9202	0.05289	7.6	6.3	4.5	epoxy		

Sample	$^{11}B/^{10}B$	S.D.	error ‰	P.E. ‰	$\delta^{11}B$	Grain type	$^{11}B/^{30}Si$	B ppm
CL-17	3.9045	0.00989	1.4	1.2	7.6	pumice/center	7.50E-03	61.4
Pre-steam	3.8669	0.00767	1.1	1.0	-1.7	pumice	5.24E-03	42.9
IMF = -42	3.8739	0.00982	1.4	1.0	0.0	pumice/edge		
	3.8746	0.00931	1.3	1.0	0.2	pumice/edge		
	3.9003	0.01014	1.4	0.9	6.5	RF		
	3.8880	0.02035	2.9	2.1	3.5	RF		
	3.8643	0.00930	1.3	1.1	-2.4	RF		
	3.8841	0.01570	2.2	1.2	2.5	RF		
	3.8579	0.04316	6.2	8.9	-3.9	glass		
	3.8613	0.06630	9.5	6.8	-3.1	glass		
	3.9224	0.05657	8.1	7.7	12.0	epoxy		
	3.9340	0.04526	6.5	4.7	14.9	fsp		
	3.8590	0.04078	5.8	3.7	-3.7	clay		
	3.9170	0.02589	3.7	1.5	10.7	epoxy		
	3.9264	0.03579	5.1	5.2	13.0	glass		
	3.9138	0.05217	7.5	6.9	9.9	glass		
	3.9095	0.03725	5.3	6.5	8.8	glass		
	3.9097	0.01020	1.5	1.2	8.9	glass		
	3.9464	0.12320	17.6	14.6	17.9	epoxy		
	3.9145	0.04642	6.6	5.5	10.0	epoxy		
	3.9360	0.04092	5.8	6.3	15.4	glass		
	3.9154	0.07363	10.5	1.4	10.3	glass		
	3.8875	0.11850	16.9	15.0	3.4	epoxy		
	3.8646	0.09687	13.8	15.9	-2.3	epoxy		
	3.8849	0.01372	2.0	1.8	2.7	glass		
	3.8134	0.00935	1.3	1.2	-15.0	epoxy		
	3.9512	0.04503	6.4	5.3	19.1	epoxy		
	3.9443	0.01467	2.1	1.3	19.4	pumice		

Sample	$^{11}B/^{10}B$	S.D.	error ‰	P.E. ‰	$\delta^{11}B$	Grain type	$^{11}B/^{30}Si$	B ppm
CL-21	3.8587	0.01398	2.0	1.4	-3.8	pumice	6.09E-03	55
Post-steam	3.8383	0.00806	1.2	0.7	-8.8	pumice	9.77E-03	89
IMF = -42	3.8210	0.02538	3.6	2.9	-13.1	pumice		
	3.8590	0.01318	1.9	1.5	-3.7	pumice		
	3.8354	0.01107	1.6	1.0	-9.5	pumice		
	3.8318	0.01271	1.8	0.8	-10.4	pumice		
	3.8540	0.00963	1.4	1.2	-4.9	pumice		
	3.8271	0.01120	1.6	1.3	-11.6	pumice		

Sample	$^{11}B/^{10}B$	S.D.	error ‰	P.E. ‰	$\delta^{11}B$	Grain type	$^{11}B/^{30}Si$	B ppm
CL21	3.8357	0.01154	1.6	1.1	-7.4	pumice		
IMF = -44	3.8265	0.01205	1.7	1.1	-9.7	pumice		
	3.8515	0.02661	3.8	1.5	-3.5	pumice		
	3.8746	0.02914	4.2	1.3	2.2	clay		
	3.8670	0.01704	2.4	1.4	0.3	pumice		
	3.8602	0.01948	2.8	0.7	-1.4	pumice		
	3.8690	0.01949	2.8	0.8	0.8	pumice		
	3.8311	0.01980	2.8	0.9	-8.6	pumice		
	3.8742	0.01997	2.9	1.4	2.1	pumice		
	3.8569	0.02907	4.2	2.0	-2.2	pumice		
	3.8399	0.01598	2.3	1.9	-6.4	pumice		
	3.8151	0.02543	3.6	1.0	-12.5	pumice		
	3.8254	0.01680	2.4	1.1	-10.0	pumice		
	3.8665	0.01985	2.8	1.5	0.2	epoxy		
	3.8457	0.01165	1.7	0.9	-5.0	pumice		
	3.7874	0.01891	2.7	2.1	-19.4	glass		
	3.8643	0.01882	2.7	1.7	-0.4	pumice		
	3.8789	0.02283	3.3	1.3	3.2	pumice		
	3.8507	0.03546	5.1	4.7	-3.7	clay	4.45E-03	36
	3.8268	0.01850	2.6	2.2	-9.6	clay		
	3.8384	0.01485	2.1	2.3	-6.8	clay		
	3.8406	0.04509	6.4	1.8	-6.2	clay		

APPENDIX B

SIMS ANALYSIS OF THE B-CONTENTS OF ORGANIC MATTER

Standards were prepared by mixing solutions of 10, 100, and 1000 ppm B (aqueous boric acid) with the B-complexing agent mannitol which is an organic compound with the chemical formula $C_6H_{14}O_6$. The proportion of mannitol was kept constant (500 mg) and only the B-content of the solution was varied. The solutions were evaporated onto B-free (p-type) silicon wafers, and Au coated for SIMS analysis. Three spot analyses were done on each sample measuring the counts on mass 11 for 20 s, and mass 12 for 30 s. The errors indicated by multiple analyses are <1‰. The resulting calibration curve is shown.

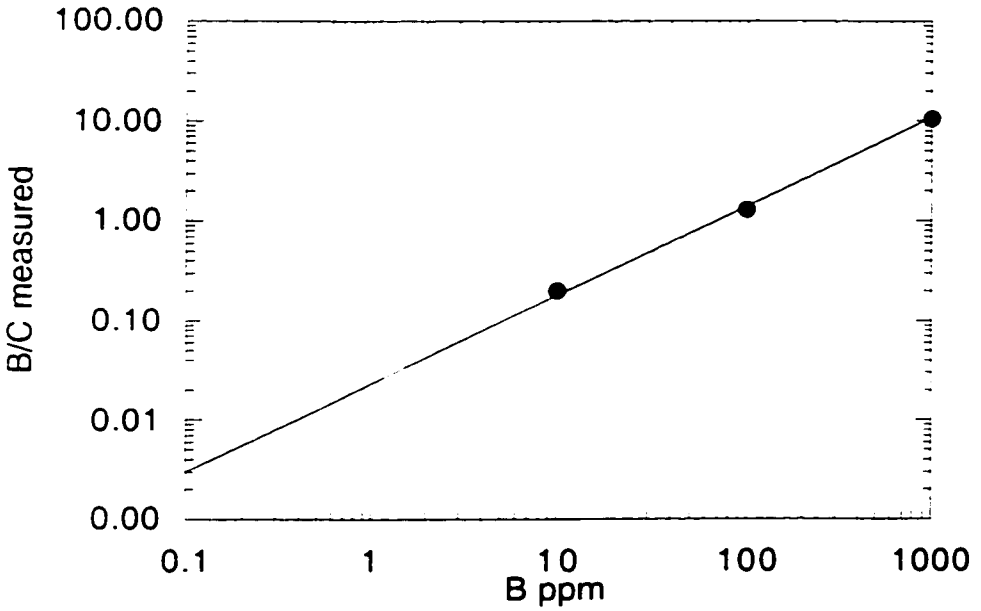

Calibration curve for organically bound B

B-content measurements on coal

Using this calibration curve the following B-content of coal was observed. Vitrinite reflectance measurements (Bostick and Pawlewicz, 1984) were used to estimate temperature.

Sample	11/12 cps	B ppm	Temp (°C)
10	0.093	0.9	300
10	0.078	0.8	300
11	0.113	1.1	280
11	0.060	0.6	280
12	0.089	0.9	250
12	0.087	0.9	250
12	0.084	0.8	250
13	0.389	3.9	225
13	0.544	5.4	225
13	0.107	1.1	225
13	0.088	0.9	225
13	0.298	3.0	225
14	1.137	11.4	220
15	0.904	9.0	215
15	0.297	3.0	215
15	0.352	3.5	215
15	0.112	1.1	215
16	0.091	0.9	210
16	0.098	1.0	210
16	0.117	1.2	210
16	0.476	4.8	210
17	0.127	1.3	205
17	0.120	1.2	205
18	2.174	21.7	200
18	3.150	31.5	200

B-isotope ratios measured on coal

It was noted that for analyses of B in organic matter, the B counts per second (cps) are much lower than for clay minerals, and they drop rapidly in the first minute of sputtering. The count rate stabilizes after about 3 minutes. Where count rates are high enough for an isotope ratio analysis, the primary beam current was increased to get a minimum of 500 cps on the least abundant mass (^{10}B). This usually required a primary current of ~5nA. The following results were obtained on the coal samples above.

Sample	11/10	S.D.	error ‰	P.E. ‰	$\delta^{11}B$	IMF
IMt-1 <2.0μ	3.8052	0.0045	0.6	0.6	-59.0	-50.0
	3.8112	0.0051	0.7	0.6	-57.5	-48.5
	3.8150	0.0044	0.6	0.6	-56.6	-47.6
	3.8106	0.0040	0.6	0.6	-57.6	-48.6
					Average =	**-48.7**

Sample	11/10	S.D.	error ‰	P.E. ‰	$\delta^{11}B$	$\delta^{11}B_{corr}$
Coal-18	3.7878	0.0716	7.2	5.5	-63.3	-14.3
Coal-16	3.7912	0.0741	7.4	2.3	-62.4	-13.4
Coal-16	3.7627	0.0647	6.5	1.9	-69.5	-20.5
Coal-13	3.7765	0.0339	3.4	1.1	-66.1	-20.1
Coal-10	3.8088	0.0952	9.6	2.3	-58.1	-12.1

Sample	11/10	S.D.	error ‰	P.E. ‰	$\delta^{11}B$	IMF
IMt-1 <2.0μ	3.8351	0.0047	0.7	0.5	-51.6	-42.6
	3.8280	0.0048	0.7	0.5	-53.3	-44.3
	3.8208	0.0064	0.9	0.5	-55.1	-46.1
	3.8205	0.0050	0.7	0.5	-55.2	-46.2
	3.8029	0.0050	0.7	0.5	-59.5	-50.5
					Average =	**-46.0**

S.D. is standard deviation of the analysis
P.E. is the predicted error.
IMF is the instrumental mass fractionation measured before and after sample analysis.